Old Dominion University

Lunar Construction Utility Vehicle

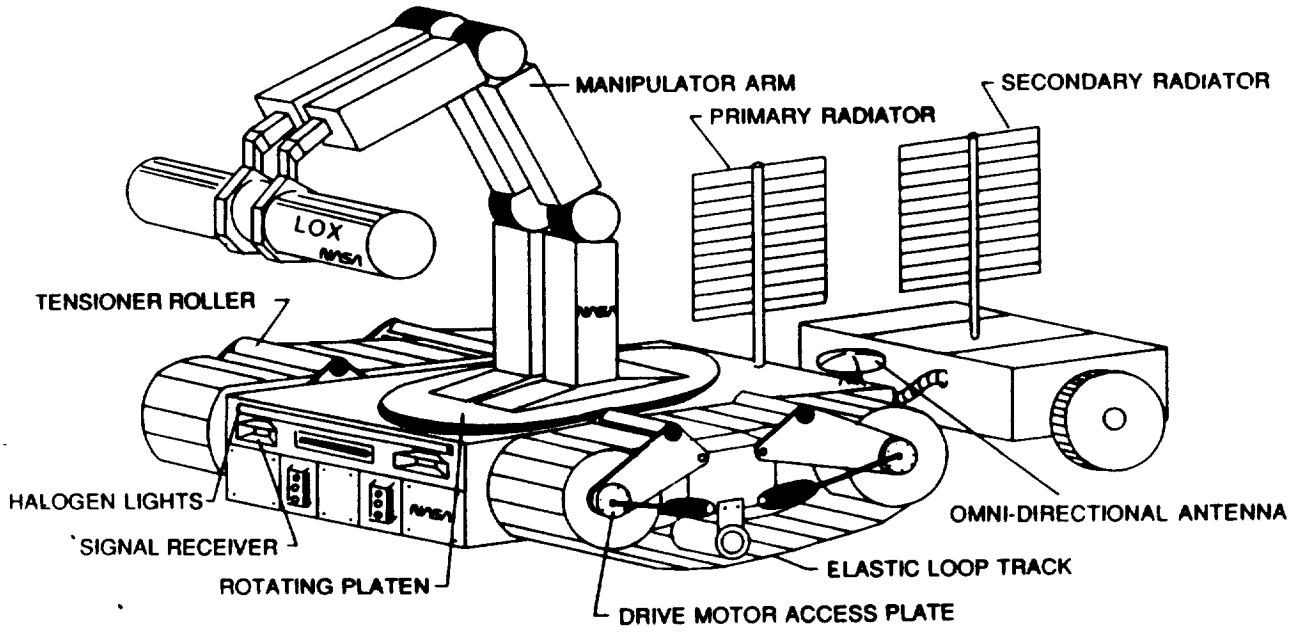

NASA/USRA Summer Report
July 1989

ODU

FOREWORD

The lunar construction utility vehicle (LCUV) was a task performed by a group of mechanical engineering students at Old Dominion University during the Spring semester of 1989. The LCUV concept was developed as part of the Advanced Space Design Program which is managed by the University Space Research Association (USRA). The conceptual report from which the constraints for this design were taken is listed as reference 10 in this report. The LCUV is a utility/construction vehicle which will aid in the robotic assembly of a lunar outpost. The vehicle is designed to operate during the initial unmanned (phase 1) construction phase. This scenario is set in the time frame 1992-2007.

Dr. John Alred was the NASA technical manager for this study; however, he has since taken the position of Assistant Director with the USRA.

This report offers both conceptual and detailed analyses. Many problems have been identified, and this work will continue for another semester with the goal of developing the details to the point where a scaled working model can be built and tested.

Questions concerning this report may be directed to:

Dr. Robert L. Ash
Old Dominion University
Department of Mechanical Engineering
and Mechanics
Norfolk, VA 23508
(804) 683-3720

ACKNOWLEGEMENTS

This work was carried out during the spring semester of 1989. The following students took part in the LCUV project:.

TECHNICAL MANAGERS

Bill Campbell
Tony Coulson
Jeff Jacobs

STUDENT ENGINEERS

Dave Alcorn
Tim Bacon
Rachelle Bentley
Jim Coritz
Charles Draper
Gary Dunne
Harry Hargis
Doug Henry
William Hughes
Salim Khaireddine
Frank Martillotti
John Nagy
Steve Nieman
Dimitri Nunez
Paul Stiles
Greg Stoltz
Joe Szabo
Tim Taylor
Mike Zydron

Dr. John Alred was the NASA mentor for the project

Dr. Robert Ash, chairman of the Mechanical Engineering Department, is the principal investigator for USRA projects at Old Dominion University.

Dr. Mason Chew is the class instructor and co-investigator for USRA projects.

Claude Bryant was the graduate teaching assistant and technical editor of this report.

Special thanks go to the student managers for the extra work they put into the project.

TABLE OF CONTENTS

LIST OF FIGURES

LIST OF TABLES

LIST OF ABBREVIATIONS

FOV - FIELD OF VIEW
GPC - GENERAL PURPOSE COMPUTER
LCUV - LUNAR CONSTRUCTION UTILITY VEHICLE
LTS - LUNAR TELEROBOTIC SERVICER
MA - MECHANICAL ARM
MCIU - MANIPULATOR CONTROLLER INTERFACE UNIT
MEM - MECHANICAL ENGINEERING AND MECHANICS
NRCC - NATIONAL RESEARCH COUNCIL OF CANADA
ODU - OLD DOMINION UNIVERSITY
PAM - PULSE AMPLITUDE MODULATION
PCM - PULSE CODE MODULATION
PDM - PULSE DURATION MODULATION
PPM - PULSE POSITION MODULATION
PTC - PYRAMIDAL TRUSS CORE
PWM - PULSE WIDTH MODULATION
REM - ROTEGEN EQUIVALENT MAMMAL
RMS - REMOTE MANIPULATOR SYSTEM
RPM - REVOLUTIONS PER MINUTE
USRA - UNIVERSITY SPACE RESEARCH ASSOCIATION
VFACS - VERTICAL FORCE ABSORBING CONNECTION SYSTEM

ABSTRACT

A NASA/USRA conceptual design for the return of man to the moon requires that a permanent lunar base be built to accommodate future missions. The build up of the base is to be accomplished robotically in this scenario. A key element of the project is the development of an all purpose construction vehicle which can serve many functions during the base assembly. The lunar construction utility vehicle will have the following capabilities:

- Self supporting including repairs
- Must offload itself from a lunar lander
- Must be telerobotic and semi-autonomous
- Must be able to transport one space station common module
- Must allow for man-rated operation
- Must be able to move lunar regolith for site preparation

The design constraints for this study were taken from reference 10 of this report. These constraints represent one conceptual scenario which is not the only possible scenario; furthermore the overall weight and size constraints are likely to move upward in the next phase of the LCUV design.

This study recommends the use of an elastic tracked vehicle. Detailed material analyses of most of the LCUV components have been accomplished. The body frame, made of pinned truss elements, has been stress analyzed using NASTRAN. A track connection system has been developed; however, kinematic and stress analyses are still required. This design recommends the use of hydrogen-oxygen fuel cells for power. Space and volume calculations will follow in a subsequent report. Thermal control has proven to be a problem which may be the most challenging technically. A tentative solution has been proposed which utilizes an onboard and towable radiator. Detailed study of the heat dissipation requirements is needed to finalize radiator sizing. Preliminary work on a man-rated cabin has begun; however, this is not required during the first mission phase of the LCUV. Finally, still in the conceptual phases, are the communication, navigation and mechanical arm systems. It is anticipated that most of the problems identified in this report will be solved and a subsequent report will be issued in July 1990.

1.0 HULL AND BODY

This report explains the hull/body section of LCUV-2. The dimensions of the frame are as follows: (1) a height of 0.7m will be used (2) a distance of 3m for the width and length will also be employed. Initially, it was decided that Pyramidal Truss Core (PTC) would be used as the frame; however, PTC employs welds which NASA does not like using because of vibrations upon launch. It then decided to use a basic truss network with the above dimensions used. Finally, a NASTRAN/PATRAN analysis was completed using Old Dominion University's CAD system.

1.1 INTRODUCTION

Initially, PTC was incorporated into our design because of its light weight, high strength, and ability to be easily manufactured according to design specifications (Reference 1). The Pyramidal Truss Core consists of a layered panel that acts as a truss system with the faces acting as the compression and tension members of the truss (Reference 1). The core of the panel acts as a diagonal truss member. The function of the PTC panels is to carry the bulk of the compressive and tensile stresses while the core of the PTC acts to transfer shear (Reference 1). Unfortunately, NASA does not like using welds, since vibrations occur at launch and thus failure is possible. What we decided on then was a simple truss network of bar elements connected by bolts and pins. The design is shown in Figure 1.1 of this report section. The length and width are each 3 meters and the height is 0.7 meters. For the actual bar elements, a hollow square section was used (see Figure 1.2). The cross-sectional area of this element is 0.016 meters squared. All of this data and more is tabulated in Table 1.1 of this report. Finally, a NASTRAN/PATRAN analysis was employed for three different loading configurations. The maximum deflection for each case was determined to be under a millimeter, implying a sturdy and most likely failure free design.

1.2 CAD ANALYSIS

A CAD analysis was used for the frame to determine where the maximum deflections and stresses occurred. The CAD system used NASTRAN/PATRAN commands. PATRAN generated the model using the proper commands such as grid and line. In PATRAN, an analysis mode was entered where bar elements were created. Also material, force, and displacement cards were employed into the design. The material of the truss used was pure aluminum. The force in each case involved a loading of 25000 Newtons. Finally the displacement cards were used where the vehicle is constrained, namely where the tracks attach to the frame.

In the second phase of the CAD analysis, NASTRAN was used. Here the NOS/VE system created the neutral file from PATRAN and hence the bulk data deck was created. Basic commands were attached

into the neutral file, these commands were employed as the case and executive control data decks. Finally the job was submitted and displacement, stress, force, bending moments, and torque records were created for all elements and nodes generated from the analysis mode of PATRAN.

Three separate loading configurations were employed in the analysis mode of PATRAN. Unfortunately, due to a limited supply of paper and ink, only two of the stress and deformation plots could be plotted and submitted within this report. The three cases are documented as follows:

CASE 1:

A load of -25000 N (y dir) was applied at the back of the frame where a bar element was not used diagonally. The reason for this occurrence was to provide in easy access to the power system in the event of a breakdown. The maximum deflection occurred where the force was applied, an excellent indicator of a rigid design. This deflection registered -0.1624E-03 m in the y direction. No deflection was recorded in the frame in any direction greater than this. The stress and deformation plot is shown in Appendix D of this report.

CASE 2:

The second analysis involved a loading configuration where the robotic arm is located. Again, a load of -25000 N was applied in the y direction (down). Also, the bar element deflected -3.4196E-03 m. Again no deflections were generated greater than this maximum one. The stress and deformation plot is shown in Appendix D of this report.

CASE 3:

Unfortunately, the second analysis is not shown. Here, a load of -25000 N was applied in the z direction to the front of the frame. This simulated a case where the vehicle may run into something. A maximum deflection again was recorded at this bar element where the force was applied. Here, a maximum deflection was found to be -2.00E-07 in the z direction.

1.3 MATERIALS

The material used for the construction of the LCUV plays an important role in the design aspects associated with the frame and loading analysis. The primary criterion in the selection of an engineering material is the extent to which that material has the characteristics required for the design. The frame must be designed to couple the forces imposed by the robotic arm and to provide sufficient support to the LCUV body. Thus, by choosing a suitable material for its construction, the frame design could provide a lightweight and practical solution to the structure analysis needed for the loading specifications.

In order for the material to perform as expected, it must be

able to endure the adverse environmental conditions that exist on the lunar surface. For example, the material will be subjected to extreme temperature gradients, low vacuum, and radiation bombardment.

In order to ensure long-lasting operation, the material used for the construction of the LCUV must be of long life and able to withstand the lunar environment. The failure of a frame component due to fatigue or loading might nullify the entire LCUV mission. Therefore, the material must exhibit the properties that will enable the LCUV to meet the required design specifications.

1.3.1 ASSUMPTIONS AND DESIGN CONSTRAINTS

Most metallic structural materials are used for load- carrying components such as fuel cells, robotic arms, and crew compartments. In this type of usage, maximum strength at minimum weight is desired. The frame of the LCUV must also be designed in order to combat the effects of the lunar environment on the material that will be used for its construction. These include temperature gradients, vacuum effects, and radiation. These three main problems are explained briefly below:

1. Temperature - the temperature on the Moon ranges from - 170°C to 130°C. Thus, materials must be used that are compatible with this temperature difference.

2. Radiation - there are a number of types of radiation encountered on the lunar surface. Therefore, the materials used for the LCUV must be immune to the penetration of harmful gamma rays.

3. Vacuum effects - sublimation of materials is a potential hazard for the LCUV. At low pressure, the material used to build the LCUV might experience evaporative losses. Hence, the need for a material that is not susceptible to sublimation is apparent.

The effects of cratering and penetration damage and welding also play an important role in the choice of materials. Taking these factors into account, the following discussion is presented in accordance with these design specifications.

1.3.2 MATERIALS FOR STRUCTURAL APPLICATION

All high strength alloys based on magnesium, aluminum, titanium, beryllium, and steel (principally stainless) are potential candidate materials (Reference 2). The refractory metals cobalt, molybdenum, tantalum, and tungsten suffer severe disadvantages in cost and weight, when considered for structural purposes; molybdenum and tungsten also exhibit very low ductility.(Reference 2) Titanium is also at a disadvantage due to its high cost. One dollar will buy 18 times as much stainless

steel, and 60 times as large a volume of aluminum as it would buy in titanium (Reference 4). Also, steel lacks the quality of being light yet strong due to its weight. Therefore, the choices will be limited to the high strength alloys of aluminum, beryllium, and magnesium.

1.3.3 TEMPERATURE EFFECTS

Temperature can have considerable effects on the structure when metals of widely different coefficients of thermal expansion are joined. The coefficient of thermal expansion is a measure of the amount by which the volume changes in response to a change in temperature. For example, the low coefficient of thermal expansion of beryllium compared to aluminum is a potential source of high thermal stresses when these metals are joined (Reference 2). Uncontrolled solar heating can cause excessive differential expansion. Thus, the material used for the frame and membrane structure will be similar, if not the same. Aluminum would be the optimal choice of material considering its high melting point which is much greater than the 130°C maximum temperature encountered on the moon.(Reference 3) Table 1.1 lists the coefficient of thermal expansion and the melting point for aluminum along with other important properties.

1.3.4 VACUUM EFFECTS

At high temperatures within a vacuum, loss of material may be of concern when considering the design of a space structure. Loss of material by direct evaporation in the low-pressure environment of space is insignificant for aluminum, beryllium, and titanium (Reference 2). In the case of magnesium, evaporative losses would be appreciable (0.004 in.) in the course of a year for a structure above 400°F (Reference 2). This value is a maximum because the mean temperature will not be a constant 400°F on the lunar surface. The effects of direct evaporation are shown in Figure 1.1. Aluminum, which is thermally compatible with the temperature gradients on the moon, seems to be the appropriate choice of material. Although titanium is also acceptable by these standards, aluminum is less expensive and more practical. A protective coating can also be applied to the aluminum in order to protect against sublimation.

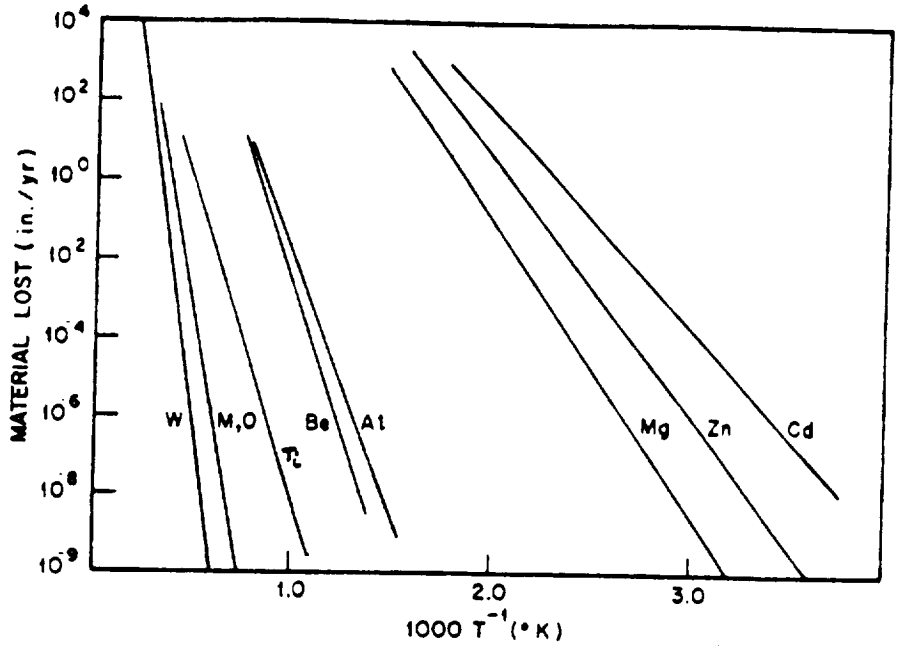

Figure 1.1 (Reference 2)
Effects of Sublimation on Space Materials

Protective coatings of low vapor pressure metals, or conversion coatings such as phosphate should be used for this type of application (Reference 2). The economics of plating are entirely reasonable for the degree of protection needed.

1.3.5 RADIATION EFFECTS

Radiation plays an important role in the design of structures that will be located on the lunar surface. The types of radiation encountered on the moon are solar galactic, and extragalactic cosmic rays, X rays and gamma rays from the Sun, solar-flare and solar wind particles, electrons and protons of the Van Allen Belts of trapped radiation, neutrons, and alpha particles. The design of the structure must be able to withstand these types of radiation. Economically speaking, aluminum would be the best choice. Aluminum is found to be an excellent deterrent for the penetration of gamma rays (Reference 3). Other materials could be used, but a protective coating must be applied in order to shield the structure from the harmful radiation. The application of a protective coating would affect the pre-flight storage and handling of the structure which might inhibit the ability to make adjustments within the frame. For example, the type of coating used might require the structure to be stored in a dust-free chamber or sterile environment in order to prevent the contamination of the protective film. Hence, the use of aluminum would prevent the need for this type of pre-flight storage.

1.3.6 CRATERING AND PENETRATION DAMAGE

The effects of cratering and penetration damage due to various lunar particles are serious potential hazards. The degree of these effects differ for each metal. Material selection can be based on the structural requirements such as skin thickness of the outer membrane. Commercially, beryllium is potentially more vulnerable to particle damage because of its brittleness (Reference 2). This limited ability to absorb impact energy can give rise to cracking or even shattering. Also, because of beryllium's low coefficient of thermal expansion, it is unlikely that it would be compatible with the aluminum parts of the frame since aluminum possesses a much different coefficient of thermal expansion. Aluminum's ductility, as well as its strength, presents itself as being the primary material for the frame and outer membrane structure.

1.3.7 WELDING STRESSES

Although aluminum is a popular structural material, one of its main weaknesses is the formation of stresses due to welding. The welding of aluminum members will be found mostly in the frame construction where the strength of these welds will be pertinent to loading specifications. Most of the structural aluminum alloys attain their strength by heat treatment or strain hardening. Welding causes local annealing which produces a zone of lower strength along both sides of the weld bead (Reference 5); therefore, allowable stresses for welded members will need to be determined so that the appropriate welds can be used to alleviate these stresses as much as possible.

1.4 CONCLUSION

The CAD analysis was a useful tool in determining if the vehicle could resist failure under loads of large amounts. Fortunately, all deflections were recorded under a millimeter, thus proving that the frame would be durable in the lunar environment. If more time had been allowed, the next step would involve a finite element analysis using NASTRAN/PATRAN for the plates attached to the frame itself.

The types of materials considered for the frame construction of the LCUV were limited to aluminum, beryllium, titanium, magnesium, steel, and their alloys. These materials were compared on the basis of their characteristics when exposed to the effects of temperature, radiation, and vacuum. By studying these effects, it was noted that aluminum seemed to be the least prone to these conditions. Aluminum also possesses the quality of being light weight yet very strong. Therefore, by using aluminum, the LCUV will attain maximum strength at minimum weight at a price that is economically reasonable.

The following is a summary of the analysis that led to the choice of aluminum for construction of the LCUV. Aluminum was chosen from a potential group of high strength materials that included magnesium, titanium, beryllium, and steel (principally stainless). The disadvantages of the use of these materials and the advantages of aluminum are listed as follows:

- Titanium - although titanium possesses the quality of being lightweight and very strong, its price is economically impractical.

- Magnesium - suffers appreciable evaporative losses when exposed in a vacuum. The need for a protective coating that will prevent sublimation might cause pre-flight storage problems. For example, the coating might require the frame to be stored in a temperature controlled, dust-free chamber or sterile environment.

- Beryllium - commercially, beryllium is brittle and is potentially more vulnerable to particle damage and cracking due to vibrations and its inability to absorb impact energy.

- Steel - although steel is strong, it is too heavy to be used for space-bound structures.

- Aluminum - its light weight and high strength is an attractive combination for use as a space-bound structure. Aluminum does not suffer appreciable evaporative losses and is an effective deterrent of harmful gamma rays. Aluminum will not be effected by the temperature differences on the lunar surface and is very practical and economical.

The properties of an aluminum alloy chosen for the LCUV have been listed in Table 1.1. These properties are subject to change as design of the LCUV continues. Our objective at this point is to establish a set of data from which our modeling procedure can expand. Hence, we have used these properties as a basis for our calculations.

Density	2.699
Melting Point	660.2
Specific Heat	
0 °C	0.2709
100 °C	0.225
300 °C	0.248
Coefficient of Thermal Expansion	
20-100 °C	23.8
200 °C	24.7
400 °C	26.7
Modulus of Elasticity	71.0
Modulus of Rigidity	26.2
Poisson's Ratio	0.334

Table 1.1 (References 3,6)
Properties of Aluminum Alloy

2.0 LOCOMOTION SYSTEM

The following section is a detailed analysis of the locomotion options available for the Lunar Utility Vehicle. Lunar soil mechanics, bearing areas and gross tractive efforts will be discussed extensively. Locomotion systems will be evaluated on effectively meeting the presented design consideration and constraints.

2.1 ASSUMPTIONS AND DESIGN CONSTRAINTS

The list provided below presents the design assumptions and design constraints used in the locomotion system analysis.

- The maximum dimensions that may be used for a propulsion system are (Reference 10):

  Length=3.4 meters
  Width=1 meter
  Height=1 meter

- Initial mass of the LCUV will not exceed 7500 kg.
- Maximum mass of the LCUV, after further integration of systems on the moon is 15,000kg.
- The locomotion system must enable the LCUV to tow the weight of another LCUV.
- The acceleration due to gravity on the surface of the moon is 1/6 that of the Earth's.
- The chosen system must be uncomplicated in its approach and require minimum maintenance.

2.2 INTRODUCTION

The basic forces, design considerations and problems of track construction for vehicles on earth will be similar to those on the moon. A vehicle of adequate power moves across the ground only if the strength of the ground is sufficient to support its weight without much resistance to motion, and provide the thrust of the ground involved in locomotion. The vertical and horizontal reaction forces to this motion are known as "flotation" and "traction". In evaluation of the reaction forces and the vehicle's overall motion characteristics, the soil properties and soil mechanics play a major factor just as they do on the earth.

Soil and surface conditions will govern the amount of sinkage and slip of a vehicle. Sinkage is defined as the amount of deformation of soil due to the vehicle's weight. Slip is a condition that occurs when the vehicle has no traction and produces no shear force on the soil. When there is little or no shear force on the soil, there is no locomotion.

One of the main reasons for applying a track to a vehicle is to provide a bearing area which would support heavy loads in soft ground (such as lunar soil). Thus the assessment of bearing capacity of tracks becomes an important part of vehicle performance and design. Two specific soil values pertaining to its strength ("c" - the soil cohesion constant and "ϕ" - the angle of internal soil friction) play a major role in bearing capacity.

The gross tractive effort is defined as the force of propulsion in the horizontal direction caused by shearing strength of soil. This force is a combination of the ground contact area and the gross vehicle weight. The gross tractive effort will not only determine the vehicle's performance but also the vehicle's towing capabilities. Soil mechanics also play a key role on the vehicle's tractive effort.

2.3 SYSTEM CANDIDATES

The following list of candidates for surface locomotion systems were considered as possibilities: wheel, jointed legs, and track. The requirements placed on the LCUV in terms of efficiency in performance of assigned tasks and load mobility conditions will be the main design criteria.

The requirements of the locomotion system being mechanically simple immediately eliminates the jointed leg candidate. Jointed leg locomotion systems have been shown to be extremely complex in nature (Reference 10). Wheeled and track locomotion systems, the primary types of rolling locomotion used on Earth, present the most favorable candidates in terms of being mechanically simple systems. A comparison of these two systems in regards to the design considerations and/or constraints will now follow.

Previous lunar vehicles have utilized the wheeled option with great success (Reference 8). Wheels are extremely reliable and mechanically efficient. The wheeled system can employ a variety of wheel types (such as pneumatic,solid,etc) and wheel sizes; however, wheeled systems possess a limited surface contact area (Reference 10). Surface contact area is key in both the maintenance of traction under loaded conditions and navigation of rough terrain.

Track locomotion systems are well suited for use on the lunar surface. As seen below in Figure 2.1, track systems have a much better distribution (foot print) than that of wheels. To achieve the same surface area in contact, a wheeled system would have to utilize wheels much greater in size and weight as compared to the need track size.

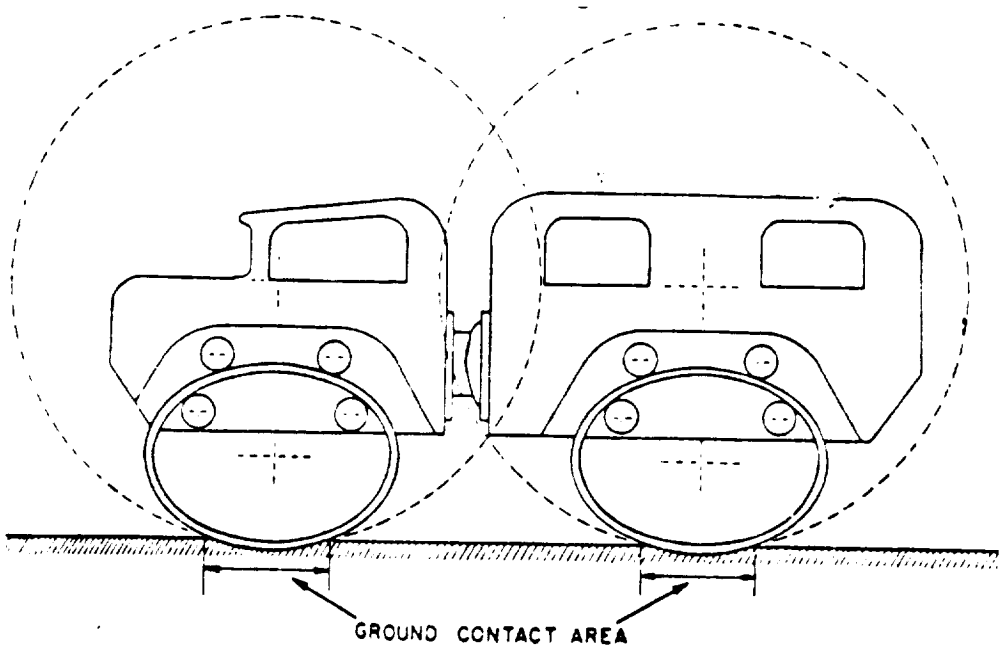

Figure 2.1 (Reference 10)
Track Contact Area

The problem of traction on the moon is amplified by its decreased gravity. Traction, as explained earlier, is caused by normal forces which are transferred to the locomotion system. Therefore to acquire equivalent traction on the lunar surface, a much larger contact area is required.

In terms of mechanical complexity, tracked systems are more complicated than wheeled systems. Track systems are also less efficient than their wheeled counterparts. However, the tracked locomotion system is the best choice for a locomotion system due to its impressive traction abilities.

	Mechanical Simplicity	Large "Footprint"	Traction in Rough Terrain	Total
Tracked System	-	+	+	+
Wheeled System	+	-	-	-
Legged System	-	-	-	-

Table 2.1
Locomotion System Decision Matrix

2.4 LUNAR SURFACE CONDITIONS

Lunar surface conditions are not as diverse as those found on earth. However, there are still great variations of conditions that must be analyzed to fully consider all aspects of the lunar surface. One such condition may be roughly explained by the existence of cohesive forces which bind soils together in numerous complex physical phenomena. These forces may be compared to the sticking power of glue which holds the soil particles together. This stickiness is known as the coefficient of soil cohesion "c" and is expressed in psi or kN/m^2.

Soils that are loose such as sand or cold "powder" snow are not necessarily held together by any kind of cohesive force. They contain loose particles that are able to move against each other. As a result, these soils create a frictional force against objects moving through them. This frictional force of soil is measured in degrees and is known as the angle of friction "ϕ".

Most soils encountered are neither purely frictional nor purely plastic, they are a combination of the two. Thus is the case with lunar soils. Average samples taken from the Apollo Missions indicate the following lunar soil properties:

	COHESION (kN/m2) "c"	ANGLE OF INTERNAL FRICTION "ϕ" DEGREES
WEAK SOIL	0.36	35 DEGREES
FIRM SOIL	1.42	45 DEGREES

TABLE 2.2 LUNAR SOIL DATA[1]

2.5 BEARING CAPACITY

One of the main reasons for applying a track to a vehicle is to provide a bearing area which would support heavy loads in soft soils. The study of the bearing capacity of tracks thus becomes an important design consideration in our Lunar Utility Vehicle.

Originally, the criterion used to measure the bearing capacity was the idea of the "mean ground pressure". Mean ground pressure is defined by the ratio of W/4sl where W = gross weight, s = length of track in contact with soil and l = the track width. This idea has been proven to have little relation to the real distribution for it takes in no account of soil properties or mechanics (Reference 8).

[1]Adapted from McAdams, Reese and Lewandowski, reference #1.

An exact analytical method to this problem would have to take into consideration all the elements involved, such as, pressure distribution, soil mechanical properties and tread form/dimensions.

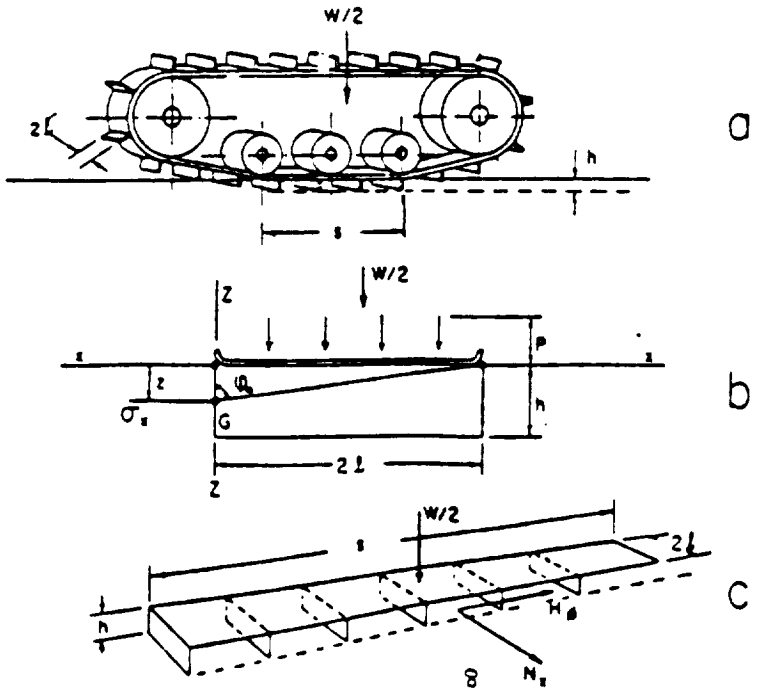

Figure 2.2 (Reference 7)
Mean Ground Pressure

The correct equation for the bearing load is a function of the soil properties and the gross contact area. These soil properties are "c" and "ϕ" as mentioned earlier in this report. Equations adopted for this purpose may be written in the following form:

$$Ws = A\ (cNc+v2Nq+1/2vbNv)\quad \text{Equation \#1}$$

where Nc, Nq, and Nv are constants depending on ϕ, b the width, A the surface area of contact, v is specific gravity and q the surcharge (initial sinkage). In the worst case of lunar soil (weak soil) we have the following values: Nc=55, Nq=35, Nv=25, c=0.36 kn/m^2, ϕ=35 degrees, and v=1.55 g/cm^3. It have been shown by Bekker (Reference 9) that if there is no initial sinkage (surcharge) the above equation in our case results as follows:

$$Ws = A\ (c\cdot Nc+1/2v\cdot b\cdot Nv)\quad \text{Equation \#2}$$

$$Ws=(2)(1)w\ ((0.36kN/m^2)(55)+1/2(1.55g/cm^3)(1kg/1000g)$$

$$(100cm/m)^3(25)b)$$

Using two tracks and given b=0.6m, h=1m,l=3.4m from the specifications of reference 10,

$$Ws = 6m^2(19.8kN/m^2+19.375kN/m^2)$$

$$Ws = 30,500N$$

In terms of mass, Wm = 18,700kg from the above equation. The specifications for mass of the Lunar Utility Vehicle has been given by reference 10 as Wm = 7500kg. The above equation for the mass of the vehicle neglected the difference between the moon's gravitational field and the earth's. It is clear that the safe mass Wm is well above the specified mass of 7500kg (References 8,9).

This equation neglects the difference between the moon's and the earth's gravitational field. In terms of safe mass Wm, the above equation yields Wm = 18,700kg. This is the maximum safe mass which would keep the load area A on the ground surface. It is clear that the bearing area of the given track specifications (W=0.6m, l=3.4m) secures a safe load area. The safe mass Wm given at 7500kg is well below the calculated safe mass (18,700 kg) for the given load area in equations #1 and #2.

2.6 TRACTIVE EFFORT

The gross tractive effort or soil thrust is caused by the shearing strength of the soil producing a force "H" on the tracks. The tractive effort is developed in the soil for the purpose of propelling a vehicle. The physical description and meaning of this may be illustrated in the following way.

The spud or cleat of a track is loaded with a vertical force "w" identified with the weight of the vehicle. The area between the spuds becomes packed with soil within the ground contact area A. When the vehicle develops a maximum tractive effort, shearing of soil occurs along this area. The force required to shear such an area is proportional to the size of the surface area and the soil coefficient of cohesion "c".

Because soil is normally a combination of both the purely plastic and purely frictional soil, as shown in Figure 2.3, a combination of those two soil properties must be included in our analysis of tractive effort. By adding these two characteristics and their effect on tractive effort we have the following:

Purely frictional case $H=W \tan \phi$	Equation #3
Purely cohesive case $H=Ac$	Equation #4

Combining the two the final equation is:

$H=Ac+W \tan \phi$	Equation #5

This equation expresses the fundamental relationship between the soil thrust (gross tractive effort "H") of the vehicle, the ground

contact area "A", the weight W, and the soil constants "c" and "ϕ". (References 8,9)

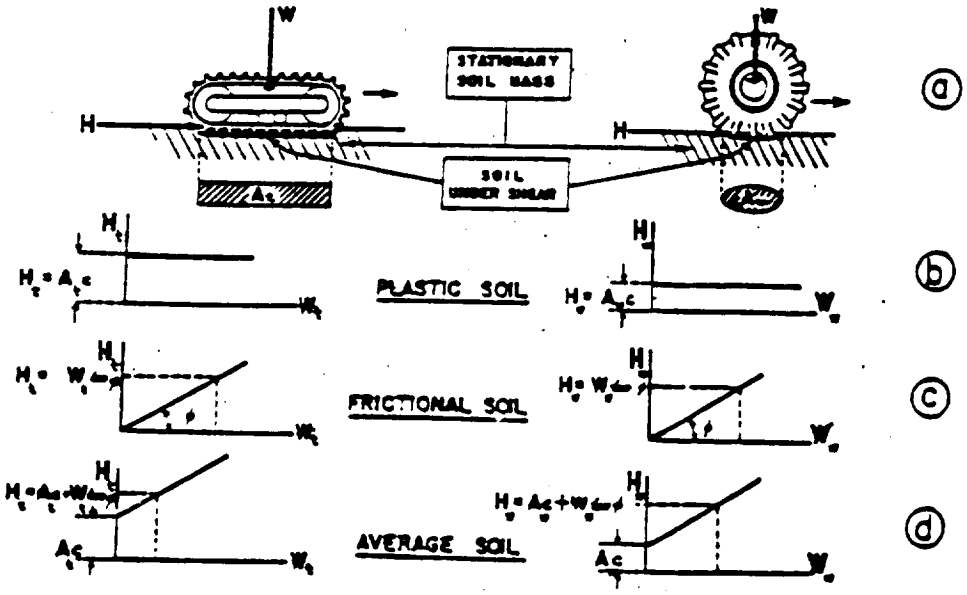

Figure 2.3 (Reference 9)
Soil Characteristics

There are two predominant factors in securing large tractive efforts: track load and track size. The more frictional the soil, the more dominant the load factor. The effect of track size greatly increases with increasing ground cohesion. Since lunar soil, like most, is a combination of both frictional and cohesive particles, the design concept for the LCUV's track load and track size must take into account both of these characteristics.

To determine the tractive effort of our Lunar Utility Vehicle we have the following from equations 3 and 4:

$$H=Ac+W \tan \phi$$

The worst case situation of lunar soil (weak soil) is given by:

$$c=0.36kN/m^2 \text{ and } \phi=35 \text{ degrees}$$

The specified area of tread contact is $A=21m^2$, $b=1.44m$ and the weight $W=30,500N$. We therefore have the following:[2]

$$H=(6m^2)(0.36kN/m^2)+(12,262.5N)(\tan 35 \text{ degrees})$$

and

[2]Equations by Bekker, references 8 and 9.

$$H=43,800N$$

The Lunar Utility Vehicle is also fully capable of favorable tractive effort in firm lunar soils. This can be shown by the following equation:

$$H=Ac+W \tan \phi$$

where $\phi=45$ degrees and $c=1.42kN/m^2$. In this case the tractive effort H=60,782.5N.

As mentioned earlier, the main tractive effort developed either by cohesive or frictional forces is related to the shear area beneath the tracks. However, it can be easily seen that there are other areas of shear (Figure 2.4). This additional shearing force is produced by the spuds of the track and must be considered for better accuracy. Equation #5 is modified in the following way:

$$H=Ac+W \tan \phi + H' \quad \text{(Reference 9)}$$

where H' is the additional shearing force produced by the spuds.

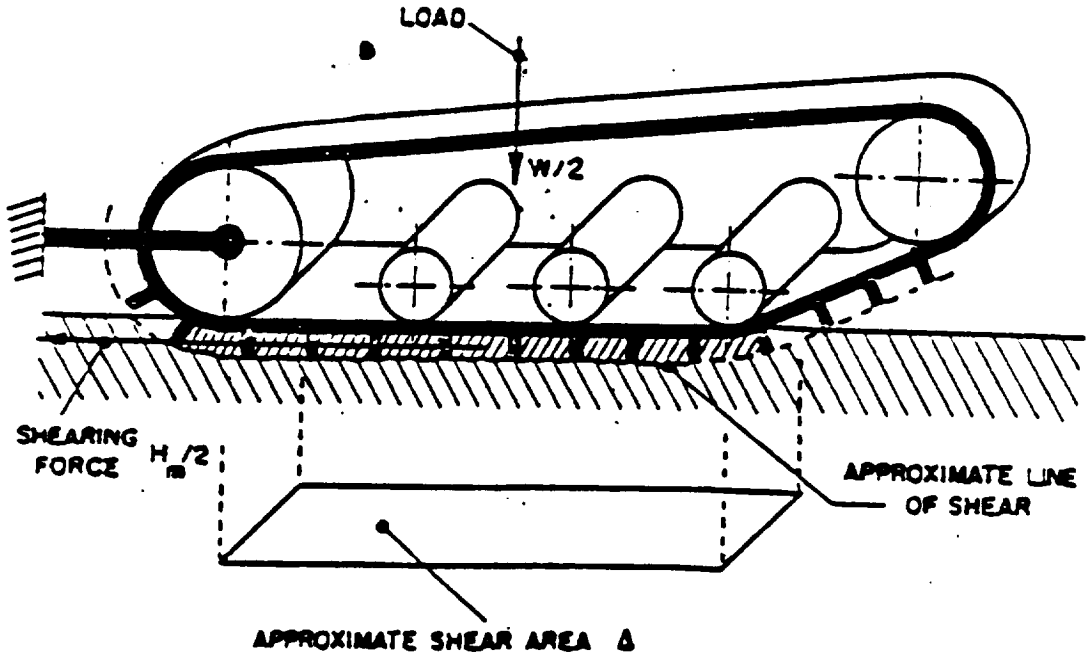

Figure 2.4 (Reference 9)
Track Shear Area

Thus by the use of spuds, the actual area of track contact in equations #3 and #4 can be increased without actually changing the tracks dimensions. This in turn will increase the gross tractive effort. Further weight and draw bar pull specifications must be provided before design of the spuds.

Figure 2.5 displays the effect of spuds in frictional and plastic soils expressed in terms of percentage of soil thrust increase ($H=Ac+W \tan\phi$).

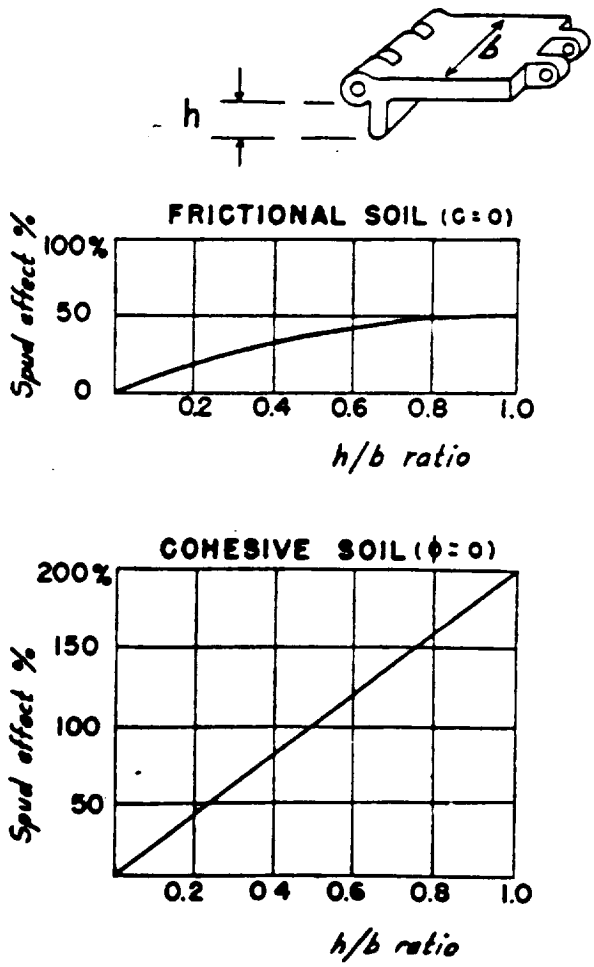

Figure 2.5 (Reference 7)
Spud Efficiency

2.7 DRAW BAR PULL

In evaluation of vehicle mobility, a quantity known as the "traction coefficient" plays a key role. Traction coefficient, known better as draw bar pull, is the amount of horizontal force (after resistance) that a vehicle can produce to tow another vehicle. Draw bar pull may be given from the following equation:

$$DP=H-R$$

where R is the resistance to motion (Reference 9).

The resistance to motion "R" is given by the following relation:

$$R = 1/[(n+1)(Kc+bKo)^{1/n}] \cdot (wg/L)^{n+1/n} \qquad \text{(Reference 7)}$$

where "L" is track length, "wg" is weight and "Kc", "Ko" and n are soil constants (Reference 7). For the lunar surface we have the following properties:

$$Ko=0.346kg/m$$

$$Kc=0.009N/m^2$$

$$n=1$$

The equations above yield R=3280N. Under the given specifications of reference 10, we have (in the worst case) the following:

$$DP=(42,882N)-(3,2820N)$$
$$DP=40,500N$$

These results are for our loaded condition where the mass of the LCUV is rated at 18,700kg. As explained earlier this is a factor of safety designed to enable us to increase the load of the LCUV from the guidelines of 7,500kg (Reference 10). Use of the above draw bar and resistance equations on the given mass of 7,500kg yields the following results:

$$R=530N$$
$$DP=(18,200N)-(530N)$$
$$DP=17,700N$$

This solution has taken into consideration the difference between the moon's and the earth's gravitational pull. However, it is clear that the draw bar pull in the worst case situation is still substantial as compared to earth tractors. Our computational results indicate that the tracked option of locomotion will more than provide the necessary brute force to accomplish the LCUV's mission.

2.8 MATERIALS

Materials play an important role in space technologies. The same is also true, possibly more so, for the Lunar Construction Utility Vehicle. Materials used for the LCUV must possess high strength. In our attempt to design materials for specific uses on the LCUV, we have used materials that are being manufactured and used today. This is an attempt to limit the amount of actual material science engineering that would have to be conducted in designing and testing "new" materials.

There are several environmental conditions to consider when investigating materials for use in space. These significant natural and induced environments to which space materials are subjected are as follows:

- Galactic Radiation
- Solar Ultraviolet Radiation
- Vacuum Effects
- Extreme Temperature Gradients

The first two of these environmental hazards are closely related. Materials selected for use on the LCUV must not only help shield radiation sensitive items, but they must also not experience ill effects from radiation. Both the ultraviolet and the soft x-ray component of the solar spectrum possesses sufficient quantum energy to induce rupture of many chemical bonds and thus initiate chemical reactions (Reference 13).

The predominant types of chemical reactions taking place due to irradiation are cross linking and chain scission (Reference 13). Both of these processes are induced by free radical formation and interaction resulting in structural changes within or between adjacent chains. The effect of ultraviolet radiation on structural metals is negligible except for a small static charge that is produced by the slight removal of electrons. The effects of actual molecular breakdown are predominantly seen in polymeric materials.

Infrared and visible radiation does not possess sufficient energy to break down molecular bonds or cause ordinary reactions. The main effect of infrared radiation is an increase in thermal agitation experienced by the material. Even polymeric materials experience minor effects from these types of radiation. The effects of visible radiation are basically negligible for all materials and are similar to those effects of thermal radiation. Compared to the thermal range, effects are somewhat less drastic and basically non-existent when compared to the possible effects in the ultraviolet range (Reference 13).

The behavior of materials in vacuum (or lunar environment) is marked by two major effects. First, evaporation of the materials or of a volatile component of the material is greatly enhanced by the total lack of atmosphere. Secondly, the layer of absorbed gases on the surfaces of many materials may be partially or entirely removed (Reference 13).

In the case of structural metals, the evaporation of material will pose little threat unless alkali metals are used. In the case of plastics, those that contain a plasticizer of high vapor pressure (cure), the loss of this constituent in the material may cause significant property changes. Plastics formed entirely from the polymerization of materials have lower vapor pressures and should be considered for space applications.

The removal of conventional lubrication materials and of the layer of absorbed gas which may act as a lubricant causes a great increase in friction. This condition may cause severe material

destruction of sliding surfaces unless special precautions are followed. It may be noted that on metals, however, removal of the absorbed layer of vapor gases on most metal surfaces has a beneficial effect in inhibiting crack formations and thus increase fatigue resistance (References 12,13).

The temperature extremes on the lunar surface present a unique variety of problems for materials. Surface temperatures can range from 120K to 374K (Reference 10). The changes from the high temperatures to the low temperatures will induce cyclical thermal stresses. Results of this temperature cycling can result in failure due to thermal induced fatigue stresses.

Temperature can produce important effects when materials of widely different coefficients of thermal expansion are in contact or joined. This can be a potential source of high thermal stresses when dealing with different thermally expanding materials. However, careful material engineering design can easily minimize this problem.

Thermal conductivity and resistance must also be addressed. Materials intended to shield various parts of the vehicle from extreme thermal gradients must possess excellent thermal resistance properties. Materials used in thermal control of the LCUV must possess excellent thermal conductivity properties.

2.8.1 ELASTIC LOOP

The track elastic loop must be made of a material that possesses high durability in elastic, thermal, stress and fatigue areas. Titanium has been recommended previously for the elastic loop material (Reference 11) . Titanium was selected because of its high strength, durability and excellent thermal properties. Specifically, the Titanium alloy (Ti-5, Al-2 Sn Alpha structure), has been recommended due to its ability to be forged into thin sheet metal parts.

One of the main considerations in choice of a loop material was material weight/strength ratio. Titanium is a relatively light metal with extremely high strength. As compared to other commonly used space metals such as aluminum alloys and nickel alloys, the titanium alloy chosen has a higher ductility and lighter weight (Reference 12). Titanium also has larger values of tensile and yield strengths than most commonly used space metals.

ALLOY	TENSILE STRENGTH	YIELD STRENGTH	ELONGATION
1000 Series Al	124 MPa	97 MPa	25%
2000 Series Al	442 MPa	345 MPa	5%
AZ31B Mn	248 MPa	159 MPa	7%
Nickel 200 Series	483 MPa	152 MPa	18%
Titanium (Ti-5,Al-2 Sn)	862 MPa	807 MPa	26%

Note: All quantities are average values

Table 2.3 (Reference 12)
Commonly Used Space Metals Vs. Titanium

Another positive aspect of using Titanium at the material for the elastic loop material is that it has been approved for flight use by the George C, Marshall Space Flight Center (Reference 11). This approval means that the material has met design criteria set forth by NASA and is deemed "safe" for use in space.

Metals present no radiation damage problems except at extremely high doses such as those experienced from the "back wash" from reactor fluxes. At such doses, some embrittlement takes place. This results in increased hardness and a decrease in creep rate. Fatigue properties are among the least to be affected. Because the elastic loop will not serve as a radiation shield, titanium is a perfectly acceptable choice as a material.
All materials might expect to suffer damage to surface properties form solar flares, however, none should show damage through $1mg/cm^2$ (Reference 13).

As explained earlier, loss of material by direct evaporation in vacuum is a major design concern. However, loss of material by direct evaporation in the low pressure environment of space is insignificant for Ti and its alloys (Reference 13). The following graph shows the sublimation or evaporation rates of some metals in vacuum at various temperatures.

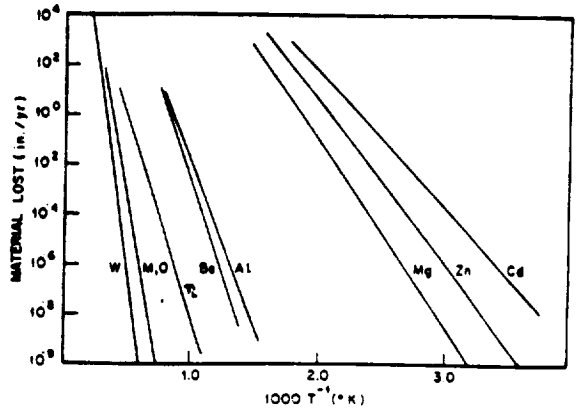

Figure 2.6 (Reference 13)
Effects of Sublimation on Space Materials

Loss of 0.1cm/yr of material has been shown to be a significant loss and thus is used as a design criteria (Reference 13). Referencing this value from Figure 2.6, the temperature at which titanium will lose 0.1cm/yr in vacuum is approximately 1250°C (973.5 K). Temperatures on the lunar surface will only reach an extreme of 100°C (373.15K). Titanium will provide an excellent material to combat the sublimation problem for the elastic loop.

The main disadvantage of the use of titanium is the cost. Titanium is a very expensive metal. Titanium is usually purchased in 25,000 lb lots at a price of $4.00/lb (price from 1985 Reference 12).

Although titanium is an expensive metal, its thermal, vacuum and radiation resistance coupled with outstanding mechanical properties make it an excellent choice for the elastic loop material.

Titanium

Advantages	Disadvantages
- Excellent thermal resistance	High cost
- Light weight	
- Excellent Mechanical properties	
- Approved for use by NASA	
- Suffers no ill effects from normal radiation	

2.8.2 GROUSERS

The grousers (cleats) on the track should be a material that can not only withstand extreme thermal and abrasive soil conditions, but also to some extent perform the cushioning function of tires. This brings into consideration the use of elastomers due to their excellent elastic properties.

In recent years the best features of certain elastomers and plastics have been combined in composites. This has lead to a new generation of tougher elastomers/plastics able to withstand the extreme conditions lunar applications. This class of elastomers is known as synthetic rubbers.

The main danger radiation presents to elastomers is changing or crosslinking of chemical bonds within the material. Although all rubber is radiation sensitive, polyurethane rubbers are ranked among the most radiation resistant as seen in table below:

Material	Radiation Stability Maximum Dosage(a) (rad)
ELASTOMERS	
Viton A	1×10^8 in diester oil at 400° F
HF4 (Poly FBA)	5×10^7 in diester oil at 400° F
Kel-F Elastomer	1×10^8
Neoprene Sealants	10^7
Nitrile (Buna-N) Sealants	10^8
Silicones	1.34×10^7
SE 551	
SE 175	8.3×10^7
Silastic 160	2×10^9 as vacuum seal
Silastic 50-24-450	1×10^7 as gasket in contact with oil at 450° F
Precision Rubber 122-70	2×10^9 as vacuum seal
Precision Rubber 151-70	1.9×10^9 as vacuum seal
LS-55	5×10^6
RTV Sealants	10^7
Polysulfide Sealants	3.5×10^7 in JP-4 fuel
PLASTICS	
Teflon	2.7×10^6
Kel-F	2×10^7

Table 2.4 (Reference 13)
Radiation Resistance of Elastomers

From the table it is clear that the most radiation resistant elastomer is silicone elastomer Silastic 160. The ultraviolet stability of the most common general purpose elastomers is listed as follows (Reference 13):

1) Silicones
2) Butyls
3) Neoprenes
4) Polysulfides
5) Natural Rubbers

Crosslinking is the predominant mechanism in the case of natural rubber, neoprones and polysulfides. It is again clear that

rubbers are highly sensitive to this form of radiation. However the resistance is still low enough to warrant damage from extreme radiation fluxes (Reference 13). Two options to prevent damage to the elastomer will now be presented.

First, a fender-shield of aluminum will be employed on the LCUV to protect the track and its components (see section 2.14). Additionally, in the case of the elastomer grousers, anti-rads may be added to the materials. Anti-rads are organic chemical additives that inhibit radiation damage to the materials to which they are added. They function by preferentially absorbing the energy induced in the compounds and releasing it thermally.

High vacuum can produce volatilization of entrapped gasses in elastomers. The rate of evaporation of each component is a complicated function of vapor pressure at a given temperature, the surface to volume ratio and thickness of elastic mechanism in question (Reference 13). The combined effects of vacuum, temperature, and high energy penetrating radiation is to increase the rate of evaporation. Silicone rubbers have been rated as one of the least susceptible elastomers to the effects of radiation. In the figure below it is clear however, that the silicone grousers will have a decreased life due to sublimation. From the provided graph below it is clear that some formulations of silicone elastomers do not suffer significant weight loss even after 90 days exposure to vacuum.

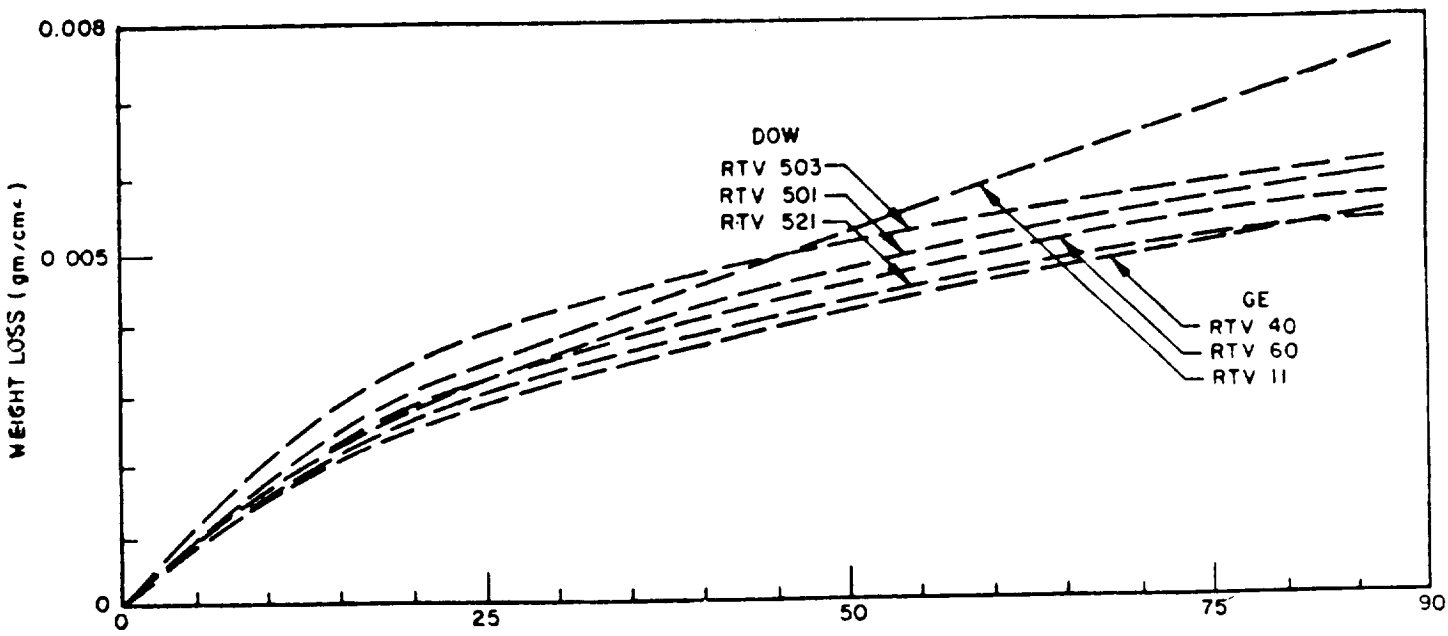

Figure 2.7 (Reference 13)
Weight Loss of Elastomers

Another severe environmental problem for elastomers is the extreme temperature gradient. Most elastomers lose their resilience at temperatures near -80°C. However, elastomers with a silicone base can operate below -100°C (Reference 13). Extremely high temperatures can cause elastomers to soften and thus allow creep. The following table provides the operating temperatures for some popular elastomers.

Elastomer	Tensile strength, ksi†	Elongation, %	Density, g/cm³	Recommended operating temp. °F	Recommended operating temp. °C
Natural rubber* (*cis*-polyisoprene)	2.5–3.5	750–850	0.93	−60 to 180	−50 to 82
SBR or Buna S* (butadiene-styrene)	0.2–3.5	400–600	0.94	−60 to 130	−50 to 82
Nitrile or Buna N* (butadiene-acrylonitrile)	0.5–0.9	450–700	1.0	−60 to 250	−50 to 120
Neoprene* (polychloroprene)	3.0–4.0	800–900	1.25	−40 to 240	−40 to 115
Silicone (polysiloxane)	0.6–1.3	100–500	1.1–1.6	−178 to 600	−115 to 315

* Pure gum vulcanizate properties. † 1000 psi = 6.89 MPa

Table 2.5 (Reference 12)
Material Properties of Elastomers

Silicone rubbers have excellent thermal, mechanical and vacuum properties; therefore silicone elastomers make an excellent choice for grouser material.

Silicone Elastomers

Advantages	Disadvantages
-Excellent thermal operation range -Excellent mechanical properties -Suffers only mild effects from vacuum	Radiation sensitive

More study and research is required to further isolate potential material design problems. It should be pointed out, however, that the materials used in the previous analysis have proven to be effective in earlier ELMS designs (Reference 11). Titanium was shown to be an excellent choice for the material to be used in constructing the elastic loop. The grouser (cleat) material had to possess elastic properties due to the nature of the application. Elastomers proved to be the best answer to this material problem. More specifically, Silicone Elastomers were chosen for the radiation and vacuum resistance.

2.9 TRACK MOBILITY SYSTEM

As presented earlier, tracks appear to be the best choice for a locomotion system for the LCUV. The next phase of this report deals with the actual track system chosen along with some of the other types of track systems considered and why they were not used.

The three types of track systems considered were as follows: "conventional" linked track with multiple idlers, pneumatic air cushioned track with space links, and an elastic loop track. The "conventional" linked track is much like those used on military vehicles and on earth moving vehicles. The conventional track itself has many individual links which are connected to the link before and after it by a pin (Reference 9). This track is supported by idler wheels which keep the track aligned and in constant contact with the ground. This system is very complex in that it has many moving parts since the individual links of the track are movable with relation to each other and it must have many idler wheels to keep the track rolling (Reference 9). The mechanical complexity of the "conventional" track along with its high weight due to the extra moving parts required for the idler wheels and connection pins excluded it from further consideration in the LCUV design.

The next type of track considered was a track which rested on a pneumatic cushion or bladder (Reference 10). This system did not have the many moving parts of the "conventional" system but was not really considered due to concerns with producing a puncture resistant bladder and preventing leaks of valuable air.

The third option,the elastic track, consists of a one piece belt which due to its own elasticity provides constant ground pressure thus eliminating the requirement for idler wheels (Reference 11). An elastic track is relatively simple in design complexity and is light weight when compared to a "conventional" track. For these reasons it was chosen as the track to be

considered for the LCUV (This is shown in Table 2.6.)

Type		
Conventional	Constant Ground Pressure	complex heavy
Pneumatic Cushion	light weight	easily punctured possibly leak
Elastic loop	few moving parts easily replaced	high deflections

Table 2.6 Track System Types

Lockheed has done much work with an elastic loop made of a titanium alloy and their work was studied extensively for the elastic loop design of the LCUV (Reference 11). As in the Lockheed design, a titanium alloy loop was considered for the LCUV.According to Bekker's maximum bearing load equation:

$$W=A(c\cdot Nc+q\cdot v\cdot Nq+0.5v\cdot b\cdot Nv) \quad \text{(Reference 9)}$$

it was determined that a track size of approximately 3.4 meters long by 0.6 meters wide would provide sufficient track area to support the design vehicle weight of 7500 kilograms times a factor of two (Reference 9). This track size was determined first by assuming that track length would be fixed at 3.4 meters and then varying the track width to find the track area which would support the desired bearing load based upon allowable mass and acceleration due to gravity. Various track widths and their resulting bearing loads are shown in Table 2.7.

Width (meters)	Length (meters)	Contact Area (meters squared)	Bearing Load (Newtons)
0.6	3.4	1.44	30500
0.8	3.4	1.92	59800

Table 2.7 Track widths and Bearing loads

Once this track width and length were determined the tractive effort, resistance to motion, and drawbar pull for the track could be determined using the equations discussed in the introduction to surface mobility section of this report. These results are shown in Table 2.8 and are based on a vehicle mass of 15000 kilograms;

a track length of 3.4 meters (2.4 meters effective length), and a width of 0.6 meters.

Width (m)	Length (m)	Tractive effort (N)	Resistance (N)	Drawbar pull (N)
0.6	3.4	35400	2110	33300

Table 2.8 Tractive effort, Resistance, and Drawbar pull

A general schematic diagram of the elastic track system is shown in Figure 2.8.

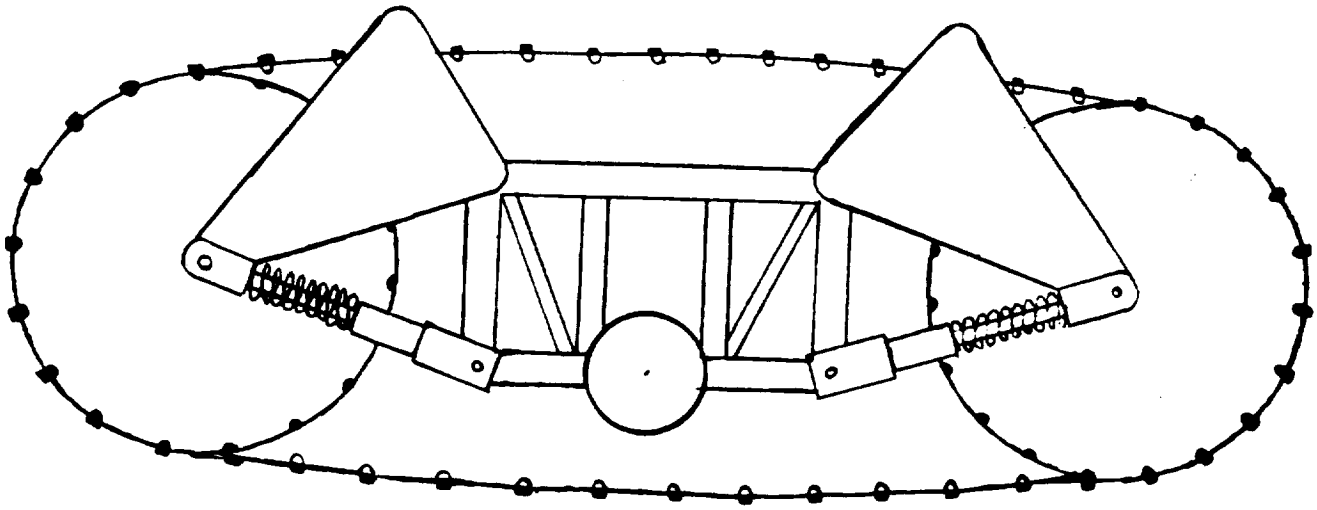

Figure 2.8 Schematic of Elastic track System (Reference 11)

2.10 INTERNAL TRACK FRAME

The internal frame of the track system is the structure on which all other components of the track are supported and is also the point at which the track is connected to the suspension and thus the main frame of the LCUV. A simple truss made of steel rectangular tubing was considered as the frame (Figure 2.8). The tube dimensions were chosen as 8.9 centimeters by 3.8 centimeters and 32 millimeters thick. The frame was chosen to have a length of 1 meter, a width of 0.6 meters, and a height of 0.6 meters. A finite element analysis was done on this frame and it was found to be more than adequately designed. As a part of this frame is the idler wheel which serves as a safety backup in case the track were to over deflect and try to over-extend in the vertical direction. This backup idler wheel would have a diameter of 0.4 meters and a thickness of 7 millimeters and would be made of steel. This wheel would come into action only if the track were to deflect approximately 8 centimeters in the middle of its horizontal span. This deflection was given as an estimate for the track deflection by Hobson Shirley of Lockheed who managed Lockheed's elastic track based Lunar vehicle (Reference 11)

2.11 SUSPENSION OF THE DRIVE DRUM

The problem of suspending the drive drum from the internal frame of the LCUV will be addressed in this section. Included in this discussion of suspension will be sections dealing with the damping of shocks and vibrations due to the rough Lunar surface.

Originally the idea of "hard mounting" the drive drum to the main frame of the LCUV was considered since this was the typical approach taken by terrestrial earth moving equipment (Reference 9). But this type of mounting allows for no shock or vibration absorption except through the deflection of the frame members through compression and tension. Since the LCUV would carry electronic equipment and would not be in a readily reparable environment it was deemed that a hard mounted system would not suffice. Still, a light weight , mechanically simple suspension is desired which will incorporate damping and structural support. The system considered to solve this problem is basically a damped -pivoted three bar mechanism. The damped pivoted system to be used in this system is shown in the schematic of the track system. The damping will be accomplished by a strut member which includes a dashpot and spring.This strut will very closely resemble a MacPherson strut which is common in automobile suspension today (Reference 15). Several different types of damping (the dashpot's function) were considered . These different types include hydraulic,pneumatic and frictional damping. The pro's and con's of each type of damping median is shown in Table 2.9.

TYPE	PRO	CON
Pneumatic	* lightweight * no need to cool	* leakage
Hydraulic	* commonly used * easy to design	* high weight * need excess fluid
Frictional	* simple construction	* wear of surfaces * needs to be cooled

Table 2.9 Damper Comparison

The first type of damping median to be eliminated was the system based upon pneumatic valving. This decision was based almost exclusively upon the fact that pneumatic systems invariably leak (Reference 9). In the Lunar environment where air is a precious commodity which can not be wasted, it was deemed that any losses due to leakage were unacceptable.

The second type of damping system originally considered was a hydraulic shock. The major concerns with the hydraulic system were finding a fluid which would operate in the wide range of

temperatures that the LCUV would be exposed to and the higher mass that the fluid would add to the total, limited mass of the vehicle. No suitable hydraulic fluid was found although it was briefly considered that the fluid used in the coolant system might be utilized as both a coolant and hydraulic fluid. This idea was abandoned when Freon was considered as the coolant fluid, since Freon is not a suitable hydraulic fluid due to its thermodynamic states during the cooling process. Failure to find a suitable fluid was the demise of the hydraulic shock concept.

A frictional damper was chosen as the shock and vibration absorber. It poses no serious problems as the air and hydraulic shocks do. Items of concern with the frictional shock include heat dissipation and wear over time. The problem of heat dissipation was solved when it was decided to incorporate a cooling system in the LCUV. Coolant lines could be run near or over the struts to keep them cool during extended use periods when excessive heating could occur. The problem of wear of the frictional surfaces of the damper is not readily solved. Wear could be reduced by using a lubricant but this would defeat the purpose of the frictional damper. Periodic replacement of the damper will probably be the only answer to the problem of wear. The surfaces in contact within the strut where friction would occur are to be metallic. For ease of construction and to prevent problems which may arise if different materials with different thermal expansions were used, both frictional surfaces will be made of the same material. The following Table 2.10 shows different materials in contact with themselves and their coefficients of static and moving friction.

Materials and Coefficients of Friction		
Material	Static coefficient	Kinetic coefficient
Mild steel	0.74	0.57
Hard steel	0.78	0.42
Nickel	1.10	0.53
Aluminum	1.05	1.40

Table 2.10 (Reference 16)
Friction Coefficients of Materials

A coil spring in conjunction with the strut would be necessary to return the strut back to its original uncompressed length after damping has occurred and also to maintain an equilibrium position of the strut. The coil spring in a typical automobile MacPherson strut application surrounds the central strut (Reference 15). For the LCUV application it would be desirable for the spring to be located within the strut cylinder in order to help protect it from the harsh, Lunar environment but this proved to be unfeasible due to the large outside diameter of the coil spring. Schematics of a typical MacPherson strut and the LCUV variation are shown in Figure 2.9.

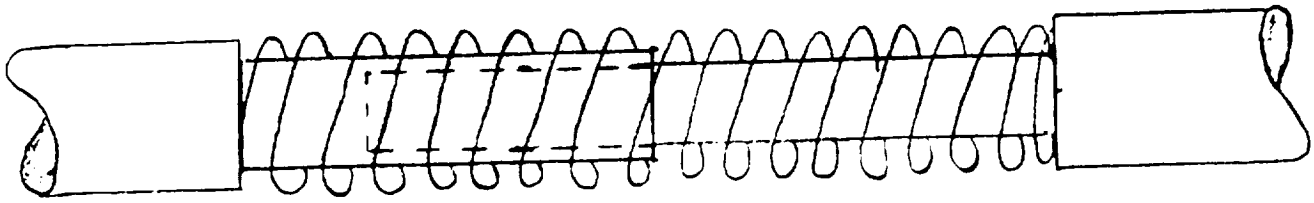

Figure 2.9. MacPherson Strut and LCUV Variation

In order to design the strut assembly it was required to perform a conservation of energy analysis to find the spring coefficient required and the radial force of the fit between the two cylinders of the strut. The energy for the system was found by equating the energy lost due to friction and the potential energy of the compressed spring with the total kinetic energy of the vehicle mass:

$$KE=0.5k\cdot x^2-u\cdot Fx$$

The maximum allowable deflection was determined from the geometry of the LCUV itself in the locations where the struts were to be applied. With the strut installed between the drive drum and the internal track frame, it was decided that a drive drum deflection of 10 centimeters would be the maximum allowable so that the track would not come off the drive drum assembly. This allowable deflection of the track was an engineering guess made with the assistance of Hobson Shirley from Lockheed (Reference 11). From the track geometry it was found that this produces a deflection for the strut of 15 centimeters (shown in Figure 2.10).

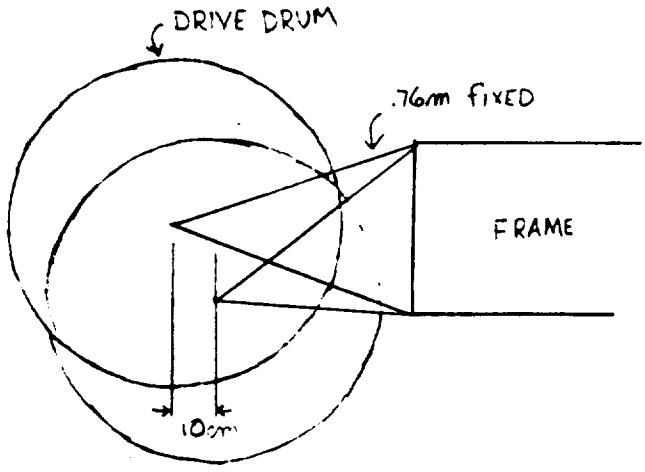

Figure 2.10 Deflection of Drive Drum and Strut

Assuming that a worst case shock to the drive drum would occur if the vehicle ran into a stationary object at full speed (0.6 meters per second) the energy that the shock would have to dissipate through friction and displacement changes would be due to the kinetic energy of the vehicle. The kinetic energy was found from the following equation:

$$KE = 0.5 \cdot m \cdot v^2$$

where the (m) is mass of the vehicle and (v) is the maximum velocity. The kinetic energy of the vehicle is 300 joules assuming a total mass of 15000 kilograms. The strut has to dissipate half this energy through the spring energy and the work lost to the frictional surfaces.In determining the work lost to friction a normal force had to be determined for the strut assembly. This force would be due to the radial force created by forcing the inner rod of the strut into the outer cylinder of the strut. The fit would have to be a tight fit in order to keep the surfaces of the cylinders in contact with each other. If this fit is considered as a press fit the radial pressure can be determined from the following equation:

$$p = E \cdot d \ [(c-b)(b-a)/(2b \cdot (c-a))] \quad \text{(Reference 6)}$$

where (E) is the Young's modulus of the material, (d) is the interference of the fit, (c) is the radius of the outside cylinder, (b) is the radius of the inner cylinder, and (a) is zero for this case. For mild steel ,a value of 207 GPa was used for Young's modulus, 1*10^-8 meters for the interference, (c) was 3 centimeters, and (b) was 2 centimeters (Reference 6). These values produced a radial pressure of 2900 Pa. This radial pressure was then assumed to produce normal forces to the cylinders which and could be determined by multiplying the average contact area between the two cylinders by the radial pressure. To find the average contact area it was assumed that the strut would change in length by 15 centimeters at full deflection which would cause the drive drum to move horizontally 10 centimeters. These values were determined by assuming that the drive drum would have a radius of 0.5 meters and would be a horizontal distance of 0.2 meters from the internal frame. The shock was also assumed to have an original nested length of 20 centimeters so that if the shock were to be extended out it would not pull apart. Using these distances the normal force to the cylinder was found to be 990 Newtons.

Using conservation of energy, and assuming that all the impact energy is dissipated through the spring and friction, the spring constant was found to be 19 100 N/m. Using this value of spring rate and using an outside diameter of 5 centimeters for the spring and going to load and spring rate tables
(Reference 16), the wire diameter of the coil spring was determined to be 7 mm. The number of active coils for the spring could be determined by using the following relation:

$$n=k/(L/f) \qquad \text{(Reference 16)}$$

where (L) is the applied load, (k) is the tabular spring rate, and (f) is the spring deflection. For the LCUV the load on the strut was found to be 2 kN and the deflection 0.15 meters. The tabular spring rate was found to be 26 500 N/m (Reference 16). Using these values the number of active coils was found to be 30. Next the free length of the spring could be determined using this relation:

$$l = (n+i)d+f \qquad \text{(Reference 16)}$$

where (d) is the wire diameter and (i) is the number of inactive coils. For this spring the number of inactive coils was set at two since a squared end spring was desired (Reference 6). The free length was found to be 0.42 meters. This spring fits into the allowable length of approximately 0.6 meters (determined by the geometry of the drive drum and frame positioning).

2.12 GROUSER DESIGN

As was discussed earlier in this report, grousers or spuds can be added to the bottom of a track to increase tractive effort and drawbar pull (Reference 9). Grousers only add additional tractive effort and drawbar pull up to a certain point before they start to decrease in their effectiveness by increasing the resistance (Reference 9). This point of dimensioning returns is related to the ratio of grouser height and track width and an experimental constant:

$$h = 0.2w \qquad \text{(Reference 9)}$$

where (h) is the grouser height and (w) is the track width. For the LCUV the track width was set at 0.6 meters, thus allowing a grouser height of 12 centimeters. This value was halved (arbitrarily) and a grouser height of 6 centimeters was used.

The optimum spacing of the grousers can also be determined:

$$s = 0.75w \qquad \text{(Reference 9)}$$

For the LCUV the optimum spacing distance would be 0.45 meters.

2.13 DRIVE DRUM AND PIVOT

The drive drum for the elastic track system houses a D.C. motor which turns the drum via a planetary gear arrangement (discussed in power and motor section). The drive drum is essentially a large spur gear itself whose gear teeth transfer motion to the track. Although time did allow adequate design of the drive drum, certain key dimensions were found. The outside diameter of the drive was set at 1 meter. This dimension was arrived by using the maximum height constraint of the track. It was felt that this height would allow for optimum obstacle

negotiation without requiring the track to pivot. The width of the drum would be 0.6 meters matching that of the track. The thickness and material were never determined.

Design of the pivot on which the drive drum, frame, and retaining roller are to be mounted was not completed (other than required lengths and a general shape). The length of the pivot arm between the internal frame and the center of the drive drum was determined to be a minimum of 0.76 meters. Extra length would have to be added for mounting purposes. The length between the retaining roller and the internal frame is to be a minimum of 0.35 meters. The length between the retaining roller and the center of the drive drum would have to be a minimum of 0.8 meters. The general shape of the pivot arm can be seen in the previous schematic of the track assembly.

2.14 TRACK PROTECTION FENDERS

Track performance is a necessary requisite for the success of the LCUV mission. In order for the LCUV to perform as expected, the track system must be able to combat the harsh environmental conditions that exist on the lunar surface. These include the effects of large temperature variations and gradients, radiation, and subsequent sublimation due to the vacuum environment. The need to protect the track from dust is also apparent due to the fact that dust particles could damage the drive drums and mechanical settings that exist within the frame of the track system.

The track consists of a titanium belt that will need protection from the lunar environment in order for it to operate as expected. A majority of this protection will be accomplished by the use of a fender arrangement that will be attached to the body of the LCUV. The fender will extend from above the track, covering the titanium belt and shielding approximately half of the drive drum (0.5 m). The main purpose of the fenders is to shield the titanium track from the harmful gamma rays that will lead to eventual sublimation and corrosion of the belt itself. The fenders will also provide ample protection from the effects of dust particles on the track system. By regulating the flow of dust particles around the LCUV, the cameras will not be subjected to poor visibility; therefore, the use of fenders for the LCUV will serve three main purposes. They can be listed as follows:

1. To provide protection from the penetration of harmful gamma rays within the titanium belt.

2. To provide dust protection for the track's moving parts.

3. To regulate the flow of dust particles around the LCUV.

2.15 CONCLUSION

A tracked Lunar Utility Vehicle will be required by NASA when it looks to inhabit the moon. Tracked locomotion systems will not only prove to be feasible, but they will be an efficient mode of locomotion for Lunar construction vehicles; furthermore, the design concepts and specifications put forth by the NASA/USRA summer report (Reference 10) have been met by the tracked locomotion system.

In terms of bearing area requirements, draw bar pull, gross tractive effort and minimum slip conditions (slip < = 40%), the LCUV design characteristics must be further studied to determine an exact array of values for various loads towed, surface conditions and vehicle properties. Once these assessments have been made, further design in the locomotion system can be completed.

3.0 SUSPENSION CONNECTION SYSTEM

The effectiveness of the connection system for a Lunar Construction Utility Vehicle, (LCUV), is vital to the machine's reliability. The connection system couples the LCUV's tracks to its hull. The Vertical Force "Absorbing" Connection System, (V-FACS), is comprised of a shaft traveling through connectors which are attached to "wings" that are in turn attached to both the hull and the track frames. These connectors will form a "mating mesh" when the shaft is placed into its operating position (Figure 3.1).

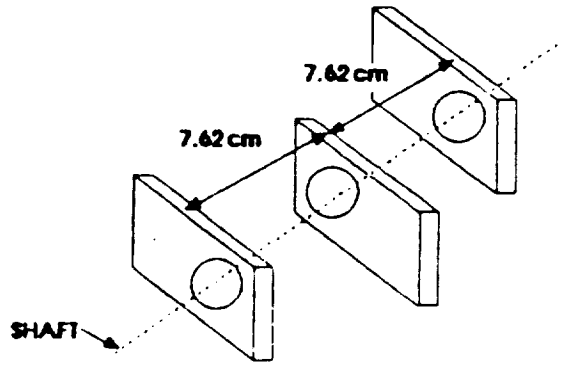

Figure 3.1
V-FACS Strut Mating Mesh

The purpose of the V-FACS is to "absorb" forces in the vertical direction that are exerted on the vehicle. This particular connection system actually transfers vertical forces that the LCUV receives. Its shaft allows rotational movement of both the hull and the track frames. To prevent this rotational movement from going beyond prescribed limits, two struts will be mounted on each side of the vehicle (Figure 3.2).

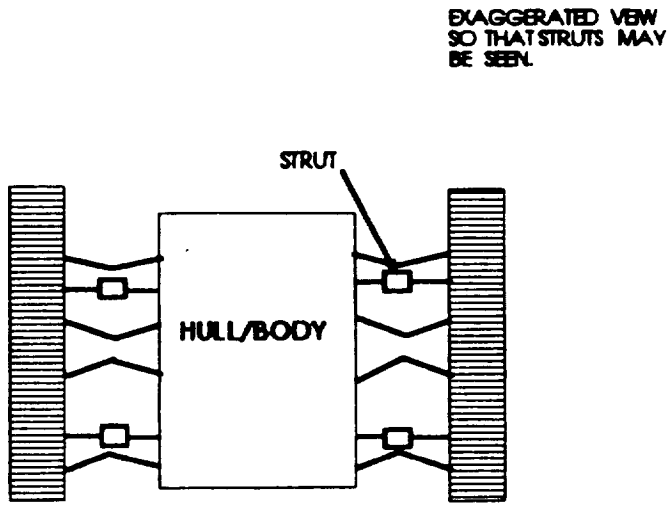

Figure 3.2
V-FACS Strut Schematic

3.1 V-FACS STRUT

The struts will follow the same design format as the struts that are located in the track frames. They will be similar to the MacPherson struts except for the damping. Whereas the MacPherson strut uses hydraulic damping, these struts will use frictional damping. The MacPherson strut's damping depends on velocity. The V-FACS strut will depend on distance of travel. A more detailed sketch of the V-FACs strut may be seen in Figure 3.3.

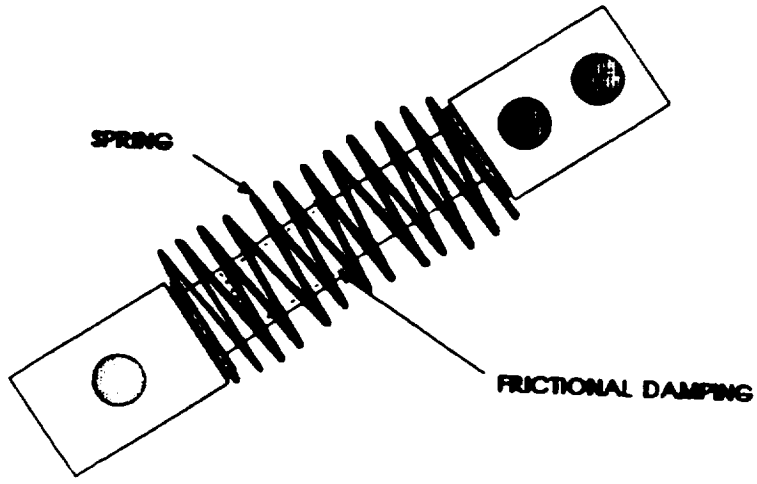

Figure 3.3
V-FACS Strut Detail

3.2 V-FACS SHAFT DESIGN

Since the primary loads on the LCUV act predominantly on the shaft of the V-FACS, its design must be reliable.

For LCUV#2, the V-FACS shaft length, on both sides of the vehicle, will be 0.9144 m. This length is a design restriction in that the track's framework is only 1 m long. It would be undesirable to design a shaft longer than is necessary. The V-FACS shaft will be made of solid aluminum with a diameter of 5.08 cm. There will be holes for pin inserts drilled and threaded on each end of the shaft.

This particular V-FACS shaft design was chosen over solid and hollow shaft designs of carbon steel. The aluminum shaft was chosen over the carbon steel shaft because of the 7500 kg weight constraint placed on the entire LCUV.

A stress analysis was performed using a 0.064 cm deflection as one of the design constraints (Reference 6). The solid aluminum shaft was found to yield a greater deflection than that of the solid and hollow steel shafts (Figure 3.4, Table 3.1);

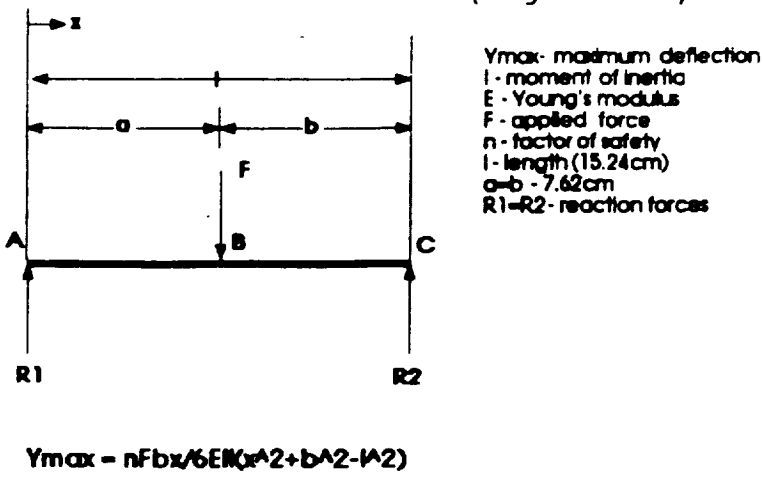

Figure 3.4
V-FACS Shaft Freebody

however, the solid aluminum shaft still falls within the 0.064 cm design criteria, and is considerably lighter in weight than the previously mentioned shafts. Its difference in maximum deflection is so small as compared to that of the hollow steel (Table 3.1), that it was chosen mainly because it weighs less.

MATERIAL	ELASTIC MODULUS (Pa)	MAXIMUM DEFLECTION (cm)	APPLIED FORCE (N)
ALUMINUM (SOLID) D=5.08cm	7.3 E^10	0.061	1.0 E^8
STEEL (SOLID) D=5.08cm	2.1 E^11	0.023	1.0 E^8
STEEL TUBE *	2.1 E^11	0.052	1.0 E^8

* Note: OD=5.08cm, ID=4.45cm

Table 3.1
Shaft Force Analysis Results

3.3 V-FACS CONNECTOR DESIGN

The role of the connector is to hold the shaft in place while allowing rotational motion to the hull and/or the tracks. The design of the connector itself was not as thorough as that of the V-FACS connector bearings. The connector's dimensions are shown in Figure 3.5.

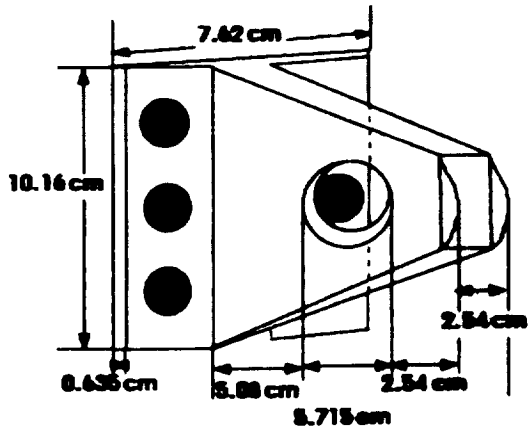

Figure 3.5
V-FACS CONNECTOR

Bearings in the V-FACS connectors are what allows the rotation of the bodies around the shaft. Self lubricating bearings are the optimum design for this case. Since the average temperature of a lunar day, -171°C to 111°C, will cause a "breakdown" in many of the common applicable lubricants (oil, grease, etc...), self

lubricating bearings become the optimum design over ball bearings. The two bearing types considered are: IGLIDGE T500 and DIXON CJ (Table 3.2, Reference 18, 19). In laboratory tests performed by the Dixon Company, it was found that the CJ bearings can withstand up to 2.41E8 Pa static load while the T500 bearing can withstand only 1.58E8 Pa (Reference 18).

BEARING TYPE	TEMPERATURE RANGE (°C)	LOAD CAPACITY (Pa)
IGLIDE T500	-100 TO 250	1.58 E^8
DIXON CJ	-179 TO 160	2.41 E^8

Table 3.2
Bearing Specifications

Dixon CJ bearings have a long term operating temperature range of -179°C to 160°C. This range is more suitable than that of the IGLIDE T500 bearing which has a long term operating temperature range of -100°C to 250°C. By inspection, it is easy to see that the IGLIDE T500 will fail before the DIXON CJ bearing when exposed to the lunar average low temperature (-171°C).

When press fitted into its housing, the Dixon CJ bearing assumes the same thermal expansion coefficient as that of its housing material. This is because its elastic modulus is lower than that of most metals (Reference 19). During normal applications, the DIXON CJ bearing will undergo simple elastic deflection. However, due to its construction (Figure 3.6), fatigue is not a limiting factor.

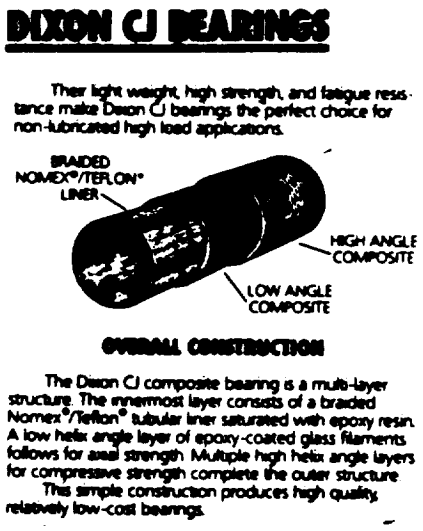

Figure 3.6 (Reference 6)
Dixon CJ Bearing

3.4 V-FACS "WING" DESIGN

The purpose of the V-FACS "wing" is the means of connection between the V-FACS connectors and the hull and the tracks (Figure 3.7). There will be 18 V-FACS "wings" (nine for each side of the vehicle). They will be placed strategically on both the hull and the tracks. Wherever a connector is to be located, there will be a "wing" coupled with it in the same position. The entire span of the "wing" will reach a maximum length of 0.9144 m.

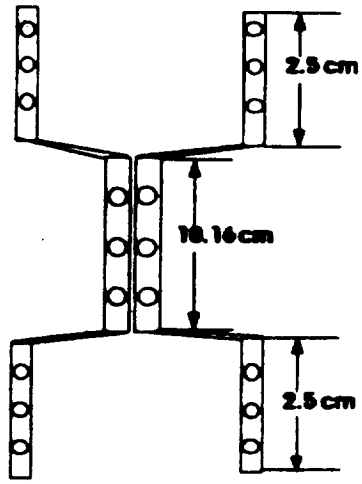

Figure 3.7
V-FACS Wing Design

3.5 CONCLUSION

The V-FACS system is a mechanically simple device that allows for a single pinned connection of the track to the frame. This particular characteristic meets the design goal of ease of maintenance. It also allows the track to rotate on the pin axis. This in turn allows the track to maintain a maximum contact area when travelling over sloped areas.

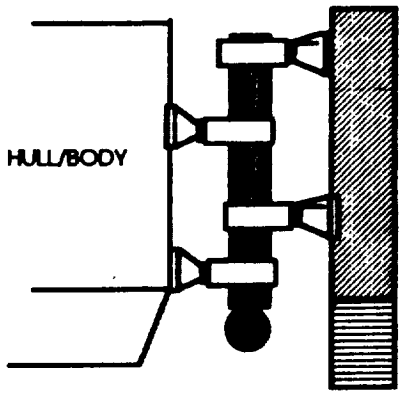

Figure 3.8
V-FACS Assembly

4.0 PAYLOAD CONNECTION

The payload connection system couples the LCUV hull with the hull of the payload. As a design requirement, the payload must be able to swivel both horizontally and vertically at the coupling.

4.1 CANDIDATE DESIGNS

Three coupling devices serve as possible candidates. The universal joint, the rzeppa joint, and the one piece flexible coupling (Reference 20, 21). An illustration of each may be seen in Figure 4.1, 4.2, and 4.3.

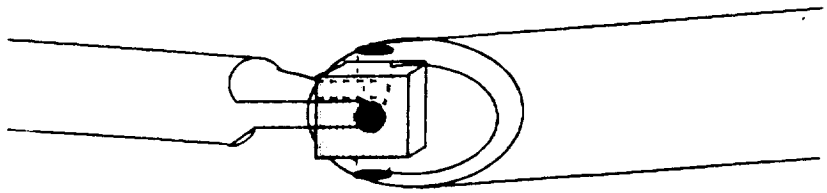

Figure 4.1
Simple Universal Joint

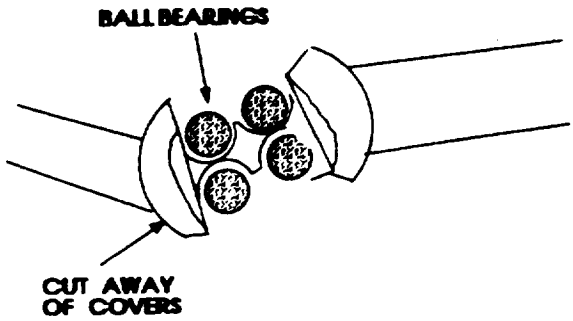

Figure 4.2
Rzeppa Joint

Figure 4.3
One Piece Flexible Coupling

The rzeppa joint consists of ball bearings in a fixed mount. Because ball bearings require lubrication (oil, grease, etc...), and common lubrications have been proven ineffective on the lunar surface (see V-FACS section), the rzeppa joint is not a feasible design. The remaining two candidates are similar as far as optimization (Table 4.1). Tests will have to be performed in order to choose the best candidate.

JOINT TYPE	PRO	CON
RZEPPA	MECHANICALLY SIMPLE	REQUIRES LUBRICATION
UNIVERSAL	MECHANICALLY SIMPLE FLEXIBLE	SEVERAL PIECES
ONE PIECE FLEXIBLE COUPLING	MECHANICALLY SIMPLE FLEXIBLE ONE PIECE	NONE

TABLE 4.1
Payload Connection Device Comparison

The coupling will be pinned to both the LCUV and the payload hulls. Its pinned connection will be similar to that of the V-FACS system.

4.2 CONCLUSION

The one piece flexible coupling is the best choice of the three alternatives considered. It's mechanically simple and doesn't require lubrication. These two characteristics make it ideally suited for lunar applications. However, due to the time constraints of this project, a complete investigation of joint mechanisms was not possible and still requires further study.

5.0 POWER SYSTEM

A large number of power supply systems are under development today. Some of these systems are at an advanced stage and would be considered good candidates for lunar application. The hydrogen-oxygen fuel cell is an excellent choice for the power supply system on the Lunar Construction Utility Vehicle. This report focuses on the design characteristics of the fuel cell. In addition, equations are included to analyze parametrically the fuel cell response to alterations in the operating conditions.

5.1 INTRODUCTION

Electricity is the most convenient form of energy. It is easy to control and to convert into other energy forms. Traditionally, the production of electricity involves the combustion of fossil fuel to release thermal energy which is converted into mechanical energy in a heat engine (Reference 22). This conversion process transforms energy that is stored in a highly ordered manner in the chemical bonds to energy associated with great disorder after the combustion process. The maximum useful power that can be obtained from this energy, is the amount which a Carnot engine would obtain operating between the temperature at which the energy was released and the natural temperature of the surroundings (Reference 23).

By means of fuel cells, it is possible to bypass the conversion-to-heat process and the associated mechanical-to-electrical process. This means that a fuel cell is an electrochemical device in which the chemical energy of a fuel is converted directly and efficiently into low voltage, direct-current electrical energy. One of the chief advantages of such a device is that the conversion, at least in theory, can be carried out isothermally; therefore, the Carnot limitation of efficiency does not apply. A fuel cell is often described as a primary battery in which the fuel and oxidizer are stored external to the battery and are fed to it as needed.

In general, the combustion reaction involves a transfer of electrons from the fuel molecules to the oxidizer molecules. The fuel cell is a device that keeps the fuel molecules from mixing with the oxidizer molecules, permitting, however the transfer of electrons by a path that may contain a load (Reference 23). Figure 5.1 illustrates the elements of a fuel cell.

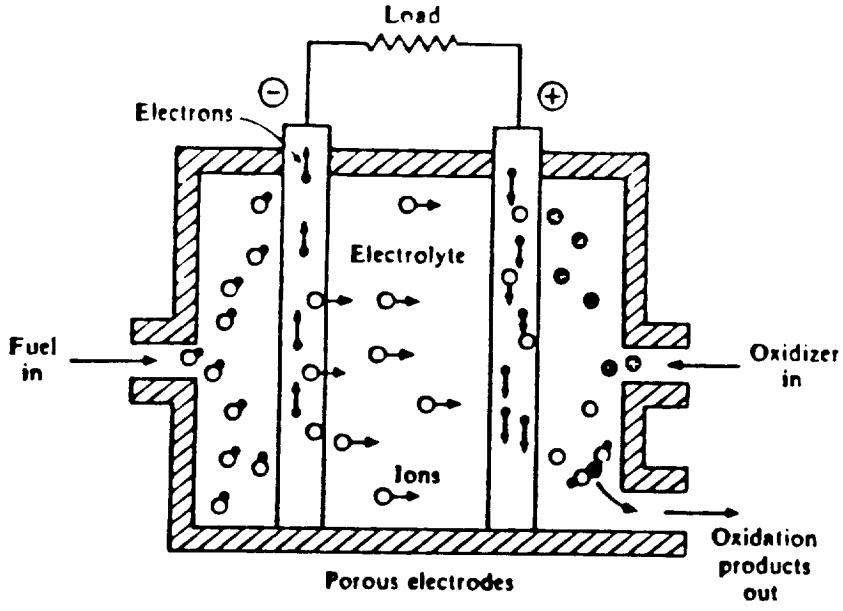

Figure 5.1 (Reference 23)
Schematic of a Fuel Cell

The alkaline hydrogen-oxygen fuel cell will be specified for use in the design of the primary power system on the Lunar Construction Utility Vehicle (LCUV). For this design several constraints had to be made:

- It must be small enough to be mounted within the LCUV.
- It must be as light in weight as possible (total weight of each vehicle is limited).
- It should consume minimum fuel.
- It must operate in an airless environment and be reliable for long periods of time.
- It must be solar independent.

There were several other power systems that were researched before the final decision was made. These power systems included batteries, radioisotope generators, solar and regenerative fuel cells. Other options will be discussed in the following paragraphs.

The battery was found to be a promising candidate for the power system of the LCUV. The main features for this design were its high power density and the ability to be recharged. This power system was not chosen for our design due to its relatively short life as compared to other power systems (Reference 23).

Photovoltaic cells have provided power for almost every spacecraft the United States and the Soviet Union have launched in the first decade of the space age. Solar cells have the advantage of high power-to-mass ratios (Reference 23). This power system was

not considered since our guidelines require a solar independent design. In addition, this system tends to be heavy because of the size of the batteries used to store the power generated (Reference 10).

Radioisotope-powered generators are especially inviting because of their reliability and simplicity. Furthermore, radioisotopes suitable for fueling such units will become more plentiful in the future as by-products of nuclear reactors. This type of energy source loses some of its appeal for terrestrial application because of its low power-to-mass ratio and the need for shields to protect humans from the radiation (Reference 23).

Regenerative hydrogen-oxygen fuel cells also show promise as a means of providing power to the LCUV. This system has the ability to convert the by-product water into hydrogen and oxygen, thereby, eliminating the need to bring extra fuel. The drawbacks to this system include the dependance on solar energy to generate power needed for the conversion process. In addition, this system has a relatively large mass (Reference 24).

5.2 HYDROGEN-OXYGEN FUEL CELL

The fuel cell operates on the well-established principle of electrochemistry; therefore, it is appropriate that we review these ideas that are necessary to the understanding of the fuel cell we have chosen (Reference 22).

The hydrogen-oxygen fuel cell consists of two geometrically opposed electrodes, separated by an ionicly conducting medium (electrolyte). For this design, the electrolyte specified will be aqueous potassium hydroxide. At one electrode (anode), the hydrogen fuel is introduced, which, in contact with the electrode and electrolyte, can ionize and release electrons to the electrode thus becoming chemically oxidized (Reference 22).

Anode Reaction: $H_2 + 2OH^- \rightarrow 2H_2O + 2e^-$

At the other electrode (cathode) the oxygen oxidant is introduced, which, on contact with the electrode and electrolyte, takes up electrons and becomes chemically reduced (Reference 22).

Cathode Reaction: $1/2O_2 + H_2O + 2e- \rightarrow 2OH^-$

When the electrodes are connected outside the cell by a conductive external circuit, electrons can flow around the circuit and perform useful work, as long as supplies of fuel and oxidant are maintained. The overall half-cell reaction for the system is shown below (Reference 22).

Overall Reaction: $H_2 + 1/2O_2 \rightarrow H_2O$ + electrical energy + heat

Figure 8.2 is a schematic of what is actually taking place in the cell (Reference 23).

5.3 VEHICLE POWER REQUIREMENTS

The power requirements for the tracking system were calculated in order to determine the mass and volume of the fuel cell that will be used in this design. The equations needed for determining the power requirements are as follows (Reference 25).

$$M = W \cdot r \cdot \cos(\alpha) \cdot \left[\frac{c \cdot A}{W \cdot \cos(\alpha)} + \tan(\phi) \right] \cdot \left[1 - \frac{K}{L \cdot s} \left[1 - \exp(-L \cdot s / K) \right] \right]$$

$$P = \frac{M \cdot v}{r \cdot (1-s)}$$

where,
P = power (W)
M = torque (N-m)
W = total weight of vehicle (N)
r = radius of drive wheel = 0.5 m
α = angle of inclination = 30 degrees (assumed maximum)
= 10 degrees (assumed normal)
c = soil cohesion = 360 N/sq m
p = coefficient of rolling resistance
ϕ = internal friction constant = 35 degrees (assumed)
K = soil constant = .025 m
L = total contact length per track = 2.4 m
s = slippage = 30 % (assumed)
A = contact area of track = 1.44 sq m
v = maximum velocity = 0.2 m/s (assumed)

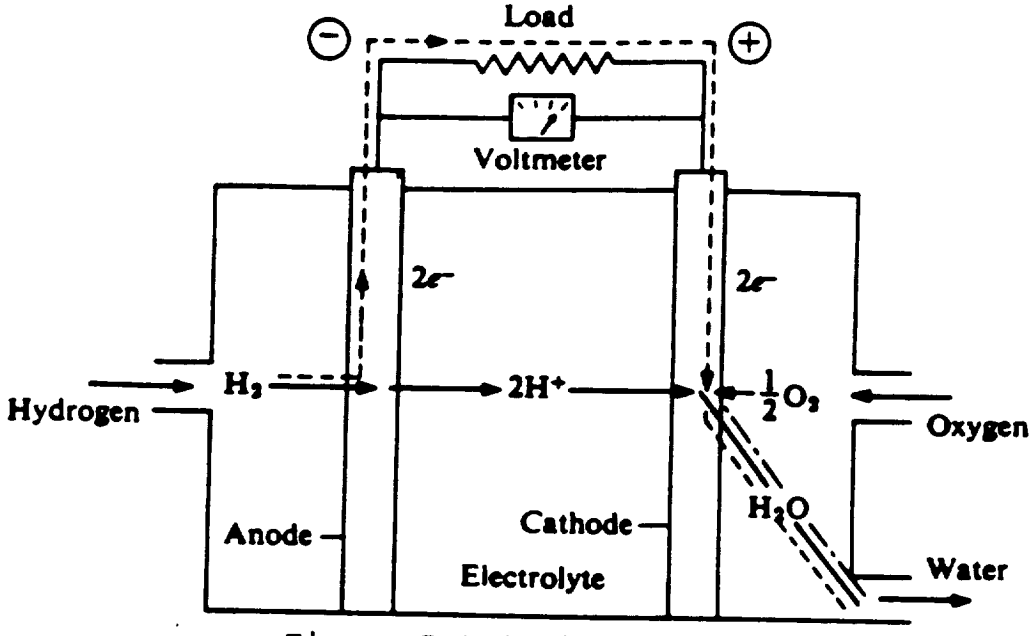

Figure 5.2 (Reference 23)
Hydrogen-Oxygen Fuel Cell

The maximum power requirement for the track system is six kilowatts. Under low power conditions this requirement may be cut to three kilowatts. The specifications for the hydrogen-oxygen fuel cell used in this design are listed in Table 8.1 (Reference 26).

Power-Weight ratio:	12 lb/KW
Dry Weight:	72 lb
Accessory Weight:	70 lb
Total Mass:	64.4 kg
Dimensions:	114.3 cm x 38.1 cm x 35.6 cm
Efficiency:	50 %
Operating Temperature:	100 Celsius
On Line Service:	10,000 hrs

Table 5.1
Specifications for Hydrogen-Oxygen Fuel Cell

5.4 MASS FLOW RATE OF FUEL AND OXIDIZER

The mass flow rate of the hydrogen fuel can be calculated by the following equation (Reference 23).

$$\text{Mass flow rate (fuel)} = \frac{P(\text{actual})}{n \cdot (\Sigma_r\ n_r \cdot \delta H_f^\circ - \Sigma_p\ n_p \cdot \delta H_f^\circ)}$$

P(actual) is the power output, and n is the efficiency of the fuel cell. The heat of formation values (H_f°) are listed in Table 8.2.

COMPOUND	Hf°kcal/mole
HYDROGEN	0
OXYGEN	0
HO	-68.32

Table 5.2 (Reference 23)
Heat of Formation Values

The mass flow rate of the oxygen oxidant is determined by the following equation (Reference 23).

$$\text{Mass flow rate (oxidant)} = \frac{\text{moles of oxidant}}{\text{moles of fuel}}\ \text{mass flow rate(fuel)}$$

The mass flow rate for both hydrogen and oxygen is listed in Table 5.3.

Operating Conditions	Mass Flow Rate of Hydrogen	Mass Flow Rate of Oxygen
Maximum	0.304 kg/hr	2.416 kg/hr
Normal	0.152 kg/hr	1.207 kg/hr

Table 5.3 (Reference 23)
Mass Flow Rate for Hydrogen and Oxygen

5.5 ELECTRODES

There are several different types of materials that can be used for construction of the electrodes in the hydrogen-oxygen fuel cell. The type of electrode used for this design is the Raney electrode. The Raney metals are metals in very divided, highly active form. They are prepared by mixing the active metal with an inactive metal, usually aluminum. This mixture is then treated with strong alkali which dissolves out the aluminum, leaving the highly developed surface structure desired for the porous electrodes (Reference 27).

The hydrogen electrode will be made from Raney nickel, by preparing the electrode structure from a sintered mixture of Raney alloy (mass fraction 60 per cent Al, 33.6 per cent Ni and 0.4 percent Cr) and ordinary nickel. Most of the aluminum is then removed with a potassium hydroxide solution (Reference 28).

This material was selected since it is relatively inexpensive, has a high mechanical strength, and is a highly active non-noble metal catalyst for hydrogen electrodes in the alkaline fuel cell. By doping the Raney nickel with chromium the catalytic activity is enhanced (Reference 28).

A similar kind of electrode can be made for the oxygen side of the fuel cell. In this case the mixture is made of ordinary nickel and Raney silver but the surface must be prepared in a slightly different way because of metallurgical problems. This material is a very good oxygen catalyst (Reference 27).

5.6 HEAT AND MASS TRANSFER

The heat and water by-products of the electrochemical reaction in the hydrogen-oxygen fuel cell must be removed. This must be done to avoid exceeding the maximum critical temperature of the cell and to prevent an excessive increase in electrolyte volume and decrease in electrolyte concentration, any one of which could cause

failure or malfunction of the cell. In addition, removal of heat and water at a controlled rate provides an effective means of maintaining the cell operating conditions within the design range. The technique we plan on using in our design for removing water as well as heat from the fuel cell is to circulate hydrogen in excess of that consumed in the electrochemical reaction. For designing this type of system there needs to be a general understanding of the mechanisms that regulate the transport and hence the rejection of the heat and water produced in an operating fuel cell (Reference 29).

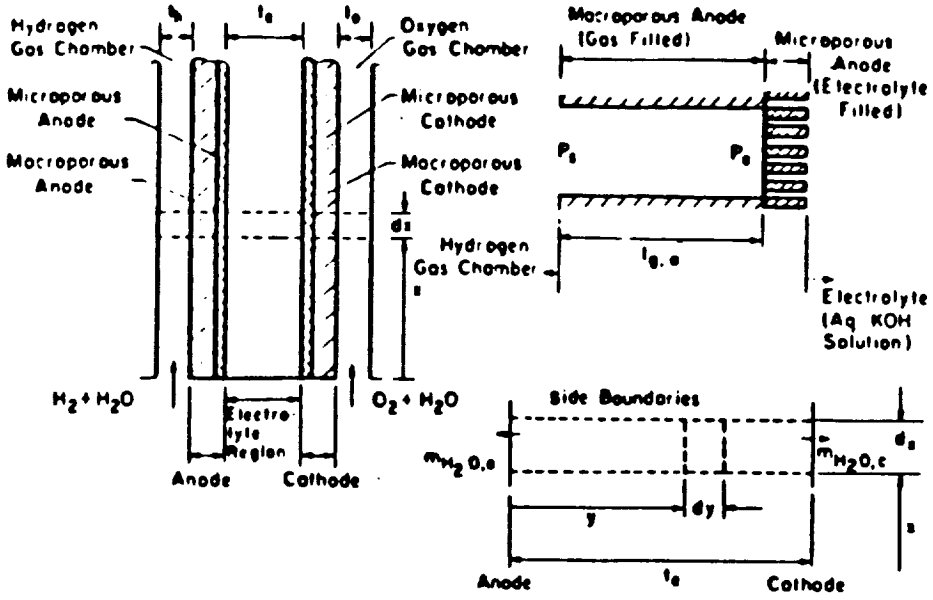

Figure 5.3 (Reference 29)

Schematic Diagram of a Cell
(a) General features
(b) Electrode Region
(c) Electrolyte Region

A schematic diagram of the cell for which the model is developed is shown in figure 5.3(a). The two electrodes consisting of macropore and micropore regions separate the gas chambers and the electrolyte. The simple pore model will be used to represent the electrodes. This model shows the porous media as a number of uniform, parallel cylindrical pores. The electrode and the electrolyte regions of the cell are shown in figures 5.3(b) and 5.3(c) respectively.

The fuel cell in figure 5.4(a) is insulated at the two ends and sides. Figure 5.4(b) shows the lumped temperature distributions at various parts of the cell.

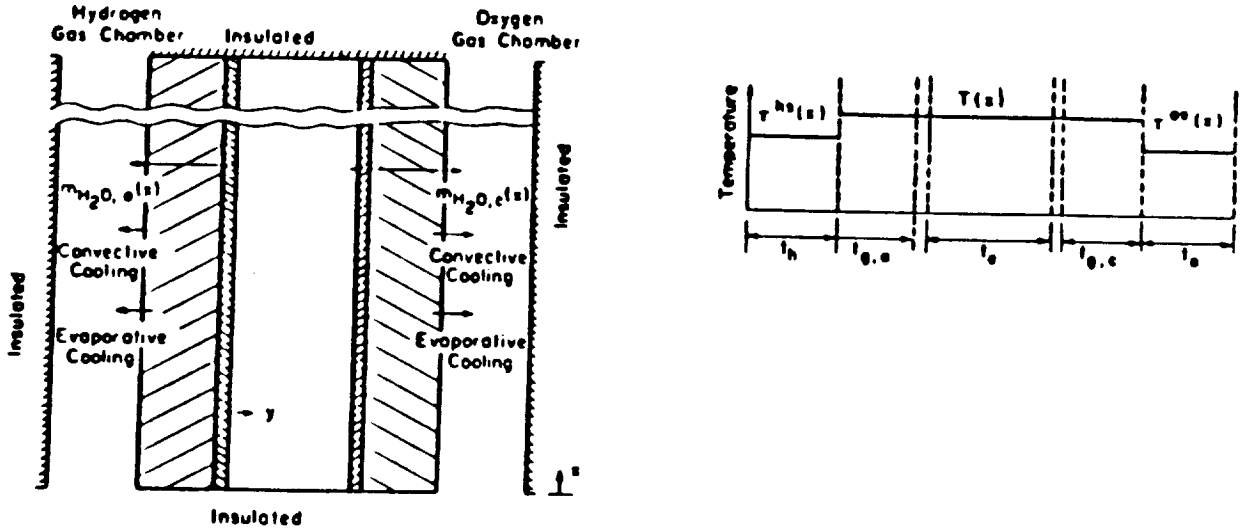

Figure 5.4 (Reference 29)

Model Description and Temperature
Distribution in a Cell Model
(a) Model Description
(b) Temperature Distribution

For the fuel cell operating in a steady-state condition, one mole of water is rejected at the hydrogen electrode for each mole of hydrogen consumed by the reaction. For binary gas mixtures at low pressures, at constant pressure and temperature across the electrode, the binary mass diffusivity is nearly independent of mixture composition. By making the assumption that a constant molar concentration of the mixture over the thickness of the macropore region at the anode at steady-state, the mass transport of water vapor can be represented by Fick's law (Reference 29).

$$M(H_2O) = \frac{(Peff \cdot D(H_2O\text{-}H_2) \cdot 18)}{R \cdot T} \cdot \frac{(Pe - P(H_2O))}{tg}$$

where Peff is the electrode porosity, $D(H_2O\text{-}H_2)$ is the diffusivity of water vapor-hydrogen mixture, R is the universal gas constant, T is the temperature of the mixture, Pe is the partial pressure of water in aqueous KOH solution, $P(H_2O)$ is the partial pressure of water vapor in the hydrogen gas chamber, tg is the thickness of the electrode. This equation is also applicable during the transients, because at low temperature, fuel cells will have a dilute mixture of hydrogen and water vapor. A similar equation will hold for the

evaporation of water vapor through the cathode (Reference 29).

Under actual transient operating conditions of the cell, the mass of the water in the electrolyte will change and the mass of the KOH will stay constant. This water gain and loss of the electrolyte will result in a change in the electrolyte and volume. Changes in the volume could be in the x direction, y direction or both. For simplicity, we will consider the change in the electrolyte in the y direction to develop the mass transfer equations for this case. The mass balance equation for KOH becomes (Reference 29):

$$\frac{\delta p(KOH)}{\delta t} = D(KOH)\ \frac{\delta^2 p(KOH)}{\delta y^2} - \frac{\delta (p(KOH)\cdot V)}{\delta y}$$

where

$$p(KOH) = p(OH^-) + p(K^+) \qquad \text{and} \qquad D(KOH) = \frac{2\ D(K^+)\ D(OH^-)}{D(K^+) + D(OH^-)}$$

p(KOH) is the density of the potassium hydroxide. D(KOH) is the binary diffusivity of the electrolyte, V is the volume average velocity and, $D(OH^-)$ and $D(K^+)$ are the diffusivities of OH^- and K^+ ions in the electrolyte (Reference 29).

The passage of two moles of electrons through the cell results in using two moles of OH^- and producing two moles of H_2O at the anode, and producing two moles of OH^- and using one mole of H_2O at the cathode. If (i) amperes per unit electrode area per second is drawn from the fuel cell, the volume average velocity per unit area for the anode and cathode may be different. The variation between the two velocities per unit area would lead to an electrolyte volume increase. In this model the volume between the electrolyte is kept constant in both the x and y directions (Reference 29).

The model mass balance equation for KOH is (Reference 29)

$$\frac{\delta p(KOH)}{\delta t} = D(KOH)\ \frac{\delta^2 p(KOH)}{\delta y^2} - V\cdot\frac{\delta p(KOH)}{\delta y}$$

From this equation the H_2O density distribution can be found by the use of conservation of volume. In the real case the mass of the KOH should stay constant (Reference 29).

The model proposed in this study, unlike, the actual case, assumes uniform porosity and complete wetproofing of the electrode structures. The resulting equations to be solved form a complex matrix and require a substantial program for their solution on the computer. The model from this research shows the actual fuel cell in a qualitative and quantitative manner, such that it can be used in analyzing fuel cell performance and response to changes in operating conditions (Reference 29).

If the current is turned off or the cell is operated at a much lower current density than it is designed for, the condensation or evaporation heat effects would involve primarily that for concentration of the electrolyte; therefore, the differential heat of vaporization of the solvent of the electrolyte should be used for these transients instead of heat of vaporization of pure water (Reference 29).

From the mathematical model transients, it is shown that a change in the operation conditions might cause an increase or decrease in the electrolyte volume, until the electrolyte concentration readjusts itself. During this process the electrode should, for a certain operating range, withstand the danger of failure. But for higher transients the electrodes might deform, dry out or become flooded, resulting in a failure of the fuel cell (Reference 29).

The model and resultant equations presented in this work have been shown to effectively represent transient response characteristics of the hydrogen-oxygen fuel cell we have chosen for our design. These equations can be used to parametrically analyze the hydrogen-oxygen fuel cell response to alterations in operating conditions (Reference 29).

5.7 CONCLUSION

The alkaline hydrogen-oxygen fuel cell appears to be the best option for the design of the power system used by the LCUV. The advantages are:

- It is small enough to be mounted within the LCUV.
- It is light in weight.
- It operates in an airless environment and is reliable for long periods of time.
- It is solar independent.

The drawback to this system involves the amount of heat that must be dissipated by a radiator. This problem will be addressed in the thermal control section of the report.

One question we encountered when designing the power system involved how the hydrogen and oxygen tanks were going to be replaced. This posed a problem since during the first stage of the mission the space station will be unmanned. The solution to this problem involves the use of robotics to perform the task of removing and replacing the tanks when necessary.

The second question we had to address was what to do with the by-product water produced by the cell reaction. The solution to this problem involves collecting the water in tanks. Since water is a valuable commodity on the moon, we propose to store it for future use by the inhabitants on the lunar base.

6.0 ELECTRIC MOTOR DRIVE SYSTEM

Since electric fuel cells are proposed to be used to power the LCUV, electric motors will be employed to drive the vehicle. Several design problems are encountered in the Lunar environment. The lunar surface is covered by what is referred to as lunar dust. This poses a serious threat to the mechanical components of the motor or any other mechanisms exposed to the environment of the Moon (Reference 30). Another negative aspect of the environment of the Moon is that atmosphere is non-existent. The problem associated with this is that heat dissipation is made difficult since heat can not be convected away from surfaces. Better methods must be developed to conduct and radiate generated heat away from the motor. One more negative characteristic of the Moon is that its magnetic field which is much smaller than that of the earth is not capable of shielding the surface from the dangerous effects of solar flares (Reference 30). This also proves to be a design problem to be addressed since the electric motor will be partially exposed to the environment. Electric motors themselves have many options associated with them: DC or AC, brushed or brushless, and direct drive or gear reduction. Each option must be analyzed to find which option is the most feasible for use on the LCUV.

6.1 ELECTRIC MOTOR DESIGN

In the beginning of this report the environmental problems associated with the Moon's surface that an electric motor will have to contend with will be discussed and the requirements of power, torque, and angular velocity to drive the tracks of the Lunar Construction Utility Vehicle (LCUV) in the worst case scenario will be presented. Methods will be developed by which certain problems can be avoided. Finally, an electric motor that meets the adjusted requirements will be specified.

6.1.1 ASSUMPTIONS AND DESIGN CONSTRAINTS

The largest influence in determining a motor for use in driving the LCUV is the environment of the Moon. There are many constraints associated with the problems affiliated with running a motor under the conditions presented by the Moon's environment. The other limiting factors are defined by the worst case scenario. The maximum requirements for torque and power to drive the tracks of the LCUV will be determined for this case.

Environmental Design Constraints:

- Temperature ranging from -171°C to 111°C.
- Damaging effect of lunar dust.
- Lack of atmosphere presents problem in convective heat dissipation from the motor.
- Effects associated with solar flares and radiation.
- Gravitational force is 1/6 that of the Earth's.

Worst Case Scenario Requirements:

- Maximum forward velocity of the vehicle is limited to 0.2 meters/second. The reason for this is due to communication delay of three seconds between the earth and the moon.
- Traversing weak soil with 30% slippage
- Pulling a disabled LCUV up a 30° incline

6.1.2 TORQUE AND POWER REQUIREMENTS

The requirements for the maximum torque will be determined for the worst case scenario defined in the assumptions and design constraints section. This demands the calculation of two separate torques, the torque required to drive the LCUV alone and the torque required to pull a disabled LCUV. From the total torque requirement and maximum angular velocity of the tracks the overall power that is required can be calculated for a direct drive motor (i.e. no gear reduction used).

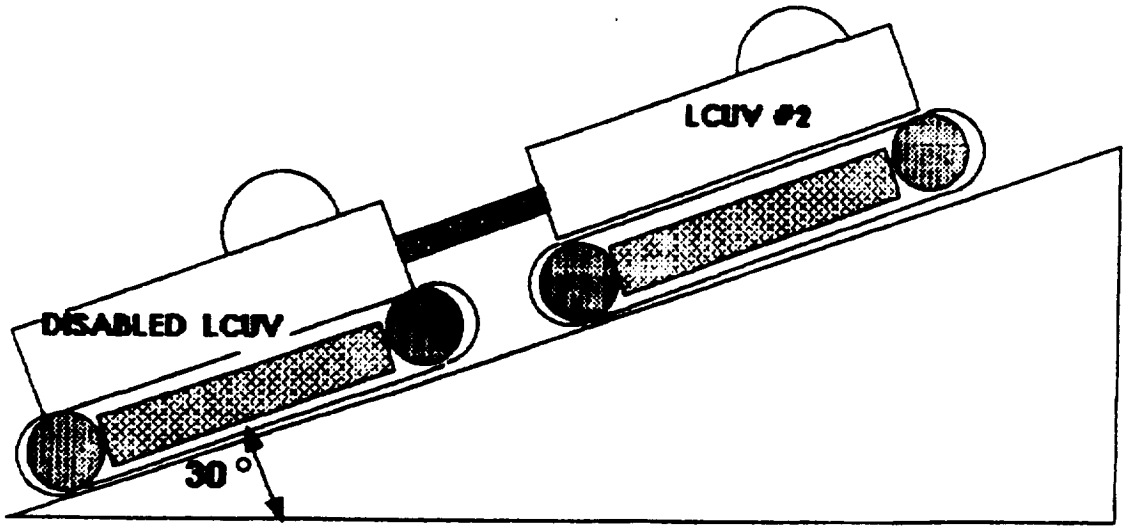

Figure 6.1
Maximum Torque Requirement

The torque required to drive a single LCUV is determined below.

$$\text{Torque:} \quad Md = W \cdot r \cdot \cos\alpha \cdot (c \cdot A/W/\cos\alpha + \tan\phi) \cdot (1-k/(L \cdot s) \cdot (1-e^{-L \cdot s/k})$$

$$\text{Angular Velocity (of drive drum):} \quad \Omega = v/r/(1-s)$$

Variables:

Md	=	Total Torque per track, (in.lbf.)
W	=	Total weight of the vehicle per track, (lbf.)
r	=	Radius of the drive wheel, (in.)
α	=	Angle of incline
L	=	Total contact length per track, (in.)
k	=	Soil Constant
ϕ	=	Internal friction constant
s	=	Percent slippage
p	=	Average track pressure
c	=	Soil cohesion constant
Pt	=	Total Power required per track, (HP)
v	=	Maximum allowable forward velocity, (in./sec.)
Ω	=	Angular velocity, (RPM)

Results: Md = 4,127 N·m, Ω = 35 RPM

The torque required to pull a disabled LCUV is given by:

Torque: $Mp = W \cdot r \cdot (p \cdot \cos\alpha + \sin\alpha)$

Angular velocity: $\Omega = v/r/(1-s)$
(of drive drum)

Results: Mp = 2,646 N·m

In this analysis the total torque required neglects the sliding friction of the disabled LCUV. From the above equations and given the worst case assumptions, the total torque required was determined to be:

M = 6,773 N·m

6.1.3 AC vs DC MOTORS

Motor efficiency is the main factor involved in determining what type of motor (AC or DC) that is the most feasible for use in driving the LCUV's tracks. Power losses are to be kept minimal. The power source for the electric motor is a hydrogen-oxygen fuel cell supplying a DC current. In order to operate an AC motor an invertor would have to be employed to convert the DC supply current into an AC current (Reference 31). When using an invertor there will be some added power loss. Since any power loss is to be avoided if possible, the DC motor proves to be more efficient than an AC motor system, and consequently it will be used on the LCUV.

6.1.4 CONVENTIONAL VS. BRUSHLESS MOTORS

The conversion of electrical energy to work in a motor is tied directly to the commutation of the DC current in the motor windings (Reference 31). It is here where the difference between the conventional and brushless motor is encountered. As the rotor turns, the magnetic field that is set up by the current through the windings also rotates. It is because of this that a means of maintaining the orientation of the field is needed. The conventional motor uses brushes which skim along a commutator as seen in figure 6.2. The brushes send a current through a pair of conductors on the commutator cylinder. The current then flows through each of the winding in a manner which is represented in figure 6.3, thus maintaining a constant orientation of current flow in the windings regardless of rotation. Since this orientation is maintained a uniform torque in one direction can be maintained.

In the case of the brushless type DC motor the commutation of current is achieved by using a shaft position encoder in conjunction with a controller (Reference 31). The position of the shaft will be determined by Hall effect sensors. These sensors detect polarities and magnitudes of magnetic fields. The signals generated by the sensors are amplified and processed by the controller. The controller in turn controls the commutation of the windings in a similar fashion as the conventional motor except without the use of brushes (see figure 6.4). Another variation of the brushless motor is that the motor windings are located on the stator instead of the rotor, and the permanent magnet is connected to the rotor (Reference 31).

There are several categories in which conventional and brushless motors can be compared, for example the ability to produce torque at high rotational speeds, peak torque, acceleration ability, effective life, reliability (maintainability), and dust protection. All of the mentioned categories must be taken into consideration in determining the appropriate type of motor that will be used.

Electromechanical commutation at high rotor speeds using brushes is limited when compared to the brushless type motor due to the fact that when using the brush motor there is heat generated by the frictional contact. In the case of brushless motor's commutation, it is not dependant on contact so frictional heat will not limit operation. Thus the brushless type motor can attain higher rotational speeds and consequently a higher torque rating.

Peak torque is predominately a function current, magnetic field strength, and number of windings, not of rotational speed. Both types of motors perform equivalently in this category.

One advantage of having the permanent magnet located on the rotor as is in the case of the brushless type motor is that higher torque to inertia ratios can be obtained. Motors with high torque to inertia ratios have better accelerational abilities so the brushless type motor is rated better in this category.

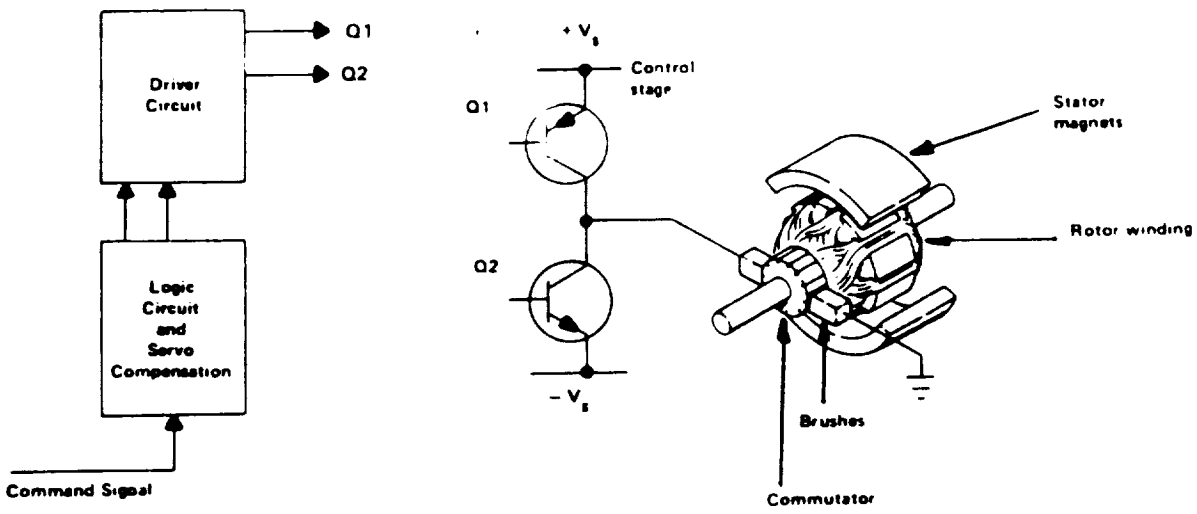

Figure 6.2 (Reference 31)

Schematic of the Commutation of Current in a Conventional DC Electric Motor

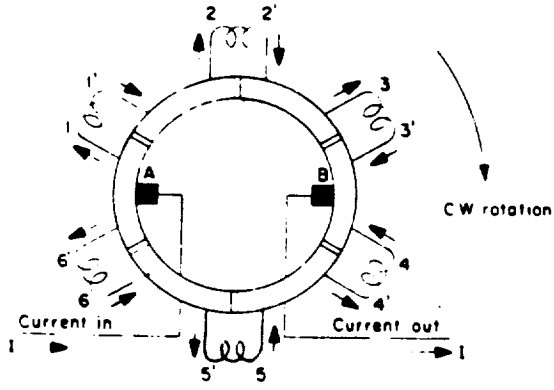

Figure 6.3 (Reference 31)

Flow of Current Through the Windings of a Conventional DC Electric Motor

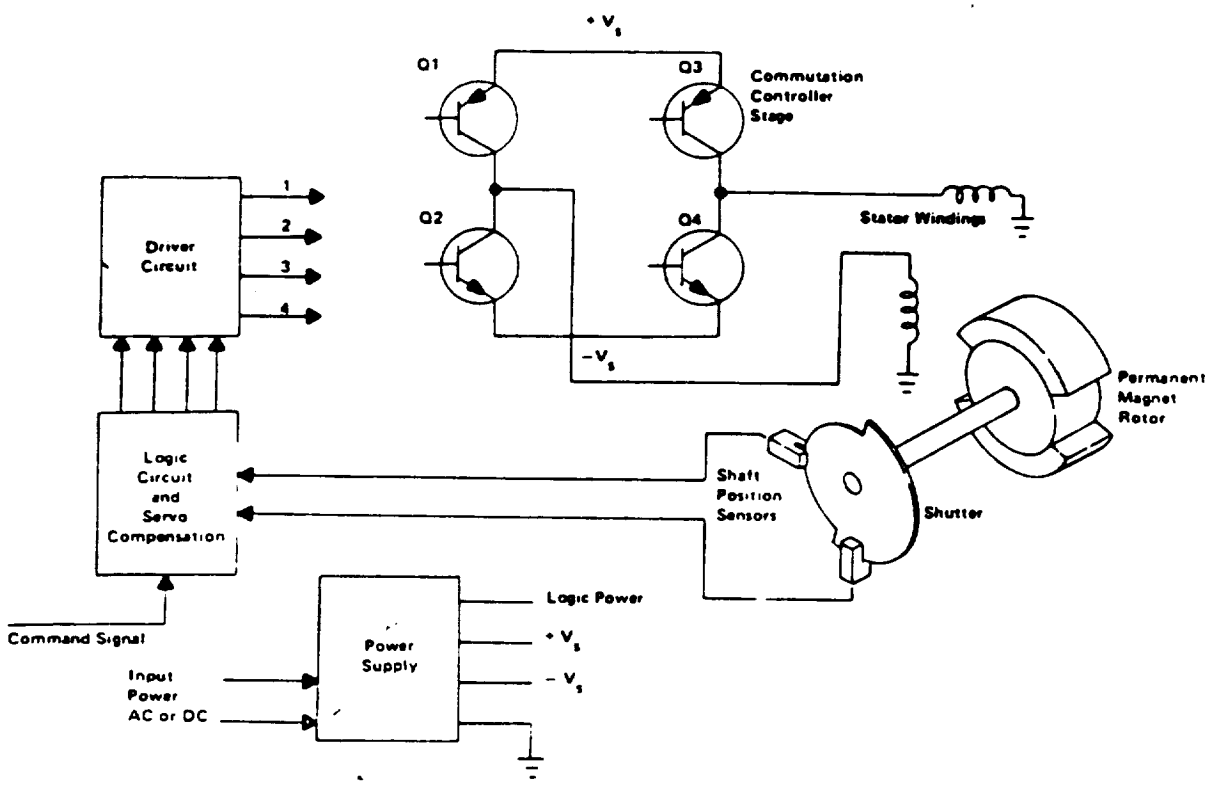

Figure 6.4 (Reference 31)

Schematic of the Commutation of Current in a Brushless DC Electric Motor

Since the brushes on the conventional DC motor are exposed to friction, as explained previously, they are prone to being replaced when worn or damaged during operation. This introduces disadvantages associated with brush type motors. The possibility of the need for manual maintenance is present and a permanently sealed casing can not be used. The brush type motor is virtually maintenance free and can be constructed with a permanently sealed casing which will prevent contaminants from entering.

CATEGORY	CONVENTIONAL	BRUSHLESS
HIGH SPEED TORQUE		X
PEAK TORQUE	-	-
EFFECTIVE LIFE		X
RELIABILITY/ MAINTAINABILITY		X
DUST PROTECTION		X

Note: the letter X denotes better ability

Table 5.1:
Comparison Table for Conventional and Brushless DC motors.

When all of the categories are taken into consideration the brushless type DC motor is equivalent to, or better than the conventional brush type motor and thus brushless option is chosen.

6.1.5 APPLICABLE MOTOR

The motor that best fits the requirements that have been defined is the R88 brushless servomotor which has been developed by Pacific Scientific company (Reference 33). Although it is not actually feasible as of yet, because the heat that will be generated in the windings during high loads would be too severe, it will be used as an example. A more appropriate motor would be one having the same construction, except linearly scaled up in characteristic abilities.

The R88 brushless DC servomotor is constructed with Samarium-cobalt permanent magnet on the rotor for high torque to inertia ratio and fast acceleration. An anti-cog magnet configuration has been included for smooth low angular velocity performance. The characteristics of the motor have been included in table 6.2. The dimensions of the R88 motor have been included in figure 6.5; also, included is a graph of the performance of the motor (figure 6.6).

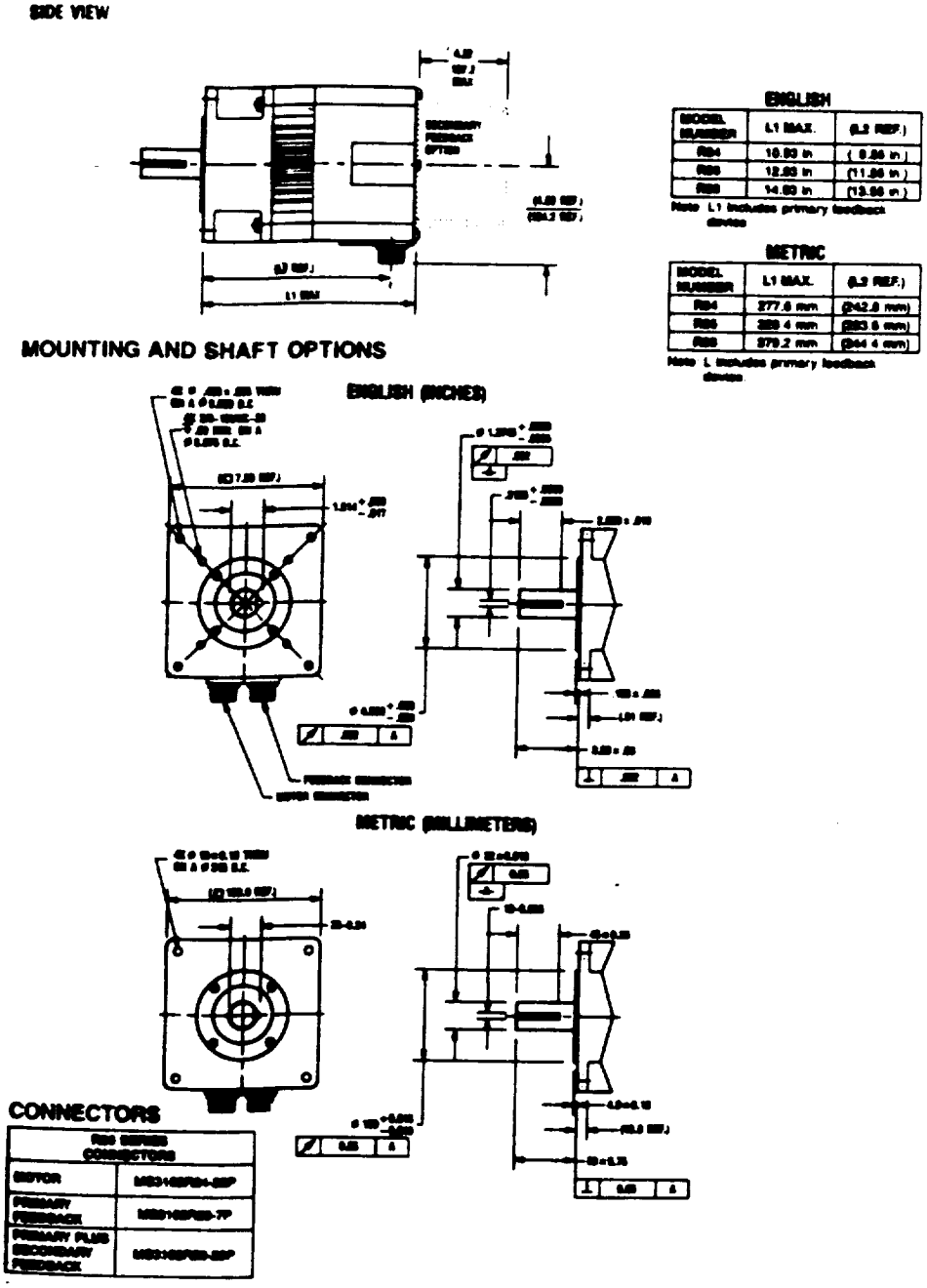

Figure 6.5 (Reference 33)
Dimensions of the R88 Series Motor

ORIGINAL PAGE IS
OF POOR QUALITY

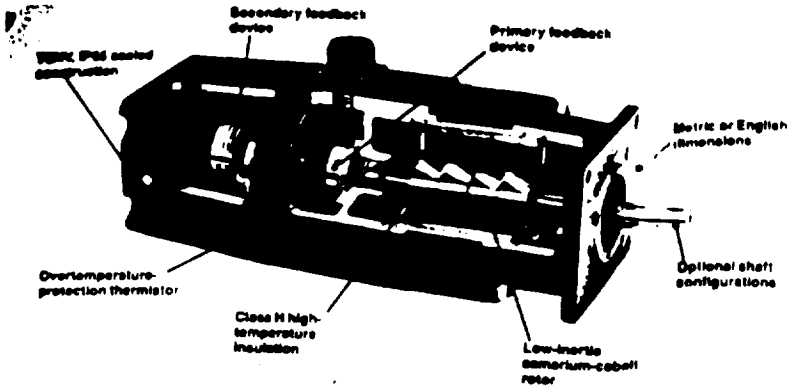

R88: H WINDING

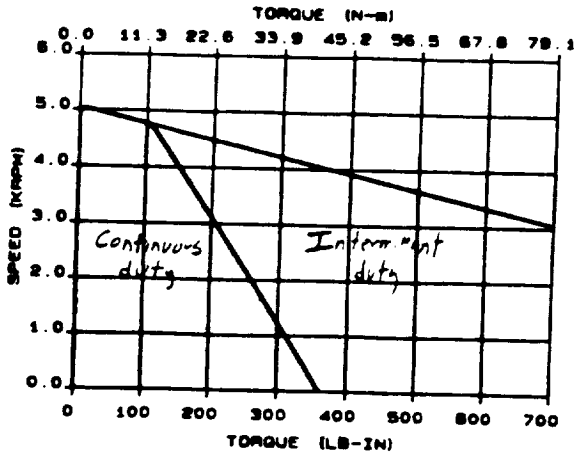

Figure 6.6 (Reference 33)
R88 Series Wound Motor
Performance Graph

MOTOR DATA	SYMBOL	UNITS	VALUE
CONTINUOUS STALL TORQUE	TCS	Nm	40 *
PEAK TORQUE	TPK	Nm	159
MAX LINEAR TORQUE (10% loss in K)	TL	Nm	54
MOTOR INERTIA	JM	kgm x10	6.8
MAX STATIC FRICTION	TF	Nm	0.56
VISCOUS DAMPING COEFFICIENT	KDV	Nm/krpm	0.20
THERMAL RESISTANCE	RTH	C/Watt	0.23
THERMAL TIME CONSTANT	TTH	Min.	59
TORQUE CONSTANT	KTP	Nm/A	0.66
VOLTAGE CONSTANT	KEP	V/krpm	69
CONTINUOUS STALL CURRENT	ICS	A	73 *
PEAK TORQUE CURRENT	IPK	A	510
COLD RESISTANCE	RC	Ω	0.07
HOT RESISTANCE	RH	Ω	0.10 *
MOTOR INDUCTANCE	L	mH	1.0

Note: * Windings at 155° C. Motor at 25° C ambient

Table 6.2 (Reference 33)
Characteristics of the R88 Brushless DC Motor

6.2 GEARING

In order to drive the tracks of the LCUV, given the required torque, power, and angular velocity with a direct drive DC electric motor a size 4363 frame (Reference 34) would have to be used. The size of this frame along with the weight of the entire unit (approximately 272kg) is far too large for use on the LCUV.

Having a smaller motor that runs at higher revolutions per minute and lower torque and using gear reduction that would be able to accomplish the same task as the larger motor would be more desirable. The efficiency of the motor will increase with higher angular velocity. In order to attain the specified power and torque requirements for the tracks, proper gearing must be utilized. In order to attain a rotational speed of 4500rpm which would yield the maximum linear torque of 54Nm specified in table 6.2 and drive the tracks at 35rpm a gear system with a gear reduction ratio of 125:1 must be developed. It was decided that the configuration shown in figure 6.7 would be the most suitable (Reference 6).

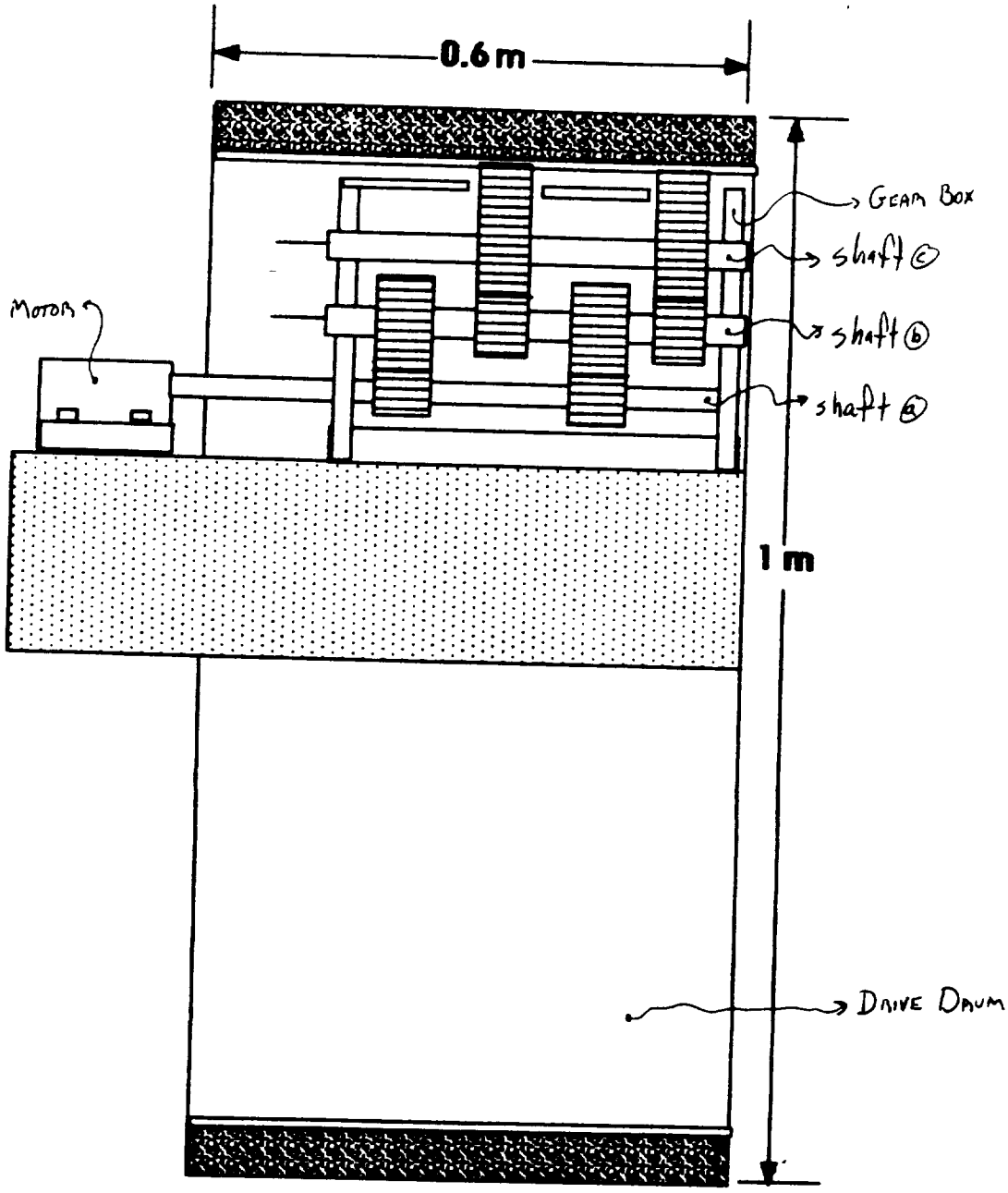

Figure 6.7
Schematic of the Gear Reduction Unit
125:1 Reduction

6.3 THE LUNAR DUST PROBLEM

The main aspect of the lunar dust that makes it a design issue is its abrasive nature. If the motor is not properly protected, the dust will substantially reduce the motors useful life (Reference 30). In order to avoid this, the motor's casing must completely enclose the motor to protect it, leaving only the shaft and front face of the motor open to the effects of the dust. The casing of the R88 model brushless DC motor is TENV sealed along with the shaft (see figure 6.5). An additional method which will be used to alleviate the effect of lunar dust on the shaft and front face is a dust cover made of flexible material. The material must be able to withstand the high operating temperatures of the motor and not in any way hinder the shaft from delivering the required torque. In the Environmental Control section of this report a dust cover made of beta cloth and teflon fiber is discussed in depth.

6.4 THERMAL DISSIPATION PROBLEM

The difficulties introduced by the absence of atmosphere on thermal dissipation of heat must be compensated for by introduction of methods to enhance heat dissipation by conduction and radiation (Reference 30). The method which has been developed to perform the task of heat removal from the motor is a radiator unit. This unit will be responsible for the heat removal needs of the entire vehicle. The heat that is generated by the motor is conducted to tubes that are wrapped around the motor and which circulate ethylene glycol. After the heat has been absorbed by the working fluid, it is carried away to the radiator which radiates the heat to the surroundings. The radiator is discussed in more detail in the Thermal Control section 7.1 of this report.

6.5 SOLAR RADIATION AND FLARE PROTECTION

The major concerns, as far as protection of the electric motor under the effects of the sun, are thermal fatigue of the materials when subjected to the frequent sharp changes in temperature and the problems affiliated with solar flares (Reference 30). As mentioned previously, the lack of atmosphere in addition to the weak magnetic field of the moon, provides little shielding from the radiational effects of the sun. The electric motor, like other external components, must be protected from these effects. A majority of the detrimental effects of the sun will be shielded by the drive drum and tracks. This in addition to the dust protection cover should be adequate in shielding the motor from unwanted radiation.

6.2 CONCLUSIONS

Taking into consideration all of the mentioned design restrictions, the electric motor that best fits the needs of the LCUV would be a brushless DC electric motor. The R88 model brushless DC motor that is developed by Pacific Scientific company has been chosen as an example, one motor will be used per track. In order to maintain a high efficiency rating, the motor will be run at high rpm's (4500 RPM at maximum forward velocity of the vehicle). Because the LCUV is to be controlled remotely during the unmanned missions, the vehicles top forward speed must be slow (approximately 0.2m/sec). A gears reduction unit with a reduction ratio of 125:1 must be used to reduce the speed of the motor from 4500 RPM to 35 RPM.

The motor that was presented in the applicable motor section, the R88 model brushless DC motor, was determined to satisfy all of the design constraints but can not be used on the LCUV because of heat generation in the windings during high loading situations. Additional means of heat removal must be designed in order for this motor to be utilized on the LCUV, or a specially designed motor must be found.

7.0 THERMAL CONTROL

Heat rejection on the lunar surface can only be accomplished by radiant heat transfer. This report provides a method for designing such a radiator. The calculations performed concentrate on the design of a radiator system for the Lunar Construction Utility Vehicle; however, the content provided can be used for other space applications.

7.1 RADIATOR DESIGN

Heat rejection on the lunar surface can only be accomplished by radiant heat transfer. The size of this radiator is determined by the amount of heat that must be rejected, temperature of the radiator surface, and the effective sink temperature. The radiator temperature is influenced by the thermodynamic cycle efficiency, pumping fluid characteristics, and the allowable material temperatures. The effective sink temperature is determined by the orientation of the radiator surface with respect to the sun and surface of the moon, as well as daytime and nighttime conditions and radiator location. The efficiency of the lunar radiator is improved by lower sink temperatures (Reference 35).

The radiator used in this design will be oriented perpendicular to the lunar surface. This type of orientation is advantageous as compared to a horizontal design since the radiator can have two active sides. By designing a radiator with two active sides, the overall dimensions will be significantly reduced (Reference 35).

The radiator material chosen for this design consists of the aluminum alloy 6061-T6 that will be coated with a zinc oxide pigment. This particular aluminum alloy was chosen since it meets the design criteria for lunar application (Reference 37). The coating selected was found to have a low absorptance-emittance ratio which is required when designing a radiator. The zinc oxide pigment is also stable under the influence of solar ultraviolet and penetrating radiation components of the space environment. In general, both of these effects will tend to raise the absorptance value (Reference 35).

Ethylene glycol will be used as the cooling fluid for the various components on the LCUV. These components include the hydrogen-oxygen fuel cell, two DC motors, and the on-board control system. The coolant temperature will range from 360 Kelvin (87 Celsius) to 369 Kelvin (96 Celsius). The boiling point for ethylene glycol is 471 Kelvin (198 Celsius) under one atmosphere of pressure, therefore, the liquid will be in the subcooled region (Reference 37).

A computer program was written by our group and has been included at the end of this report. The intent of this program was to aid in the design of our radiator system for the LCUV. In addition, this program can be used for other space applications using different parameters (Reference 35).

7.1.1 HEAT REJECTION CALCULATIONS

The first phase of the design process involves determining the rate of heat rejection required by the radiator. In this design heat must be removed from the hydrogen-oxygen fuel cell, DC motors, and the on-board control system. The rate of heat rejection required by this system was calculated for each individual component. The results are listed in Table 7.1.

Component	Heat Dissipation for Normal Operating Conditions	Heat Dissipation for Maximum Operating Conditions
DC Motors	3 KW	6 KW
Controls	negligible	negligible
Fuel Cell	3 KW	6 KW

Table 7.1
Heat Dissipation Requirements

Once the rate of heat rejection has been calculated, the mass flow rate will need to be determined. For these calculations the mass flow rate of the cooling fluid through a 2.54 cm diameter pipe is defined to be 0.54 kg/second. This mass flow rate was chosen in order that a turbulent flow would be produced. The reason behind this type of flow pattern will be discussed in the next section.

The temperature of the cooling fluid at the radiator outlet was chosen to be 360 Kelvin (87 Celsius). By using this temperature the specific heat of the cooling fluid can be determined. Since the specific heat of the cooling fluid varies slightly with temperature, only a small error is introduced into the calculations.

The temperature of the cooling fluid at the radiator inlet can be found by rearranging the following equation (Reference 35).

$$Q = w \cdot Cp \ (T_{fi} - T_{fo})$$

The relation between the temperatures of the cooling fluid and the radiator wall temperatures can be obtained by taking a heat balance at any location on the radiator. The heat balance is made between the radiative and convective heat flow for a unit area. The temperature drop through the wall is assumed to be small; therefore, the outside wall temperature is approximately equal to the inside wall temperature. Equating the convective and radiative heat flow results in the following expression shown below

(Reference 35).[1]

$$Hr \cdot (T_f - T_w) = \sigma \cdot \epsilon \cdot (T_w^4 - T_s^4)$$

Rearranging this equation gives the general expression for the radiator wall temperature (Reference 35).

$$T_w = T_f - \sigma \cdot \epsilon \cdot (T_w^4 - T_s^4)/Hr$$

The inlet radiator wall temperature becomes (Reference 35),

$$T_{wi} = T_{fi} - \sigma \cdot \epsilon \cdot (T_{wi}^4 - T_s^4)/Hr$$

The outlet radiator wall temperature becomes (Reference 35),

$$T_{wo} = T_{fo} - \sigma \cdot \epsilon \cdot (T_{wo}^4 - T_s^4)/Hr$$

In these equations for calculating the radiator wall temperatures the convective heat transfer coefficient can be estimated (Reference 35). The method for determining the convective heat transfer coefficient will be demonstrated in the next section. In addition, the effective sink temperature can be calculated as shown in a subsequent section.

7.1.2 CONVECTIVE HEAT TRANSFER COEFFICIENT

A popular method for computing the local Nusselt number for fully developed turbulent flow in a smooth circular tube is the Dittus-Boelter equation. The expression for this equation is as follows (Reference 38).

$$Nu = 0.023\ Re^{4/5} \cdot Pr^n$$

where n=0.3 for cooling. This equation has been confirmed experimentally for the following range of conditions (Reference 38):

1) $0.7 < Pr < 160$

2) $Re > 10{,}000$

3) $L/D > 10$

This equation should be used only for small to moderate differences in the cooling fluid temperature and radiator wall temperature.

Since the average Nusselt number for the entire tube depends

---

[1]Note: A list of subscripts and symbols are included in Appendix B.

on the inlet conditions, as well as on the Reynolds and Prandtl number, generally applicable equations are not available. However, to a first approximation, the foregoing equation may be used to obtain a reasonable estimate of the average Nusselt number. When determining the average Nusselt number all fluid properties should be evaluated at the arithmetic average of the inlet and outlet fluid temperatures (Reference 38).

Once the Nusselt number has been determined, the convective heat transfer coefficient can be calculated. The expression for the convective heat transfer coefficient is (Reference 38)

$$Hr = (Nu \cdot K)/D$$

7.1.3 EFFECTIVE SINK TEMPERATURE

Variables that affect the sink temperature (Ts) of a radiator are lunation, radiator location, and orientation. The radiator is subject to three different sinks: (1) the surface of the moon, which is assumed to be a black body, (2) space, and (3) the sun. For this reason equations must be developed expressing the effective sink temperature as a function of the three sink variables. The heat rejection rate for a .305 by .305 meter (1 by 1 foot) section of radiator with two active sides can be expressed in terms of radiator orientation, location, and lunation as (Reference 35)

$$q = 2 \cdot \epsilon \cdot \sigma \cdot T_{w,av}^4 - F_1 \cdot \epsilon \cdot \sigma \cdot T_m^4 - F_2 \cdot \epsilon \cdot \sigma \cdot T_m^4 - |G_s \cdot \alpha_s \cdot \cos\theta_n|$$

Since F1+F2=1.0, the above equation becomes: (Reference 37)[2]

$$q = 2 \cdot \epsilon \cdot \sigma \cdot T_{w,av}^4 - \epsilon \cdot \sigma \cdot T_m^4 - |G_s \cdot \alpha_s \cdot \cos\theta_n|$$

The lunar temperature (Tm) is given in figure 7.1. In our calculations we assumed that the LCUV would be operated at 45 degrees latitude. In addition, the radiator average wall temperature (Tw,av) for these calculations is the integrated average of the temperature of the radiator surfaces. The method for determining this will be given in the next section.

[2]Note: F1 and F2 are the shape factors for the radiator.

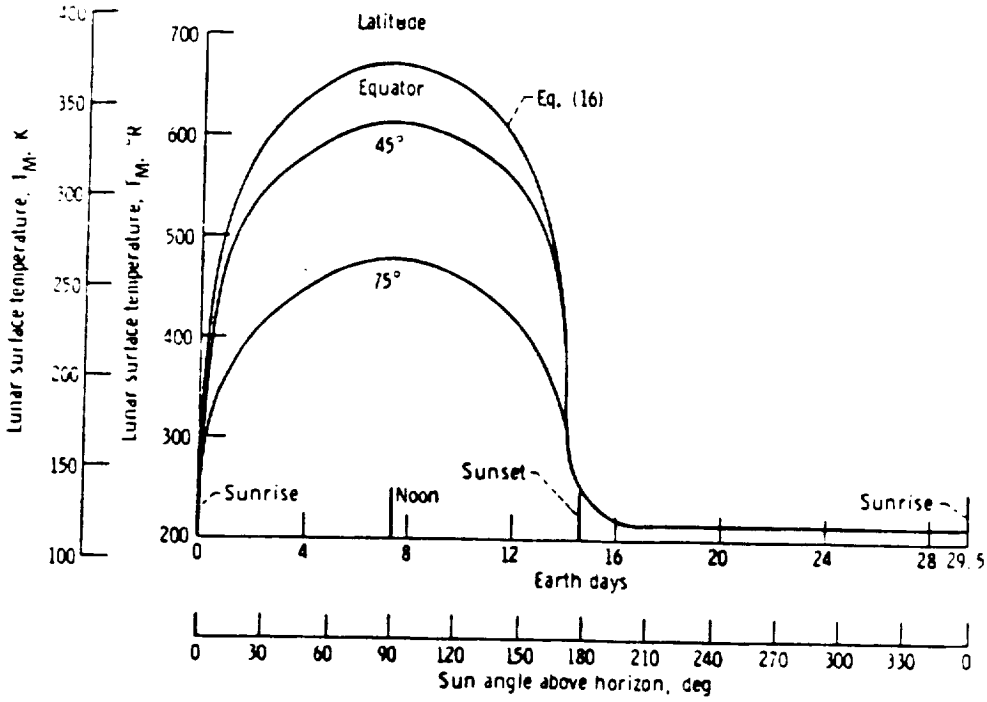

Figure 7.1 (Reference 35)
Lunar Surface Temperature

The heat rejection rate for a .305 by .305 meter section of a radiator with one active side can be expressed in terms of average wall and sink temperature by the following equation (Reference 37).

$$q = \sigma \cdot \epsilon \cdot (T_{w,av}^4 - T_s^4)$$

Since our design for the radiator has two active sides, the right side of this equation must be multiplied by 2.0.

For the radiator with two active sides, the last two equations can be combined to yield (Reference 35)

$$2 \cdot \epsilon \cdot \sigma \cdot T_{w,av}^4 - \epsilon \cdot \sigma \cdot T_m^4 - |G_s \cdot \alpha_s \cdot \cos\theta_n| =$$

$$2 \cdot \epsilon \cdot \sigma \cdot (T_{w,av}^4 - T_s^4)$$

Solving for the sink temperature results in

$$T_s = \left[\frac{T_m^4}{2} + \left| \frac{G_s \cdot}{2 \cdot \alpha} \left[\frac{\alpha_s}{\epsilon} \right] \cos \theta_n \right| \right]^{1/4}$$

7.1.4 RADIATOR WALL TEMPERATURE

When the heat rejection process is one similar to condensing, the fluid temperature is uniform and nearly constant from inlet to exit conditions. For this case, the arithmetic average of the inlet and exit wall temperatures can be used for average radiator wall temperatures. However, in a radiator, the temperature of the fluid decreases from inlet to outlet so that an integrated average should be used for this case. The expression for the radiator average wall temperature is shown below (Reference 35).

7.1.5 PRIME RADIATOR AREA

The prime radiator area (AR) can now be determined by using the following equation (Reference 35).

$$AR = Q/\sigma \cdot \epsilon \cdot (T_{w,av}^4 - T_s^4)$$

The radiator designed for the LCUV will have two active sides.

7.2 CONCLUSION

There will be two radiators used in order to reject heat from the fuel cell, two motors, and on-board control system. The primary radiator will be attached to the back of the vehicle behind the operator's bubble and will accommodate normal operating conditions during solar night. This radiator will have a prime area of 7.3 square meters. Since there are two active sides to the radiator, the overall dimensions will be 1.2 meters long by 3.0 meters high. If conditions become greater than normal for solar night operation a secondary radiator will be required. This secondary radiator can be attached to the vehicle by a trailer and will have a prime area of 15.0 square meters. The overall dimensions for this radiator will be 2.7 meters long by 2.7 meters high. The placement of these two radiators was chosen in order that they would not interfere with the LCUV working parts.

The advantages of this design include:

- This method of design can be used for any type of space applications.
- This radiator can be used with any type of coolant fluid.
- Radiant heat transfer is the only method to dissipate heat on the lunar surface.

The disadvantages of this design include:

- This radiator is quite large, especially under maximum power conditions.
- A pump must be designed for circulation of the coolant fluid.

8.0 ENVIRONMENTAL CONTROL

This paper will develop ways to provide environmental control of important areas of the Lunar Construction and Utility Vehicle. The purpose of this facet of the design is to develop ways to provide a manual control area that is protected from dust, debris, meteoroid showers, and radiation, while still allowing the vehicle operator to have an unobstructed view of the working area. A double pane system of glass, made of lithium-aluminumsilicate as the inner pane and fused-silica as the outer pane, placed over the cabin area will allow such protection and visibility. This design also includes a garment to protect movable parts from dust and debris, including the motors in the wheel well and the motors of the robotic arm. The cabin area will also be protected. A combination of Beta Cloth and Teflon TFE, similar to the garment used in the design of the Skylab Extravehicular Mobility Unit, will accomplish the desired result.

When dealing with space applications, environmental control becomes difficult. In this facet of the design, areas such as the manned control area, which will be referred to as the cabin, and the joints and openings of movable parts need to be kept free from dust and debris. Each area has special considerations that need to be taken into account due to the effects of the lunar environment. For example, the cabin area needs to be made of a transparent material that will allow the operator of the LCUV to have an unobstructed view of the working area. The covering of the movable parts, which shall be referred to as boots, need to be flexible and durable.

These designs are easily developed on earth. However, the harsh environment of the moon causes very different effects due to the large temperature gradients and radiation fluxes. The temperature and radiation changes have varying effects on all materials in this environment. An added problem that exist in the lunar environment is that of micrometeoroid showers. This becomes especially important if the operator is allowed to work while partially suited.

8.1 CABIN DESIGN

Although the initial stage of a lunar base buildup will not be manned, there will be an eventual need for a cabin area where manual control of the LCUV can take place. This section will outline some of the basic considerations of the cabin area.

8.1.1 ASSUMPTIONS

1) The vehicle will not need transparent material to cover the cabin area until the manned stages of the Split-Mission Project (Reference 10).

2) The cabin area will be covered by the same material being designed for the boot when the transparent spherical cover is not in place.

3) The Skylab Extravehicular Mobility Unit,(Reference 39), or a comparable spacesuit will be worn during operation of the vehicle.

The cabin area will be 1.5 meters in diameter. The covering of this area will be in the shape of a semi-hemispherical shell. This sphere will be made out of a material that will allow the controller 360 degree visibility while operating the vehicle from inside the cabin. The sphere can be assembled and disassembled by use of the robotic arm. The sphere will have three keywicks that will allow the bubble to be locked and unlocked by rotation; see Figure 8.1 for dimensions of the keywicks.

8.1.2 MATERIAL BACKGROUND

There are many types of materials that could be considered for the design of a transparent sphere. Due to project limitations on time, only glass materials were investigated.

Some problems when considering the use of glass are the absorption of X- and gamma radiation. The absorption of these types of radiation causes the formation of color centers, resulting in absorption bands with peaks at specific wavelengths (Reference 40). Most silicate glasses color brown under high energy radiation, 10^5 R or more. Phosphate glasses color purple, but have much narrower absorption bands. Ultraviolet radiation also produces coloration in glasses containing pairs of certain elements; e.g. As and Mn, As and Fe, Sb and Mn, and Sb and Fe; but this is highly dependent upon the ultraviolet wavelength (Reference 41).

Arutunian and Seppi (Reference 42) subjected transparent materials to x-ray irradiation to determine how ionizing radiation affected their optical transmission. The materials used were aluminate glass, polystyrene, plexiglass, allycarbonate and polyvinyl acetate. Figures 8.2 and 8.3 (Reference 41) show the transmission of solar radiation at the surface of the earth as a function of dosage. Often materials are also commonly used in infrared transmission including quartz, fused silica, and several glasses. Penetrating radiation induces in all of these materials changes similar to those discussed previously (Reference 42). Figure 8.4 (Reference 43) presents the charges in transmission efficiencies produced by gamma-irradiation of four different materials used in space infrared optics.

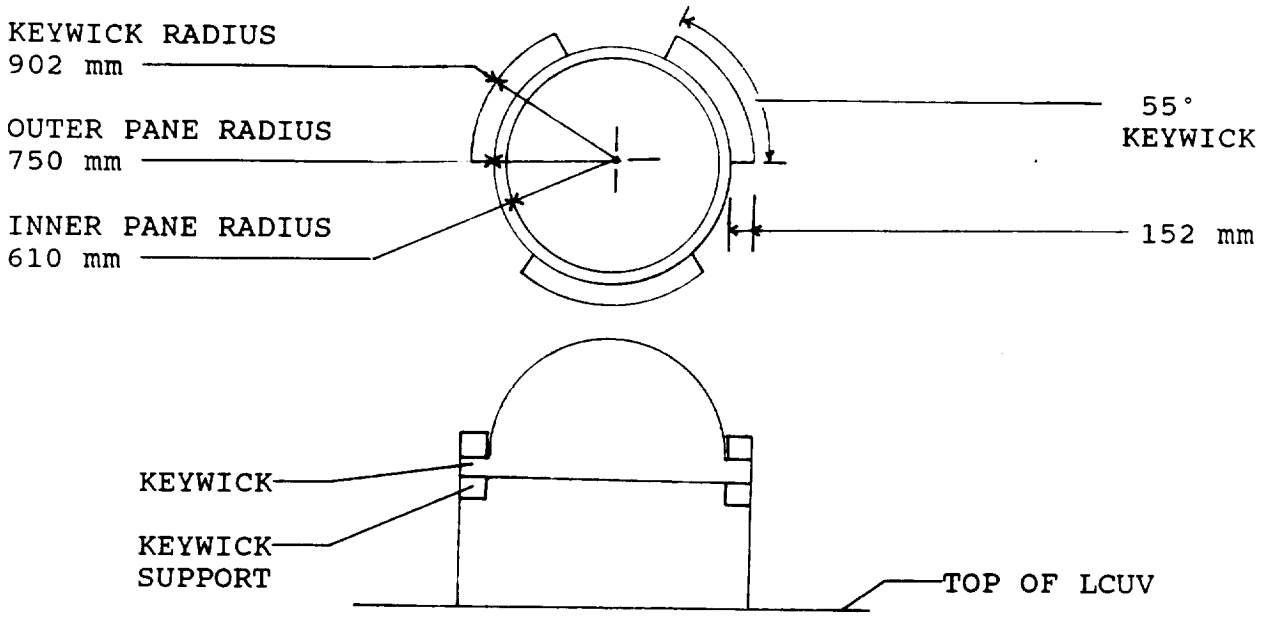

Figure 8.1
Manual Control Area Cover

"It is obvious that many materials can be used in space applications, however, materials which are resistant to the effects of the total space environment must be used. It is important to realize that the materials themselves will determine in large part temperature control requirements and the ability to fulfill them" (Reference 44). Knowing that large temperature variations exist on the moon, low coefficients of thermal expansion and high resistance to thermal shock are necessary properties of any material used in space design.

Many types of glasses have been used in space technology. Examples of the use of glass in space come as early as 1958 in which the Vanguard I satellite used a 1/16 inch thick quartz solar cell cover (Reference 45). The first optical material used as viewing windows was an aluminum silicate glass used on the Mercury-Atlas which was first orbited on September 13, 1961 (Reference 46). "Today, the space shuttle uses a three pane system for its crews viewing purposes...The innermost pane of the shuttle is constructed of tempered aluminosilicate glass to withstand the crew's compartmental pressure. The center pane is constructed of low expansion fused silica glass due to its high optical quality and excellent thermal shock resistance. The outer pane is made of the same material as the inner pane" (Reference 47).

After obtaining information about past uses of glass in space technology, engineers from various glass manufacturers were consulted. Various questions were asked about the types of glass materials used in space applications and how these glasses would react to the effects of the lunar environment and to the effects of the stresses placed on it by shaping it into a hemispherical shell. Results of the conversations are displayed in Table 8.1.

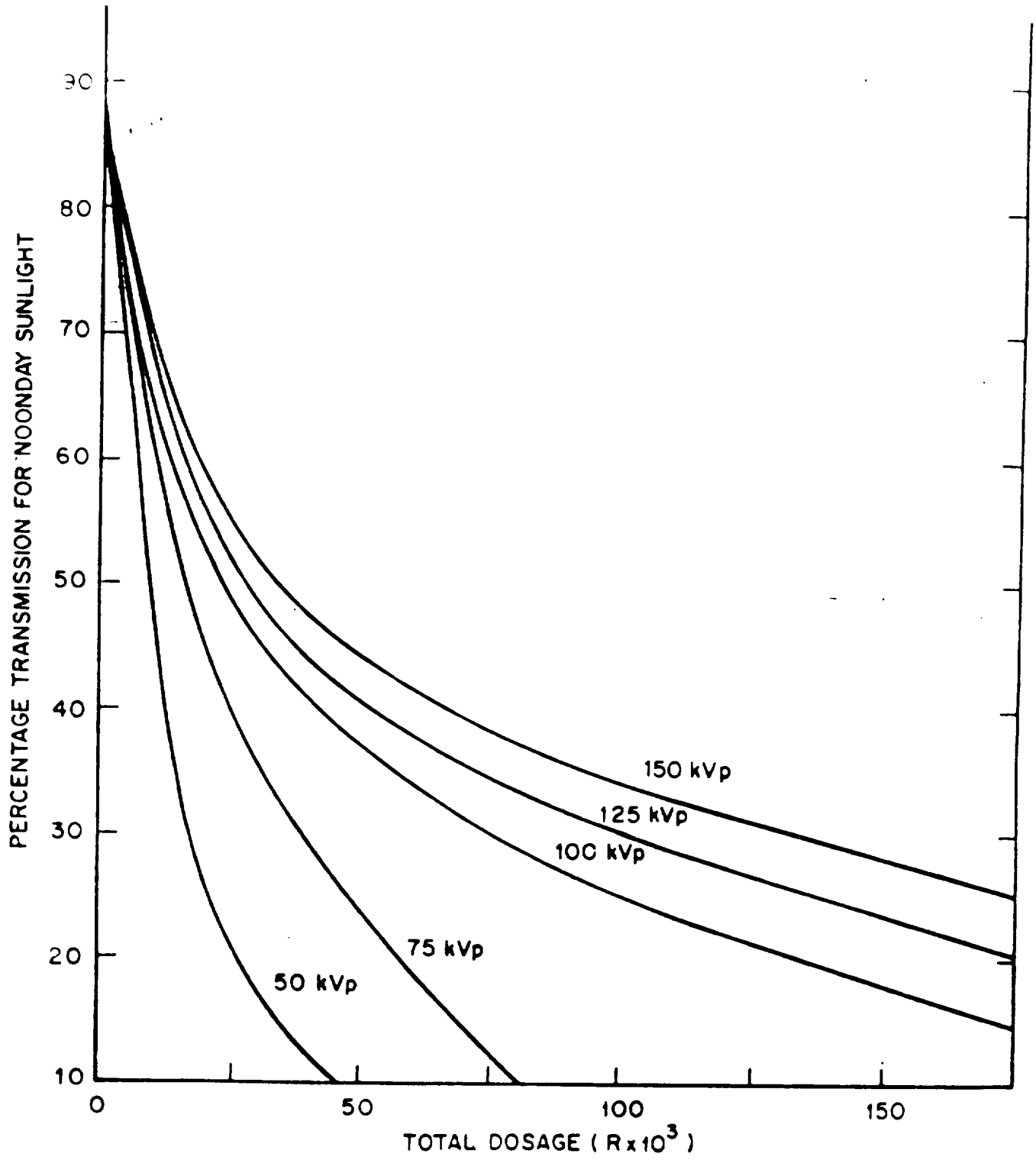

Figure 8.2 (Reference 41)
Transmission of Commercial-Grade Aluminosilicate
Glass After Irradiation by X-Rays of Various Energies

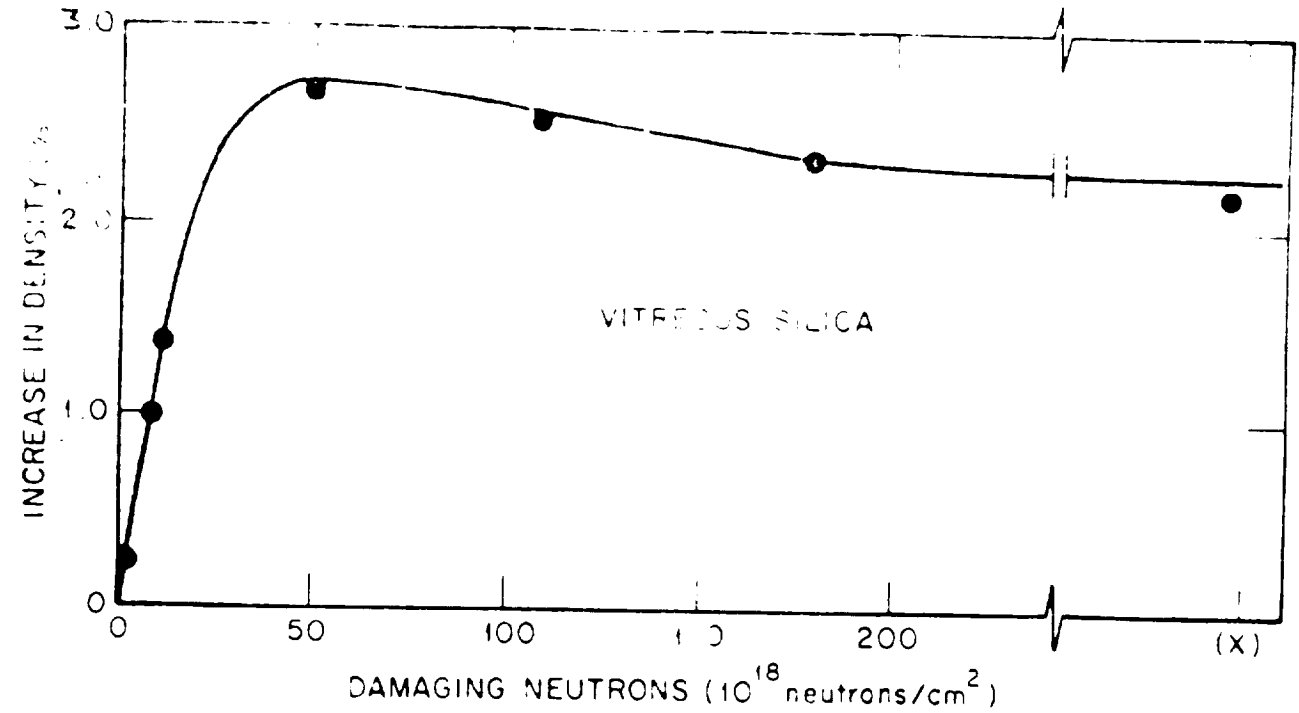

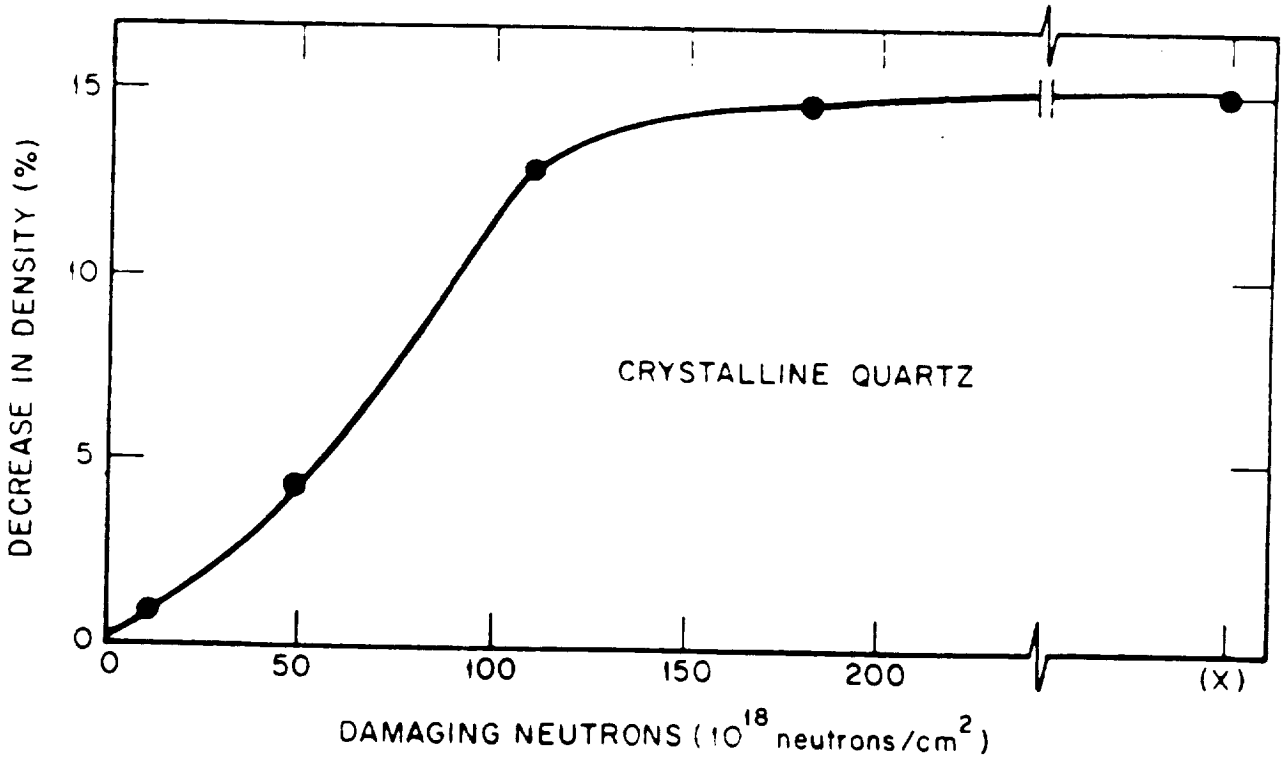

Figure 8.3 (Reference 41)
Change in Density of Vitreous Silica and Quartz on Irradiation in Nuclear Reactors. The dosage at (x) is estimated at 250 to 400.

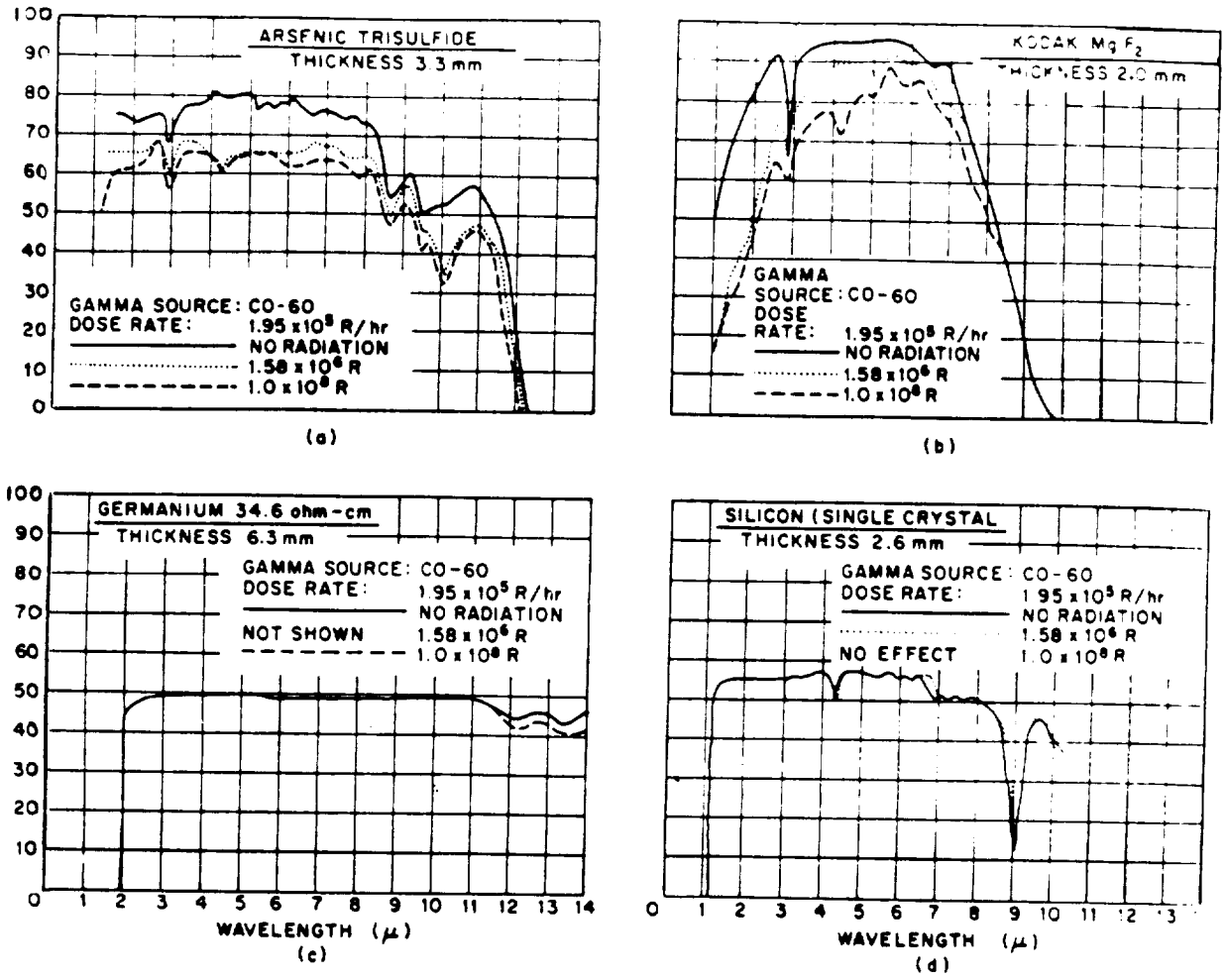

Figure 8.4
Effects of high level radiation on transmission efficiency of four materials presently used for space vehicles.

	MATERIAL	COMMENTS
CABIN COVER COMPONENTS	CORNING GLASS	(REFERENCE 10)
DOUBLE PANE (INNER)	TEMPERED LITHIUM ALUMINO SILICATE	USED PREVIOUSLY HIGH MELTING TEMPERATURE ABRASION RESISTANT HIGH STRESS
DOUBLE PANE (OUTER)	FUSED SILICA	STRENGTHENED HIGH MELTING TEMPERATURE LOW EXPANSION NO DARKENING
FILM MATERIAL	ZECONIA SILICATE HAFNIA SILICATE TANTILIA SILICATE SCANDIA SILICATE	ALL RECOMMENDED FOR USE IN SPACE VEHICLES

Table 8.1
Cabin Cover Materials

H Misca (Reference 48) felt that there are a several different types of glasses that could handle the environmental effects, but because of aluminosilicate's long history of success, it is the material to use. Mixing the aluminosilicate with lithium will give the resulting material, lithium aluminumsilicate, the strength to deal with higher bending stresses. This will allow it to stay strong in the spherical shape (Reference 48). Because aluminosilicate will darken from the radiation exposure, Misca also recommends using a double pane system. The outer pane will be made out fused silica or Silicon Dioxide. The reason for using silicon dioxide is to strengthen the glass. It also has a low coefficient of expansion, and it is considered a high temperature glass (melting between 1200-1400 degrees Celsius). This type of glass will not darken due to radiation, and it will provide added strength and protection against micrometeoroid impact.

Placing a highly reflective film on the outer and inner pane of the Si-O2 glass will allow the inner pane a longer period before the radiation will darken it. Added protective films should be placed on the inner pane as well to help reduce the effects of the damaging ultraviolet, infrared, and x-rays (Reference 48). Some useful films (Reference 50) for the inner pane are shown in Table 8.1.

8.1.3 DESIGN DECISIONS

A double pane system will be used as shown in Figure 8.1. The inner pane will be made of 12.7 millimeters thick tempered lithium-aluminosilicate glass and has a silicate or reflective coating that will reflect the infrared and ultraviolet rays. This will aid in both thermal control and the problem of glass darkening. The outer pane should be 1.59 millimeters thick to help prevent it from cracking due micrometeoroid impacts. It should be coated with a high efficiency antireflective coating to improve visible light transmission. This is similar to that used on the space shuttle's forward windows (Reference 47).
A summary of the design choices and the primary reasons for these choices are outlined in Table 8.2.

The film information that has been obtained is general in nature. The thicknesses expressed by Meskot (Reference #10) were based primarily on the those taken from the space shuttle's press information (Reference 47). There has been a modification of the inner surface due to the lack of pressurization of the lunar vehicle. The total weight of the covering was calculated to be 64 kilograms (Reference 50). A summary of the weights of each component of the glass sphere is shown in Table 8.3.

DECISION	RATIONALE
GLASS	UNOBSTRUCTED VISIBILITY
SPHERICAL SHAPE	NO BLIND SPOTS
KEYWICK LOCK	SIMPLE DESIGN CAN BE PRESSURIZED
DOUBLE PANES	HIGH STRENGTH LONG LIFE RADIATION RESISTANT FACILITATES PRESSURIZATION
FILM COATED INNER PANE	PROVEN SPACE DESIGN
REFLECTIVE FILM OUTER PANE	ADDS STRENGTH PREVENTS DARKENING

Table 8.2
Cabin Area Design Summary

	INNER PANE	OUTER PANE
MATERIAL	LITHIUM-ALUMINUM SILICATE	FUSED SILICA
DIAMETER (m)	1.22	1.5
THICKNESS (cm)	1.27	1.59
MASS (kg/m^2)	4.68	5.95
INNER SURFACE AREA (m^2)	4.67	7.07
MASS (kg)	21.9	42.1
LUNAR WEIGHT (N)	35.7	68.7
NOTE: PROPERTIES BASED ON FLOAT GLASS (REFERENCE 50)		

Table 8.3
Cabin Area Covering Weights

8.1.4 PRESSURIZATION

One of the design assumptions was that the operator would always be in his space suit. Consideration was also given to the possible pressurization of the LCUV. If the operator were allowed to remove his hands from the suit gloves during operation of the vehicle, the task could probably be done more efficiently while allowing the pilot to be more comfortable during long work sessions aboard the LCUV.

The glasses that are recommended have withstood a proof pressure of 8600 psi at 115 degrees °C and 0.017 relative humidity on the space shuttle (Reference 47). It is also possible for humans to work in environments for a period of time with a pressure as low as 5 psia (Reference 52). The space shuttle has been hit by a micrometeoroid in the glass area resulting in a small indention with no leakage (Reference 53). This leads us to believe that pressurization of the cabin at a low pressure is possible; however, until further research on the details of this design can be obtained, this design will recommend a pressureless cabin.

Safety considerations caused the pressurized cabin option to be scrapped. If the glass covering were cracked and a sudden loss of pressure resulted, the operator would be subject to a life threatening situation. If he lived through the explosive decompression, he would need to repressurized his hands quickly in order to prevent permanent injury. Pressurization also complicates

and adds weight to the design. Since the design goals are to keep the overall mass as low as possible and to simplify the details, pressurization was ruled out for this initial design of the LCUV.

8.2 DUST COVERING DESIGN

The coverings that will be used to keep dust and other debris out of working parts of the LCUV will be referred to as boots. The proposed coverings will be placed over the wheel wells of the tracks, mechanical arm joints, and the cabin area.

The main problem for this design was finding a material that was flexible enough to move with the equipment and seal the parts from dust. The materials that were considered are Dupont Teflon TFE fiber, and Beta Cloth, made by the Owens-Corning Corporation. Both Beta Cloth and Teflon fibers have been used in the Skylab Extra Vehicular Mobility Unit. The properties of the two materials that were used for the spacesuit design are shown in Table 8.4 (Reference 39). Because the extravehicular garment assembly (or spacesuit) has many of the same general requirement as the boot, the materials used in the EVA suit have been considered in the boot design.

8.2.1 MATERIAL BACKGROUND

The general requirements of the EVA suit and the boot are similar. Both must have the following material properties: they must resist high temperature while reflecting the suns rays, be resistant to abrasion and scratching; and be able to withstand high velocity meteoroid impacts, while not letting the dust and debris stick to the cover. As Table 8.4 shows, Beta Cloth and Teflon TFE when combined, have the properties needed for the boot material.

	MATERIAL	FUNCTION
OUTER COVERING OF INTERVEHICULAR MOBILITY UNIT	BETA CLOTH	WOVEN GLASS FIBERS GOOD INSULATOR
	TEFLON TFE	HARD AND FLEXIBLE FLUOROCARBON MATERIAL HIGH TEMPERATURE MATERIAL ABRASION RESISTANT SCRATCH RESISTANT STICK RESISTANT
INTEGRATED THERMAL MICROMETEOROID GARMENT	10 LAYERS MIXED WITH:	
	BETA CLOTH	SAME AS ABOVE
	KAPTAN	INSULATING MATERIAL
	TEFLON TFE	SAME AS ABOVE
	COMBINATION	PROTECTS AGAINST SOLAR RADIATION AND MICRO-METEOROID IMPACT

Table 8.4 (Reference 39)

Extravehicular Mobility Unit Outer Materials

One of the main problems with this design is the longevity of the materials being used. This is also a problem with the EVA suit design; the exact useful life span of the spacesuit has not yet been determined (Reference 55). To express why the Teflon fiber is being used in the boot design, Table 8.5 shows some general properties of the fiber. Teflon fiber is the most chemically-resistant fiber known. Molecules of Teflon fiber are electrically neutral and have no strong polar forces binding them together, as in the case of nylon or cellulosic fibers. The unique molecular structure of this Teflon fiber also accounts for the fibers stability at extreme temperature conditions. The fiber softens at elevated temperatures and becomes less ductile at sub-zero temperature; however, experience indicates that adequate toughness and strength are available for uses at temperatures as low as -268°C and as high as 288°C. The fibers are found to be most ductile and flexible between 288°C and -268°C. The maximum temperature Teflon TFE fiber can be exposed for long periods of time is 288°C, but brief exposures to temperatures as high as 316°C can be tolerated (Reference 57). Sunlight resistance and radiation resistance is a necessity to any material used on the lunar surface. The sunlight and weather resistance of this fiber is outstanding according to DuPont (Reference 58). Three years continuous use in Miami, Florida, produced only a 2% loss in yarn strength (Reference 59). "The effects of high radiation and vacuum conditions of this fiber are given in by (Figure 8.5)" (Reference 57).

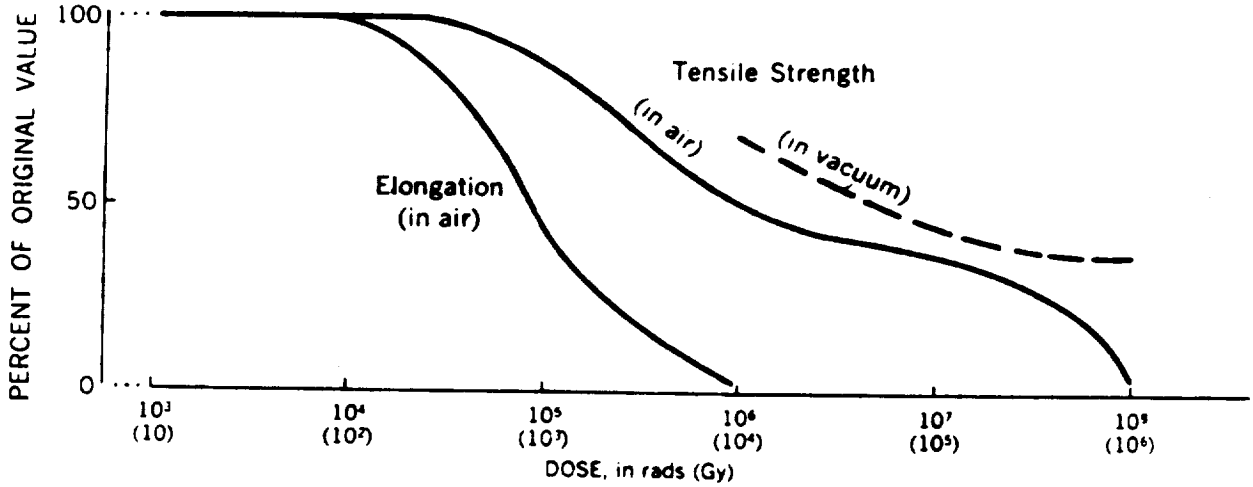

Figure 8.5 (Reference 57)
Effects of Radiation on Teflon

TYPICAL PROPERTIES FOR UNBLEACHED YARNS OF TEFLON TFE FIBER		
YARN DENIER (1 GRAM PER 9000 METERS)	400	1200
STRESS STRAIN PROPERTIES		
STRENGTH TEST TENSILE STRENGTH (MPa) BREAKING STRENGTH (N) BREAKING TENACITY (G/DEN) ELONGATION AT BREAK (%) INITIAL MODULUS (G/DEN)	 359 7.6 2.0 19 13	 290 18.7 1.6 35 8.3
LOOP TEST TENSILE STRENGTH (MPa) BREAKING STRENGTH (N) ELONGATION AT BREAK (%)	 214 8.0 8.5	 197 24.5 18
THERMAL PROPERTIES	BOTH	
SHRINKAGE AFTER 30 MIN. (%) IN WATER AT 100°C IN AIR AT 177°C	 2.5 6.0	
SPECIFIC HEAT (CAL/G/°C)	0.25	
THERMAL CONDUCTIVITY (W/m² K/cm thk.)	3.8	
ZERO STRENGTH TEMPERATURE (°C)	310	
GEL TEMPERATURE (°C)	327	
SUBLIMATION RATE (% WT. LOSS/HR) AT 290 °C AT 430 °C	 0.00002 1.5	
GENERAL PROPERTIES		
SPECIFIC GRAVITY	2.1	
MOISTURE REGAIN (%)	0.0	
FILAMENT DIAMETER (mm)	0.02	

Table 8.5
Properties of TFE Fluorocarbon Yarns

8.2.3 DESIGN DECISIONS

The final design of the boot cannot yet be detailed. It is known that the material to be used will be a Beta Cloth and Teflon TFE mixture interwoven much the same as the outer garment of the EVA. The part of the design that cannot be finalized deals with the thickness of the interwoven material. Powell (Reference 54) explained, "Every specific use of the Teflon TFE fiber needs its own testing in order to find out the fibers specific reaction due to a mixture of materials in a certain environment."

8.3 CONCLUSIONS

As shown, trying to provide a safe and clean environment with the conditions that exist on the moon is very demanding. A double pane hemispherical shell made of fused-silica on the outside and lithium-aluminumsilicate on the inside was chosen as the cover of the manual control area of the LCUV. A fiber mixture of Beta Cloth and Teflon TFE has been chosen to keep vital areas free from dust, debris, and meteoroid showers. This material is very flexible and has been shown to stand up to severe conditions and large temperature variations. This work is somewhat general in nature. Once the details of the LCUV begin to emerge, a detailed design of the boots and coverings can be accomplished.

9.0 RADIATION SHIELDING

This report explains the radiation hazards present on the lunar surface. Radiation has two effects on humans, somatic and genetic. Its chief energy form is that of ionizing matter. A strategy to shield man from radiation has three steps: (1) aluminum is used on the hardshell casing of the lunar vehicle, (2) Kapton films meshed with quartz fibers are blanketed in the interior of the module, (3) a protective coating of aluminum will then be applied to the exterior of the lunar vehicle. Concluding remarks will address the feasibility and safety issues.

9.1 RADIATION TYPES

Ionizing radiation is man's greatest concern. "In this category are solar, galactic, and extragalactic cosmic rays, X rays and gamma rays from the Sun, solar flare and solar wind particles, electrons and protons of the Van Allen Belts of trapped radiation, neutrons, and alpha particles (Reference 60)." Why does radiation due to the Sun exist on the Moon and not on the Earth? The Earth's atmosphere and magnetic fields act as a shield, blocking out harmful radiation rays. The Moon, however, does not have an atmosphere and therefore has no radiation shielding (Reference 60). Knowing that radiation now exists on the Moon, what is its chief source? This question leads us into the discussion of the 'Cosmic Barrier'. 'Cosmic Barrier', as its name infers, involves cosmic radiation. Cosmic radiation involves primary and secondary radiation (Reference 61). Secondary radiation is what man encounters on earth everyday. This type of radiation is not harmful due to the earth's atmosphere and magnetic field like shielding. However, primary radiation is what man encounters in space and it is this type that proves detrimental to his well being. Of this primary radiation exists solar cosmic rays and galactic rays, where "The most energetic charged particles reaching the Moon's surface come from outside the solar system in the form of galactic cosmic rays (Reference 62)." As Table 9.1 shows, the penetration depth for galactic cosmic rays is greater than that of solar cosmic rays (Reference 62). Galactic cosmic rays originate out of the solar system; however, solar cosmic rays are associated with the solar flares. These solar flares produce radiation in the form of high and low energy (Reference 61). Certain flares occur once every four or five years, and some occur once every ten years (Reference 61). Knowing the extreme hazards of radiation, we can draw conclusions about exactly what the lunar vehicle will experience. On the other hand, radiation of the energy nonionizing form is not a real threat to man's safety in the lunar vehicle. "The nonionizing radiation consists of infrared and ultraviolet light from the Sun, visible light, and microwaves in the radio-frequency spectra (Reference 60)." These types of radiation have no real penetration abilities, and what little they have is blocked from the hardshell casing of the lunar vehicle, which would most likely be aluminum.

SOURCE	MeV PER NUCLEON	PROTON FLUX (Ncm^-2 S^-1)	PENETRATION DEPTH (cm)
SOLAR WIND	10 E-3	10 E8	10 E-6
SOLAR COSMIC	1 TO 100	100	0.001 TO 1
GALACTIC	100 TO 10 E4	1	0.001 TO 1

Table 9.1
Radiation Environment at Lunar Surface

9.2 BIOLOGICAL EFFECTS OF RADIATION

In space, human contact with radiation can prove detrimental to his well being. There are two types of harmful effects possible to man due to radiation exposure. They are somatic and genetic effects (Reference 63). The somatic effect causes permanent cellular damage to man (Reference 63). If his cells begin to deteriorate so will the rest of his body. Genetic effects will not affect man directly but his offspring may be born with genetic defects (Reference 63). A certain case documented a mother and father who were in space and later conceived healthy children (Reference 60). Obviously, there was no genetic effect, but these astronauts were only in space for 24 hours (Reference 60). The lunar base, on the other hand, would be a permanent settlement; therefore, a major concern to man would be the genetic effect he had on his offspring due to radiation effects. American physicist, Dr. Arthur Rinfert, had an idea as to how to solve the problem. Dr. Rinfert suggested storing spermatozoa from the astronaut before he is exposed to the radiation involved in a lunar habitat (Reference 60). This is a simple solution to a problem that man may have to face in later years.

We must understand that the radiation limits for astronauts are very difficult to obtain. However, maximum radiation levels were established from the Apollo Project (Reference 60). 980 REM is the maximum dose for feet, ankles, and hands (Reference 60). "The roentgen equivalent mammal (REM), is the amount of any ionizing radiation absorbed that has the same relative biological effectiveness as one roentgen of X rays (Reference 60)." Again from the Apollo Project, 700 REM is the maximum permissible dose for the entire body, and 200 REM is the maximum for the eyes and blood-forming organs. From Table 9.2, one can compare and estimate the impact radiation sources have on humans (Reference 63).

LIFESTYLE	SOURCE OF RADIATION	ANNUAL DOSE (mREM)
WHERE YOU LIVE	COSMIC RADIATION AT SEA LEVEL (1)	30
HOME	WOOD	30
	CONCRETE	34
	BRICK	34
	STONE	36
	GROUND	15
	EATING, DRINKING BREATHING	25
HOW YOU LIVE	JET FLIGHTS	4 (2)
TELEVISION	BLACK AND WHITE	1
	COLOR	2
MEDICAL	X-RAY CHEST	150
	X-RAY DENTAL	20

Note: 1. Add 1 mrem for every 30 m above sea level
2. Multiply by the number of long flights

Table 9.2 (reference 63)
Compute Your Own Radiation Dose

9.3 STRATEGIES IN RADIATION EXPOSURE

At this point, the extremely hazardous conditions that the lunar vehicle will be experiencing have been explained. Thus, the problem is how do we devise and construct a shielding to protect the Lunar base inhabitants. Today, few solutions have been documented to do this. Our proposed solution involves three steps. First of all, a hardshell casing material for the lunar vehicle must be designed. Secondly, Kapton films meshed with quartz fibers will be placed in areas that astronauts will work. Finally, as an extra precaution, a protective coating of aluminum will be applied to the outside of the lunar vehicle. The hardshell casing material of the module must first be designed. Taking into account the weight and cost of materials, aluminum is a good choice. Aluminum is an excellent shield of gamma rays, and it is a very light metal (Reference 64). After narrowing the category of material to aluminum, the next step is to define an aluminum type. Pure aluminum would be the optimal choice, since it is also fairly strong. Having this characteristic will prove beneficial since it may also provide protection from falling meteoroids. It should be noted that pure aluminum in its early stages is soft. However, it

can be hardened by cold working and alloying (Reference 64). From Table 9.3, note that pure aluminum has a melting point that is well over the maximum temperature of 130° C at the Moon's equator (Reference 64). This is indeed another plus to our decision of choosing pure aluminum. Concluding remarks on the choice of pure aluminum are that it is: (1) an excellent shield in the protection against gamma rays; (2) a moderate strength material; (3) light weight and fairly low in cost; (4) easily hardened; (5) has a melting point well over the maximum temperature reached on the Lunar surface.

The second step in this protection process is the placement of Kapton films in areas where man will interact and systems that may be damaged from exposure of radiation. These Kapton films are used for insulation in satellites, providing for thermal control (Reference 66). However, when Kapton films are used with quartz fibers they can reject the Sun's harmful radiation (Reference 66). Quartz fibers are made from Stevens #581 fabric or quartz paper (Reference 66). "Simple calculations indicate that in a square centimeter of quartz paper there 130,000 fibers. There are only 25,000 fibers in #581 fabric (listed in Table 9.4). This quartz paper is much more efficient; it reflects 80% of the Sun's visible energy (Reference 66)." Therefore, having the quartz paper meshed with the Kapton films would not only prove as an insulator, but more importantly it would serve as a radiation shield. This may seem like an extra expense since the pure aluminum hardshell casing is already being used as a shield; however, the Kapton films meshed with the quartz fibers would provide an extra layer of protection in the event that radiation passed through the hardshell casing of pure aluminum. Very briefly, a protective coating of aluminum will be applied to the outside of the lunar vehicle. This coating will provide in an extra layer of protection to the vehicle and to anyone operating it. This too may seem like an extra expense; however, safety is the most important objective in our design analysis. Also, Phase I of the Lunar Split Mission (Reference 10) is unmanned, and any damage that occurs due to radiation could slow the process of construction.

9.4 CONCLUSION

We have come to understand that "the greatest threat to man in space is the radiation he encounters there (Reference 60)." For a manned or unmanned lunar vehicle, certain precautions must be undertaken and solutions must be designed to deal with this problem. A solution to this problem is use aluminum as a shielding material and to employ Kapton film as a secondary shield. The Kapton film meshed with quartz fibers has the added benefit of providing a way to thermally insulate the vehicle from the sun. The actual design details of this proposal have not yet been determined. It should be noted that adding to thick of an aluminum shield can actually increase the radiation levels by exciting secondary reactions. This problem and the details of this report are both a subject for further study.

10.0 COMMUNICATION SYSTEM

One of the major components of any space vehicle is its communication system. The purpose of a communication system is to provide a command link from Earth to the space vehicle. The command link for the LCUV represents the communications link from Earth to the vehicle and will relay instructions to the vehicle. Commands will be needed for routine operation and control of the LCUV; some commands may be provided for changing the emphasis of the vehicles mission, should unexpected conditions arise; others may be required to correct erratic operation of the space vehicle (Reference 67).

The need for a reliable command link from the Earth to the lunar surface is important since it provides the only means to influence the lunar vehicle after it is launched. The correct performance of all maneuvers depends on the accuracy of command and instruction transmission. Hence, the foremost requirement for command links is reliability of transmission; transmission error rates must be very low (Reference 67). In order to ensure proper vehicle performance, the transmission error rate for the LCUV must be designed to be extremely low so as to prevent malfunctions that would result in a mission loss.

10.1 ASSUMPTIONS AND DESIGN CONSTRAINTS

The LCUV is a two phase operation. Phase I is the unmanned portion of the mission in which all of the vehicles maneuvers are controlled from Earth. Therefore, the need for a command/control link from the Earth to the lunar surface is apparent. This link will be the only means of communication between the LCUV and the Earth base site. Phase II of the mission incorporates the presence of humans on the lunar surface into the operation of the LCUV. This will require a voice link from the lunar base site to Earth. On the lunar surface, the LCUV will be operated by remote control from the base site or manually by humans within the LCUV. Thus, a line of sight remote control system and a voice link from the base site to the LCUV is needed. The following information is presented with regard to both phases of the mission (Reference 10).

In order for the LCUV to operate as expected, radio waves must effectively overcome extraterrestrial noise sources. There are a number of unavoidable sources of noise which are Earth bound. These noises include components introduced by absorption of radio waves in propagation through the ionosphere and troposphere, atmospherics from electrical discharges in the atmosphere (which are a severe problem at low frequencies), unavoidable radiation from the ground near an antenna site into the backlobes of the antenna and losses within the antenna itself (Reference 70).

Another major design constraint is the time delay that exists between the Earth and Moon when radio waves are transmitted from source to receiver. This time delay is approximately 2.6 sec round-trip (Reference 68). The transmission time delay is a function of the transmission distance and is shown in figure 10.1.

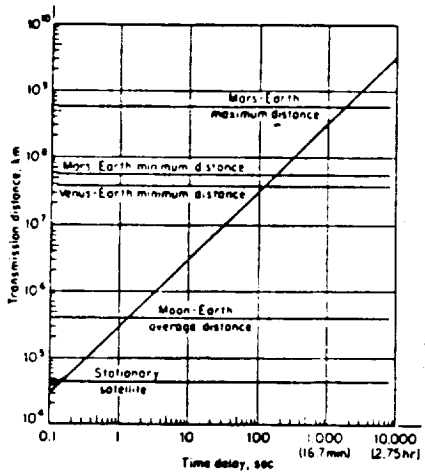

Figure 10.1 (reference 68)
Transmission Delay Time

The LCUV will utilize microwave transmission of the commands from Earth to the lunar surface. Microwaves have been used successfully in the past, and will be implemented in order to ensure radio transmission. The location of microwaves with regard to frequency and wavelength can be seen in figure 10.2.

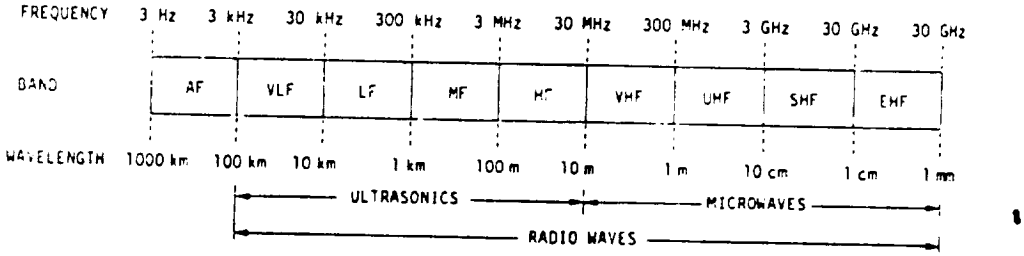

Figure 10.2 (Reference 72)
Wave Spectrum

10.2 PHASE I COMMAND/CONTROL LINK

The command/control link will be used to stop, start, steer, maneuver, and change the speed of the vehicle, to vary the setting of the camera lens, and to perform various construction operations (Reference 68). The information carried on the command link will generally include commands and instructions. For example, when the LCUV is commanded to assume a certain orientation, the command would be "orient vehicle" and the instruction would specify the vehicle's direction in a reference frame which is sensed by the vehicle (Reference 67).

In the past, two kinds of command link techniques have been employed for space vehicles: tone systems and digital systems. Tone systems can be considered a form of analog transmission. In the tone-actuated command system, a command tone modulated on a carrier is transmitted to the space vehicle. This tone is received and recognized by a filter. The received signal in the filter output then actuates a switch which leads to the execution of the command (Reference 67). Digital transmission is the transmittal of digital pulses between two points in a communications system. The original source information may already be in digital form or it may be analog signals that must be converted to digital pulses prior to transmission and converted back to analog form at the receive end (Reference 69).

Tone-actuated systems are capable of relaying only a very small number of different commands (7 to 10 at the most). Practical systems that have been developed require a 15 kc bandwidth for 7 tones (Reference 67). The total available command frequency band at 136 Mc permits only a limited number of about 25 tones (Reference 67). This would require a common use of one command tone for different space vehicles and leads to the possibility of causing unscheduled command functions. The tone system is quite unsecured, and unauthorized commanding of the LCUV would be rather simple. Another limitation of the tone system is the required high signal-to-noise ratio of 20 to 30 dB (Reference 67).

The foregoing disadvantages have spurred the use of more digital transmission systems in space vehicles. The primary advantage of digital transmission is noise immunity. Analog signals are more susceptible than digital pulses to undesired amplitude, frequency, and phase vibrations (Reference 69). This is because with digital, it is not necessary to evaluate these parameters as precisely as with analog transmission. Instead, the received pulses are evaluated during a sample interval, and a simple determination is made whether the pulse is above or below a certain threshold (Reference 69). Also, digital pulses are better suited to processing and multiplexing than analog signals. Digital pulses can be stored easily, whereas analog signals cannot (Reference 69). Another important feature of the digital system is that the transmission rate can be easily changed to adapt to different environments and to interface with different types of equipment.

Considering the various operations that are involved in the communication link between Earth and the LCUV, it seems as though digital transmission will be more effective than the tone system. Also, the more sophisticated digital system will become more powerful in the future as technological advances are made in the field of digital communication. The following is a summary of the disadvantages and advantages of tone and digital systems that led to the choice of digital transmittance for the LCUV.

Disadvantages of tone-actuated systems:

- Capable of relaying only a very small number of different commands
- Total available frequency band permits limited number of signals
- System is unsecured, and unauthorized commanding is rather simple
- Requires high signal-to-noise ratio

Advantages of digital transmission:

- Less susceptible to noise
- Digital pulses can be stored easily
- Transmission rate can be easily changed
- Can easily interface with different types of equipment

Although the LCUV will utilize digital transmission of command signals, the following is a list of the disadvantages of the digital system that need to be recognized in the design of the command/control link:

Disadvantages of digital transmission:

- Requires more bandwidth
- Analog signals need to be converted to digital codes prior to transmission and converted back to analog at the receiver
- Requires precise time synchronization between transmitter and receiver clocks
- Digital systems are incompatible with existing analog facilities
(Reference 69)

10.2.1 PULSE MODULATION

Pulse modulation includes many different methods of transferring pulses from a source to a destination. The four predominant methods are pulse width modulation (PWM), pulse position modulation (PPM), pulse amplitude modulation (PAM), and pulse code modulation (PCM) (Reference 69). These four methods of pulse modulation are summarized below and shown in Fig.3.

1. PWM. This method is sometimes called pulse duration modulation (PDM). The pulse width (active portion of the duty cycle) is proportional to the amplitude of the analog signal.

2. PPM. The position of a constant-width pulse within a prescribed time slot is varied according to the amplitude of the analog signal.

3. PAM. The amplitude of a constant-width, constant position pulse is varied according to the amplitude of the analog signal.

4. PCM. The analog signal is sampled and converted to a fixed-length, serial binary number for transmission. The binary number varies according to the amplitude of the analog signal. (Reference 69).

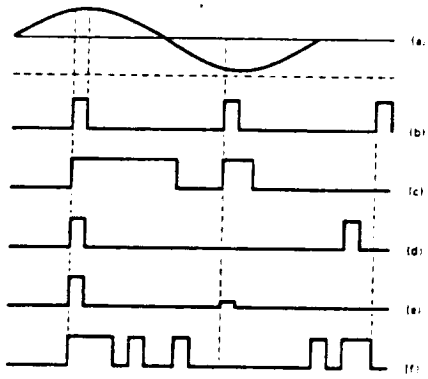

Figure 10.3 (Reference 69)
Pulse modulation: (a) analog signal; (b) sample pulse; (c) PWM; (d) PPM; (e) PAM; (f) PCM

PAM is used as an intermediate form of modulation and is seldom used by itself. PWM and PPM are used in special purpose communication systems (usually for the military) (Reference 69) PCM is by far the most prevalent method of pulse transmission and was chosen to be used in the LCUV. PCM will be the next topic of discussion.

10.2.2 PULSE CODE MODULATION

Pulse Code Modulation (PCM) is the only one of the previously mentioned pulse modulation techniques that is a digital transmission system. With PCM, the pulses are of fixed length and fixed amplitude (Reference 69). PCM is a binary system. Pulses are transmitted within a prescribed time slot. A pulse or lack of a pulse within this time slot represents a logic 1 or a logic 0 condition (Reference 69).

The use of PCM allows messages to be handled and processed by binary circuitry. Binary transmission also greatly facilitates processing of the received messages on Earth. Also, binary data representation is very flexible and versatile. This will allow the PCM equipment to adapt to more solid state devices and can be made highly reliable, small, and rugged (Reference 67). The equipment alignment within the LCUV is noncritical because of its digital circuitry (Reference 67). The PCM method of pulse modulation was chosen to be used in the LCUV because of its advantages over other

pulse modulation techniques. PCM advantages are summarized on the following page.

Advantages of Pulse Code Modulation (PCM):

- Only method suitable for handling digital information
- Uses binary representation (binary data representation is flexible and versatile)
- PCM equipment is small, reliable, and rugged
- PCM equipment alignment is noncritical

10.2.3 VEHICLE ANTENNAS

The selection of the antenna subsystems to be used on the LCUV mission is constrained by vehicle orientation, power consumption, and vehicle geometry. The physical dimensions of the LCUV are limited, therefore design compromises must be made in the configurations of the antenna. This will ultimately affect the area of the antenna gain. Also, the power required to transmit messages from the vehicle to Earth must be minimal since the power produced by the fuel cells is an important commodity.

In general, three different missions must be fulfilled by the LCUV antenna system:

1. High data-rate transmission from vehicle to Earth - "high gain" antenna

2. Low data-rate transmission from vehicle - "omnidirectional" antenna

3. Command transmission from Earth to vehicle - "omnidirectional" and/or high gain antenna (Reference 70)

The first mission involves the use of relatively directive antennas which are pointed at Earth by the vehicle-control system. this will enable the LCUV to transmit directly to Earth. Another method assumes the data from the LCUV is being transmitted to Earth via a parent vehicle as a radio relay. The latter method would eliminate the need for a steerable Earth-oriented antenna on the vehicle and minimize its power requirements (Reference 68). However, in order to maintain the communication link from the vehicle to Earth, the use of additional radio relays is apparent if the vehicle will operate beyond line of sight of the transmitting parent vehicle.

After considering the design constraints on the antenna subsystem, the following radio relay design provides the optimum performance while consuming minimal power during Phase I of the operation:

The LCUV will be equipped with two omnidirectional antennas. One will be used to receive transmitted commands directly from Earth while the other is used to relay data from the LCUV to a parent vehicle which will transmit the information to Earth. Since

there are no power limitations effecting the Earth's command transmission, no relay is required and the signals can be transmitted directly to the LCUV. The launched payload that will accompany the LCUV will act as the parent vehicle which will be equipped with a 4 ft. (1.22 m) reflector directional antenna. This will be a stationary antenna that will be used to relay data from the LCUV to Earth. Since the power needed to transmit from the parent antenna to Earth is a function of the effective area of the receiving antenna, the power source accompanying the transmitter can be minimal with regard to the large Earth-bound receiver. A receiving antenna detects an amount of power given by Equation 1.

$$W_R = P \cdot A_R = W_T \cdot A_R / 4 / \pi / R^2 \qquad \text{Eq.1 (Reference 71)}$$

Where : R = distance from transmitter
W_T= transmitter power radiated
A_R= receiving antenna effective area

Therefore, the only constraining factor associated with the use of a large Earth-bound receiver is the cost of construction. It must be decided whether to transmit a more powerful signal from the lunar surface thus consuming more power or to limit the power usage by constructing a large receiving antenna on Earth. Figure 10.4 shows the relationship between the diameter of the receiving antenna and its probable cost. Therefore, depending on the budget associated with the LCUV operation, it must be determined which alternative is more attractive.

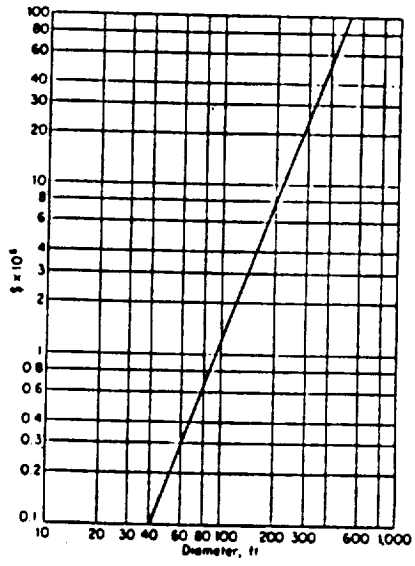

Figure 10.4 (Reference 70)
Approximate Antenna Cost

10.2.4 TRANSMITTANCE ERROR CORRECTION AND DETECTION

One of the most important features regarding microwave transmission is command verification. Since the operation of the LCUV relies entirely on commands received from Earth, it is important to transmit these messages reliably and accurately. A command that is interpreted incorrectly might result in a costly mission loss. Therefore, error correction and detection systems incorporated into the communication link will provide assured reliability.

Assuming the command is encoded properly at the Earth base site, the message is modulated and then transmitted via microwaves by a directional antenna to the omnidirectional antenna mounted on the vehicle. In the LCUV, the received signal is demodulated and decoded; the commands and instruction words with the necessary synchronization signals are fed to the proper vehicle systems (Reference 67). Before the commands are executed, it is desirable to verify the transmitted signal. This verification can be accomplished by two methods:

1. Once the command is received at the LCUV, complete retransmission of the command from the LCUV to the Earth station can occur where the messages would be compared in order to detect any errors. Only in the case of complete matching is an execution transmitted.

2. The complete command message can be transmitted and stored in the LCUV. The message is then transmitted from Earth a second time; then both messages are compared in the LCUV. The command is executed only if the two messages match (Reference 67).

The latter method offers an attractive alternative and will be used in the LCUV communication link due to the fact that it does not require as much power consumption as complete retransmission of the command from the LCUV to Earth. Although this method is more power efficient, it does require some storage in the vehicle.

One of the most substantial design constraints associated with the LCUV is the time delay accompanying command transmission. The time delay encountered in transmission from the Earth to the LCUV is approximately 2.3 sec. round-trip. With a vehicle speed of 0.2 m/sec. and a TV frame of 1 picture every 2.6 sec. lunar round-trip, a picture is received on Earth for each 0.52 m of vehicle motion (Reference 68). Thus, the LCUV will cover approximately 1m between the time a command is transmitted and the time finally seen by the Earth-bound base. This time lag problem can be alleviated by insertion of a predictor function in the control loop and an indication of the velocity vector on the Earth-based display (Reference 68). This aspect of the LCUV transmission link will need to be carefully designed and tested in order to insure reliable operation of the vehicle.

10.3 PHASE II COMMAND/CONTROL LINK

Phase II of the Lunar Split Mission (Reference 10) involves the presence of humans on the lunar surface. Once the lunar base is suitable for astronaut occupancy, the communication system will serve two functions:

1. Provide communication on the lunar surface from base site to LCUV
2. Provide communication from base site on lunar surface to Earth

These functions will include a voice link from the lunar base to the LCUV, remote control of the LCUV from the lunar base, and a voice link from the lunar base to Earth. The need for direct transmission of commands from Earth to the LCUV will no longer be required since the vehicle will receive its messages from the lunar base. The use of pulse code modulation (PCM) for the remote control of the LCUV from the lunar base will enable the vehicle to operate without having to change the onboard PCM equipment. This will also allow the LCUV to receive messages directly from Earth if ever the need arises. Therefore, the communication system will become more flexible and integrated during Phase II of the LCUV operation.

10.3.1 VEHICLE ANTENNAS

During Phase II of the operation, the LCUV antenna subsystem will consist of two omnidirectional antennas mounted on the vehicle along with the reflecting antenna accompanying the parent vehicle. These antennas will serve two purposes:

1. Provide means for remote control of LCUV from the lunar base

2. Provide voice link from LCUV to lunar base

The LCUV will need to operate within the line of sight of the lunar base in order to eliminate the need for radio relays on the lunar surface. Transmitting and receiving antennas on masts of 30 and 60 m tall, respectively, will permit point-to-point communication (to the horizon) over a path of less than 15 km. (Reference 68). Figure 10.5 shows the lunar horizon distance nomogram relating antenna size to transmittance distance.

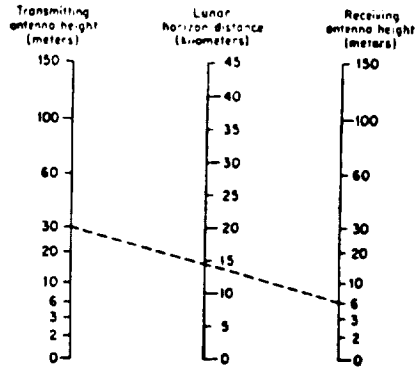

Figure 10.5 (Reference 68)
Lunar Horizon Distance Nomogram

As the LCUV mission progresses, the addition of radio relays can be implemented in order to provide a wider range of LCUV operation. Also, reliable communication over 100 km distances can be obtained by ground-wave propagation, using the lower frequency portion of the spectrum (Reference 68).

10.4 CONCLUSION

The use of an efficient and reliable communication link from Earth to the lunar surface is an essential aspect of the LCUV. The system proposed for the LCUV involves the use of digital microwave transmission and pulse code modulation (PCM). Command verification and error detection will be incorporated into the system in order to ensure reliable and accurate transmission. The antenna configurations include two omnidirectional antennas mounted on the LCUV and a 4 ft (1.22 m) reflector antenna used for transmission to Earth from the parent vehicle located on the lunar surface. After considering each alternative available for designing a communication link, the most practical and economical methods were chosen. Before this system can be used, it must first be thoroughly tested and proven reliable since it will be the only means of communicating with the LCUV after it is launched. Failure of the communication link will result in total failure of the LCUV mission. Therefore, careful design and exacting detail are required in order to ensure a successful operation.

11.0 MECHANICAL ARM

The primary design driver for the Lunar Construction Utility Vehicle (LCUV) is its ability to perform a wide variety of construction tasks (Reference 10). The mechanical arm (MA) is an important component because of the need to perform many of the various tasks. These tasks will be accomplished by a variety of attachments. The two main attachments that are of primary importance for the lunar mission are the backhoe device and the hoisting mechanism. The backhoe will be responsible for excavating on the lunar surface. The hoisting devices primary concern is the ability to lift certain modules such as:

1. Habitation module
2. Materials processing
3. Interconnect Nodes
4. Airlock
5. Flexible tunnels

(Reference 10)

These main attachments and others will be discussed in greater detail in a latter section of this report. These attachments will be designed so that they can be easily interchanged on the mechanical arm. Our primary goal is to develop a mechanical arm that will facilitate excavating and hoisting processes for the phase one development of a Lunar Base facility. The following steps were taken for the development of the mechanical arm.

1. Establish the general design requirements, constraints, and limitations.
2. Investigation of the lunar environment; i.e., soil for excavating purposes, reduced gravity, and frequent temperature changes, etc.
3. Investigation of actuation systems - electrical and hydraulic.
4. Investigation of controls; i.e., thermal and MA.
5. Specific attachments of arm.
6. Design and analysis of arm.

11.1 ASSUMPTIONS AND DESIGN CONSTRAINTS

The two main drivers for the sizing of this arm are the height of the lunar lander and the optimum partial burial depth for application of the radiation shielding material. The MA is 15 m in length from its base to the point of attachment of the backhoe or hoist implements. These two main attachments, the backhoe and hoist implements, will serve a number of purposes during the early construction phases of the lunar base. The backhoe attachment will have a holding capacity of $0.6m^3$ with dimensions to be specified later in the report. The time required to excavate $500m_3$ of soil will be 48 hours. This assumes three and one half minutes to fill the backhoe and empty it into the side-dump box or onto the lunar

surface. If a partially buried environment is required, the backhoe system will be utilized. If the modules are to be placed on the surface, then the backhoe could not be used because the required length of the MA would be too long to allow the distribution of regolith along the top of the habitation module. The backhoe will be able to perform some site preparation such as the clearing of large lunar rocks which may be required prior to transport of the habitation module from the landing site to the lunar base site.

The crane attachment is better defined as a series of attachments associated with crane or hoisting processes. An attachment for the Lunar Telerobotic Servicer (LTS) will be required to give the LTS access to places it would not have access to from its position of the LCUV. A forklift attachment will be implemented for lifting relatively small payloads or engine pallets from the lander and transferring them to an LCUV for transport to the lunar base site. The hoisting mechanism may be used to aid in the placement and connection of habitation modules and module interconnect nodes during expansion of the lunar base. It is suggested that the backhoe and the required crane attachments be housed in a tool crib which retains them in the required position for the MA to change from component to component quickly and easily. If a number of different tasks are to be carried out in the same area, this crib could travel on an LCUV and remain on site during the process (Reference 10).

Besides the constraints and limitations developed in the previous section of this paper, there are other environmental constraints which pose serious problems. For example, thermal control of the arm. The heat generated by the drive motors and electronics of the arm system will have to be dissipated during all operations. The development of a radiator for the LCUV will hopefully aid in the solution to this problem. Lunar soil and dust is another problem. It could be a very serious problem if the dust or soil enters the manipulator arm joints. A protective covering for the joints will have to be developed. This covering must not inhibit the mobility of the arm to perform the required construction tasks. Another design problem is the fact that construction vehicles with mechanical arms have not been developed for Lunar use. This caused a problem in locating information on mechanical arms with construction capabilities that can operate in the Lunar environment. A majority of the information that will be used in the development of the MA is from the Remote Manipulator System (RMS) on the Space Shuttle. This is the only Manipulator system that is presently being used in space. Much of the control aspects of the MA will be developed similar to the RMS. The final constraint and most dominant is the absence of human operators during the unmanned phase of exploration and surface preparation (Reference 73). One solution to this problem is the use of telerobotics.

Some other constraints that must be considered are:

- Mechanical simplicity
- Minimal weight
- Adaptability to task changes
- Robotic maintenance and repair

Major concerns:

- Power needed for hoisting and digging to be accomplished
- Heat dissipation of motors
- Assurance that vehicle will not tip over when lifting is being performed

Added Assumptions:

- Motors capable of providing required torque
- Deployable spades available to provide support
- Length of arm booms
- Thermally controlled
- Able to work in harsh environment with minimal maintenance

A promising design of a MA will be one that takes advantage of the lunar environment and will operate within the constraints it imposes (Reference 10). Current terrestrial construction equipment such as the bulldozers and backhoes typically depend on weight for counter balance and the reaction to the application force. The fact that the moon has a gravitational field 1/6 that of the Earth presents another problem in producing traction forces with such equipment, since the normal forces created by the vehicle will be less on the moon. This gravitational constraint leads to the next topic, the lunar environment.

11.2 LUNAR ENVIRONMENTAL EFFECTS

The mechanical arm must be designed to work in the severe lunar environment. This environment is characterized by:

- Lack of atmosphere
- Reduced gravity (1/6 of the earth)
- Diversity of soil
- Exposure to solar and galactic cosmic radiation
- Exposure to dust and visibility problems
- Extreme temperature fluctuations (-170°C to 130°C)

The 1/6 reduction of gravity causes a major problem with the lifting of objects. To create the necessary opposing force required to perform the task of lifting or excavating on the lunar surface, the mechanical arm module will incorporate two deployable spades. The volume displaced by these spades to support the fully

loaded MA is 1 m^3 per spade. If the load is to be moved a distance around the center of gravity of the LCUV, then two more deployable structures utilizing only support pads may be mounted opposite to the spades. Each of these systems will be a fixed part of the MA module and will be contained on the module when not in use. They may be driven into the lunar surface using the backhoe attachment, but they must also be able to retract to accommodate the MA use as a crane. To simplify the removal of the spades, the MA may provide locomotion in the direction of the spades thus pulling them free from the regolith (Reference 10).

The lunar soil can be described as well-graded silty sands with an average particle size between 0.040 and 0.130 mm. The density of in situ bulk lunar soil, as determined from large diameter core tube samples, is typically 1.4 to 1.9 g/cm^3. The bulk density increases to support the overburden in lunar gravity. Spheres, angular shards, and fragile reentrant vesicular grains are among the diverse shapes found in most lunar soils. The most abundant particles composing the soil are igneous or breccia lithic grains, mineral grains, glass fragments, and the unique lunar agglutinates (Reference 74).

Some important environmental factors are the fluctuations in temperature of a lunar day and the effects of radiation during the day. Thermal control and radiation shielding will be developed to compensate for these factors. These are the conditions that the mechanical arm will face in the lunar environment.

11.3 BACKGROUND

A robotic manipulator may be defined as a multidegree of freedom open-loop chain of mechanical linkages and joints. It is designed to perform mechanical operations which normally require the manipulative skills of humans. These mechanisms, driven by actuators, are capable of moving an object from initial to final locations or along prescribed trajectories (Reference 75).

Remotely operated robotic manipulator arms are used in all types of applications. The only arm in space that is presently being used is the Remote Manipulator System (RMS) on the shuttle. Since this is the case, much of the information used to design the mechanical arm for the LCUV has come from this existing design. The development of the RMS was done by SPAR Ltd. in Canada. The manipulator system, the results of a cooperative program between the National Research Council of Canada (NRCC) and NASA, consists of the arm, a display and control panel, (including 2 hand controllers), and a manipulator controller unit that interfaces with the Orbiter computer (Reference 76). The RMS is Canada's contribution to the space program. In return for the RMS, NASA signed an agreement to buy other flight units from Canada. The agreement will also give Canada a price break on shuttle launches. NASA also agreed not to contract with any other firm to build a competitive system. The arm is presently being used aboard the shuttle to retrieve and service satellites. On later missions the

arm may be used to deploy satellites, change modules on satellites needing repairs, and help build large structures in space (Reference 77).

The RMS is approximately 50 ft. long and weighs 994 lbs. Like a human arm, this mechanical arm has a shoulder elbow and wrist joints, plus a "hand" that can capture payloads (Reference 77). SPAR Ltd. indicated there were three main constraints in building the RMS:

- Site of gear boxes and motors to move arm
- Controls system to be used
- Computer software for arm

These constraints and others listed earlier concern the development of the MA for the LCUV. The details of this design will now be developed.

11.4 HYDRAULIC vs ELECTRICAL ACTUATION SYSTEMS

The robotic arm will be used to perform construction tasks. The ability to perform these tasks depends on the actuation of the arm's joints. The two types of actuation systems that will be examined are the hydraulic and electromechanical. The factors that will be used in determining the choice of actuation systems are:

- Temperature effects
- Maintenance standards
- Lifting capacity

Holzbock (Reference 78) declares that for the same power output hydraulic actuators are smaller than electrical actuators; and since they have less mass, they are dynamically superior to electric actuators. On the other hand, electric actuators are easy to use and maintain.

11.4.1 HYDRAULIC SYSTEMS

One of the principle advantages of a hydraulic system is an approximate 8:1 power advantage over electrical systems. Young explains that another potential advantage is the low compressibility of hydraulic fluids, which in turn causes the stiffness of the actuator to be high, thus leading to a high natural frequency and a rapid response (Reference 78).

11.4.2 ELECTROMECHANICAL SYSTEMS

The use of electrical motors for the mechanical actuation of robotic limbs is very appealing since a wide range of suitable devices are available. Also flexible methods of control and electrical power for the recharging of the power storage batteries are available (Reference 78).

11.4.3 TEMPERATURE EFFECTS

The lunar environment is exceedingly different from that of the earth. The temperature ranges from approximately -140°C to 150°C. Young's research notes that it is desirable that a dual purpose temperature stabilizing system, which can either heat or cool, should be used in such cases. Motors and fans used in lunar equipment are cooled with the aid of heat-dissipating coatings of beryllium oxide microspheres in silicon rubber. The temperature dependency of hydraulic system fluid viscosity could cause a problem with performance of the system since at extremely cold temperatures the fluid becomes very viscous and may freeze.
The most commonly used electromechanical system is the permanent magnet DC brushless motor. Permanent magnets have a physical property known as the Currie Point. This occurs when a magnet loses its magnetism immediately upon reaching a critical temperature. The magnetic material consists of Neodymium, Iron, and Boron and has a Currie Point between 120°C and 150°C. This could cause a problem because it is just within the limits of the maximum lunar temperature range. As mentioned earlier, this problem could be avoided by the use of heat dissipating coatings.

11.4.4 MAINTENANCE STANDARDS

The electromechanical actuator is virtually maintenance free, whereas, the hydraulic system has critical filtering requirements. Another factor concerning the maintenance of the hydraulic system is that the fluid it uses must remain particle free. These strict requirements make the electromechanical system the better suited for lunar application. As stated in Reference 79:

> "Hydraulic systems should not be used on the Moon due to the high maintenance requirements anticipated resulting from the vacuum, high radiation, and regolith dust environment".

11.4.5 LIFTING CAPACITY

The ability to lift is increased with the use of a hydraulic actuating system than with an electromechanical system. This is known to be true because of the estimated 8:1 power advantage of the hydraulic system. Although this is an important factor, this becomes less of an advantage on the moon because of the 1/6 gravity reduction, which allows the electromechanical system to have 6 times greater lifting capacity than on the earth. See Table 11.1 for a comparison of these two systems.

11.4.6 SYSTEM COMPARISON

	HYDRAULIC	ELECTRICAL
TEMPERATURE	FLUID MAY FREEZE	HIGH TEMPERATURE MAY AFFECT MAGNETIC PROPERTIES *
MAINTENANCE STANDARDS	CRITICAL FILTERING REQUIREMENTS	MAINTENANCE FREE
LIFTING CAPACITY	8:1 POWER ADVANTAGE OVER ELECTRICAL SYSTEMS	ELECTRICAL SYSTEMS MORE EFFECTIVE IN LOW GRAVITY

* Note: Currie point - 120°C to 150°C

TABLE 11.1
Hydraulic Actuation vs. Electrical Actuation

Each systems advantages and disadvantages for use on the lunar surface have been considered, and the determining factor is the complexity of the systems maintenance requirements. The electromechanical actuator is relatively maintenance free, whereas, the hydraulic system has high maintenance requirements. The optimum design is to have simple maintenance requirements. The hydraulic system would not provide this. Therefore the electromechanical actuation system is the preferred choice. The type of motor that will be used to power the actuation system is a brushless DC motor similar to the one used for the RMS on the space shuttle. Heath (Reference 78) identifies two distinct characteristics of direct current motors:

1. They have the capability of being reversed. By reversing the polarity of the applied power, the direction of motor rotation is reversed.
2. By changing the applied voltage, the speed of the motor is varied.

Direct current motors are discussed in further detail in Section 6.1.3 of this report. The brushless motor will also work with an planetary gear system to provide the needed torque for lifting capabilities.

11.5 CONTROL OF ARM

The development of the control aspects of the MA is very complex. Dr. Jen K. Huang, a professor and expert in the controls field at Old Dominion University, indicated that a complete development of the controls for the MA would be too complex to obtain in one semester. He also indicated that the testing of control systems is required to accurately develop a system. In this section, a comparison between Non-Servo and Servo control will be examined. Also, an overview of the type of system that will interpret the commands and modes of control will be examined. Lastly, thermal control and a list of the various types of control will be inspected.

11.5.1 NON-SERVO VS. SERVO CONTROL

Non-servo controlled robots move their arms in an open-loop fashion between exact end positions on each axis or along predetermined trajectories in accordance with fixed sequences (Reference 75). The arm motion of a non-servo robot is limited by mechanically adjustable hardstops on each mechanical joint or axis. This will only allow each axis to move in an open loop fashion to only two positions. This would be unfeasible for our design since feedback of position is not incorporated. Controls of the MA must be able to incorporate a computer. In order to use the computer, the position of all joints to be controlled must be known. Therefore a control without feedback is unfeasible. For our purposes, a manipulator with position control and force feedback must be used. Figure 11.1 shows some of the parametric manipulator relationships. Note that the complexity and cost of this type of system is a lot larger than other manipulators. The system that will be used on the MA will need to be complex to serve the number of various tasks associated with the MA.

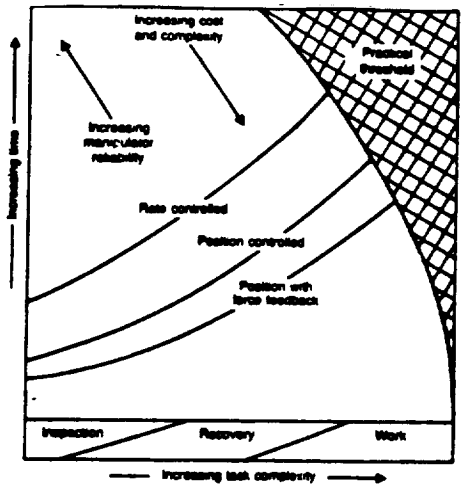

Figure 11.1 (Reference 75)
Parametric Manipulator Relationships

Servo controlled robots incorporate feedback devices on the joints or actuators of the manipulator which continuously measure the position of each axis (Reference 75). With the feedback devices incorporated, it will permit the control to stop each axis of the manipulator at any point within its total range, rather than only two positions that non-servo control can obtain. Servo control robots have a more manipulative capability than non-servo control robots in the sense that they are able to position a tool or a gripper (i.e. backhoe & hoist) anywhere within the workspace. The controllers of non-servo robots may be electronic sequencers, minicomputers, or microprocessors based on the control systems needed. This class of control systems has magnetic or solid state electronic memory devices for storing a taught sequence of motions in digital form. For example, if a simulation of the arm was performed on earth, the computer could store these movements for later use. This type of servo control will be used for the MA of the LCUV.

One type of servo control is the 'Continuous Path Control'. This type of control is used where continuous path of the end-effector or attachment (i.e. backhoe & hoist) is of primary importance to the application. The continuous path motions are produce by interpolating each joint control variable from its initial value to the desired final value (Reference 75). This process allows for minimal movement of each joint in attaining the final positions. This will give the MA a controlled predictable path. All of the joints' variables are interpolated to complete the motions simultaneously, thus giving a coordinated joint motion (Reference 75).

The three basic continuous path controls that will be used are as follows:

1. Conventional Servo Control - This control uses no information about where the path goes in the future. The controller may have a stored representation of the path it is to follow, but to determine the device signals to the arm's brushless dc motors and planetary gear system, all calculations will be based on the past and present tracking error.

2. Preview/Feedforward Control - This control uses some knowledge about how the path changes immediately ahead of the robot's current location, in addition to the past and present tracking error that will be used by the servo controller.

3. Path Planning/Trajectory Calculation - this control involves using an available description of the path the manipulator should follow from one point to another.

11.6 CONTROL MODES

Telerobotics, which is defined as the remote computer-assisted manipulation of equipment, materials, and systems autonomy, includes intelligent automated control. Monitoring and diagnosis will be used simultaneously to effectively operate the MA in the unmanned phase of operation.

The arm will be monitored by television cameras, and a large computer will handle the surface operations. Telerobotic operations from earth such as, the selection of primary control modes, braking of motors, end effector control, and vehicle motion control will be available. Hand controllers on earth will be used to perform rotational and translational motion. Like the shuttle, telerobotic control from earth will be routed through a Manipulator Controller Interface Unit (MCIU). This is the main interface with the General Purpose Computer (GPC), the control and display panel, the electrical subsystem and the end effector attachments. The MCIU collects and formats the data, and transmits it to the appropriate part of the system (Reference 80). See Figure 11.6 for a conceptual design of the system.

The MA will be controlled in a variety of automatic and manual modes. For safety purposes, a back up mode of operation will be developed that will override the GPC and utilize hard wired commands to drive the joints. There will be five modes of operation that will allow the vehicle to be controlled in both the unmanned and manned phase of the LCUV mission. They are listed as follows:

- Manual Augmented
- Automatic - command auto sequence
  pre-programmed auto sequence
- Single joint drive
- Direct drive
- Backup drive channels

11.7 THERMAL CONTROL

The thermal control of the MA will be similar to that of the RMS. The RMS thermal control system maintains the temperature of all the elements of the arm safely. By using insulating blankets, thermostatically controlled heaters, and radiators, thermal control is obtained (Reference 10). Controls for temperature monitoring will be accomplished by placing sensors on the motors which are the most critical thermal points of the arm. If the temperature is too high, the operator will be alerted and these sensors on the arm will automatically switch the power off.

11.8 OTHER CONTROLS

The following is a list of various controls that will be implemented in the operation of the MA:

- Control for motor strain
- Bucket attachment sensors used to control its speed of closure
- Displacement lag control
- Accelerometer used to prevent arm collisions with foreign objects (ie. lunar rocks, other LCUV's etc.)

11.9 INDIVIDUAL JOINT CONTROL

All linear motions must be made by combined rotations of various joints just as the human arm does (Reference 77). Each joint of the arm will have a complex array of gears and motors that not only have to move the arm into proper position, but they must compensate for wobbling resulting from movement of the LCUV.

11.10 ATTACHMENTS

A backhoe attachment will be used primarily for excavation of soil and soil handling for site preparation. This includes digging, trenching, and leveling of the lunar surface. The backhoe will be attached to the end of the mechanical arm. The backhoe will consist of two independent quarter circle type buckets arranged so as to generate equal and opposite forces for either digging or clamping. The soil will first be cultivated using a rotary device with sharp blades that can be attached to the rear of the vehicle. Then the arm will drive the bucket into the soil for excavation purposes. A worm gear system will be used to open and close the bucket attachment. A clockwise or counter-clockwise motion of the worm gear will cause this effect. The bucket will be equipped with sensors that will detect strains resulting from the attempted opening or closing of the attachment. If a maximum strain is exceeded, the power will be terminated.

A tiller will be used to cultivate the soil prior to excavation by use of the bucket attachment. This tiller is designed so that it can hook on to the connection link of the LCUV and then be pulled across the lunar surface. There will be a number of circular blades that will rotate on an enclosed axle. The axle is enclosed to prevent lunar dust from inhibiting the rotation of the device.

Finally, a blade attachment will be used to push and level the lunar soil. It will be attached to the LCUV via the connection link.

11.11 HOISTING MECHANISM

This attachment will be used for lifting the habitation module, materials processing modules, and interconnect nodes. The attachment will utilize a hook device. This hook can be inserted into a circular fixture located on the specific modules that need to moved. Pre-flight simulation tests must be conducted in order to ensure reliable operation of these attachments on the lunar surface.

11.12 CONCLUSION

The development of the mechanical arm was very complex. Many aspects were considered, such as constraints and assumptions which played a major role in the design. The major concern was the power requirements needed to hoist and dig on the lunar surface. An assumed maximum load of 6450 N was applied to the end of the arm at a distance 6.56 m away from the vehicle so that the vehicle would not tip. An assumed maximum moment was determined. From this moment an assumed maximum torque needed for the motors for lifting capabilities of the arm was determined. The overall design of the arm will include :

- Three booms totaling 15m with 3 degrees of freedom
- Electrical Actuation System
- Servo Control "Continuous Path Control"
- Two main attachments (Hoist and Digging Mechanism)
- Brushless D.C. Motors with planetary gear set.

The present design will need much more design and analysis before it will be a complete design. Tests and simulations must be performed to ensure a safe and reliable arm.

12.0 OPTICAL SYSTEM

The Lunar Construction Utility Vehicle (LCUV) is required to operate both manually and remotely from an Earth based station. It is during the un-manned mission that the use of proper lighting packages, camera configurations, and a means of position determination is crucial.

The problems that will be discussed in the assumptions and design constraints section demand the use of an adequate means of lighting for both lunar day and night situations. There are several ways that the lighting packages may be situated on the LCUV, many of these configurations will be looked into and the arrangement that best fits the constraints will be chosen.

A large amount of information that will aid the Earth station in maneuvering the vehicle will be provided by the cameras that will be mounted on the LCUV. Like the lighting packages, the cameras can be arranged in many different ways. The arrangement that best optimizes power usage and complies with the design constraints will be selected.

The position of the vehicle and the distance an object is away from the vehicle is information that will be required by the Earth station when guiding the vehicle. The instrument that will be determining this information will have to contend with the unfavorable environmental conditions of the Moon in addition to producing reliable data. There are numerous method by which this task can be accomplished. Some of the more favorable rangefinding techniques are by the use of microwave or laser. Each of these options must be looked into and the option that both produces the most reliable data and maximizes power utilization will be employed.

12.1 ASSUMPTIONS AND DESIGN CONSTRAINTS

Much of the restrictions that are established for guidelines in designing the lighting configurations and navigational aids are set by the environment and composition of the Moon's surface (Reference 10). Because the moon does not have an atmosphere, as the Earth does, diffuse reflection of light (light scattering) is not possible (Reference 10). This causes areas which are brightly illuminated contrasted by areas of vast shadowing. An additional problem that is presented is what is called washout (Reference 10). Washout is caused when light impinges upon the Moon's surface within 30 of the normal of the surface, when this occurs the light reflects back to space and none is diffusely reflected. The one major aspect of the Moon's surface composition that presents a design restriction is its ability to reflect light. Albedo is a measure of the reflective ability of substance. The Moon's albedo rating is roughly 9% (Reference 10).

Design Constraints:

- Temperature ranging -171°C to 111°C.
- Effects associated with solar flares and radiation.
- Effects associated with the lack of atmosphere.
- Limited diffuse reflection of incoming light.
- Shadowing.
- Washout.
- Moving down light.
- Low albedo rating of Moon's surface.
- Minimal power consumption

12.2 LIGHTING ARRANGEMENT

Since the main object in designing the lighting packages to be used on the LCUV is to maintain a low power draw from the fuel cells, it is essential that the lights are mounted to optimize the area that is covered. Another item that must be considered is that the conditions for lighting needs during the unmanned mission are different than that of the manned mission. The constraints that were mentioned beforehand that were set by the environment of the Moon will primarily effect the angular range of tilt that the lights are capable of. In order to avoid to effects of shadowing the lights will have to be mounted a sufficient distance above the surface.

The arrangement that has been decided upon for use on the LCUV (see figure 12.1) is comprised of four lights mounted 5 feet and having the capability of extending to 10 feet above the surface on each corner of the vehicle giving the capacity of illuminating any area around the vehicle. Each of the lights are capable of a lighting power of 200 lumens which is sufficient during the worst case situation of the lunar night. The stands which support the lights will have the ability of 360° rotation in the horizontal plane, this will aid in concentrating light on certain areas. A camera and rangefinder arrangement is included on each stand for a diversity of views. For a maximum range of view, the camera/light/rangefinder arrangement will have an angular tilt ability in the vertical direction ranging from 60° below the horizon and 60° above the horizon.

In addition to the above mentioned lighting arrangement a light stand will be located in the center of the vehicle that will support the main camera and rangefinder arrangement. This particular stand will have the capability of extending to a height of 15 feet above the surface for long range viewing. Similar to the corner stands, the main stand is capable of 360° rotation and vertical tilts ranging from 60° below horizon and 60° above horizon.

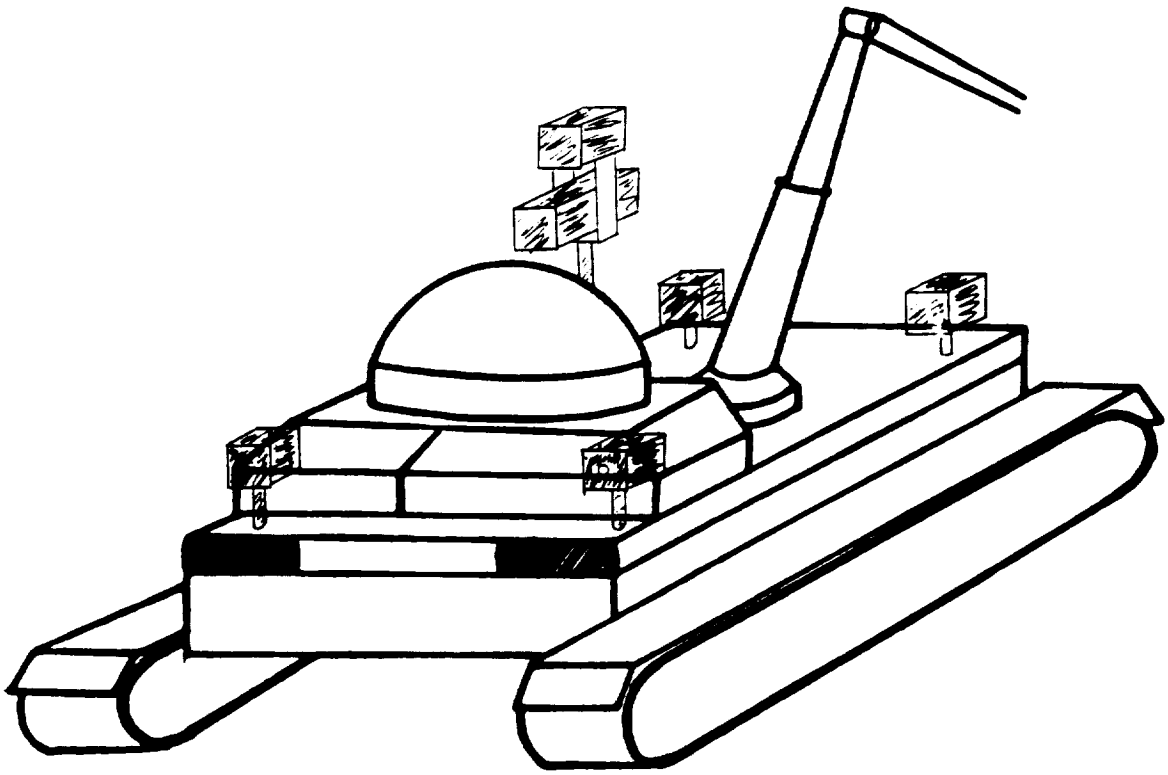

Figure 12.1
LCUV Arrangement of Optical Aids.

12.3 CAMERAS

The camera system that is going to be put to use on the LCUV has to have the following capabilities:

- Automatic focus
- Wide range of view
- Switching capability (transmit one or more views)
- Transmit pictures of all working cameras every six seconds.
- Automatic attenuation to light conditions

The cameras will be aligned in the way that is shown in figure as was described previously. An actual working camera that works under the conditions specified in the design constraints section of this report has not been found as of now but one that is capable is possible.

12.4 NAVIGATION AND RANGEFINDING

Accurate vehicle to object data in aiding the navigation of the LCUV is essential. There are many methods by which this can be accomplished all of which use the basic concept of time of flight of a waveform. First, a signal in the form of a wave of some sort is sent out. The time that is consumed before the wave returns is then measured. With this information, in addition to the speed of the wave, the total distance traveled can be determined. This distance is actually twice the distance between the object and the source/collector of the waves. The waveforms that will be considered are microwave, and light (i.e. laser).

The major drawback associated with the use of microwave radar rangefinders is that they suffer from diffraction, there is limited angular resolution for a given antenna and reflector size (Reference 82). This limits the accuracy that can be attained when trying to range on the moons surface. Since the accuracy of the data that is acquired is of utmost importance for navigational purposes the microwave radar rangefinding device will not be considered hereafter.

The laser rangefinding device is capable of achieving remarkable accuracies using the same principle of measurement that is used in the microwave radar rangefinder, that being the time of flight response phase delay measurement method described previously and also shown in figure 12.2. The reason why the laser rangefinding device is capable of better accuracies than the microwave radar device is because of the properties of the waveforms that are used. As described previously, the microwave is susceptible to diffraction as when the wave impinges upon a small or unpolished surface whereas the laser light beam is concentrated and does not diffract (i.e., the beam is coherent) (Reference 85).

The LCUV will have five laser rangefinders (one on the main stand and four on each of the four corners stands of the vehicle) that will be used; when they are not in use they will be turned off in order to conserve power.

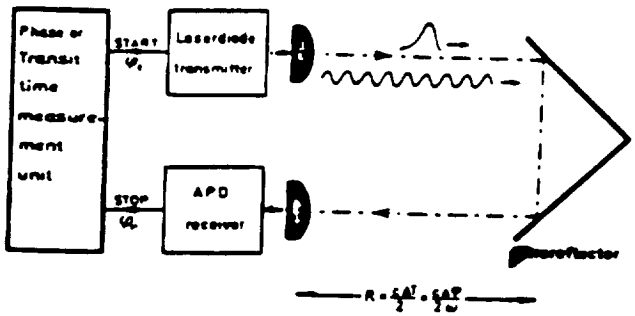

Figure 12.2 (Reference 82)
Time-of-Flight of a laser pulse from a laser rangefinder.

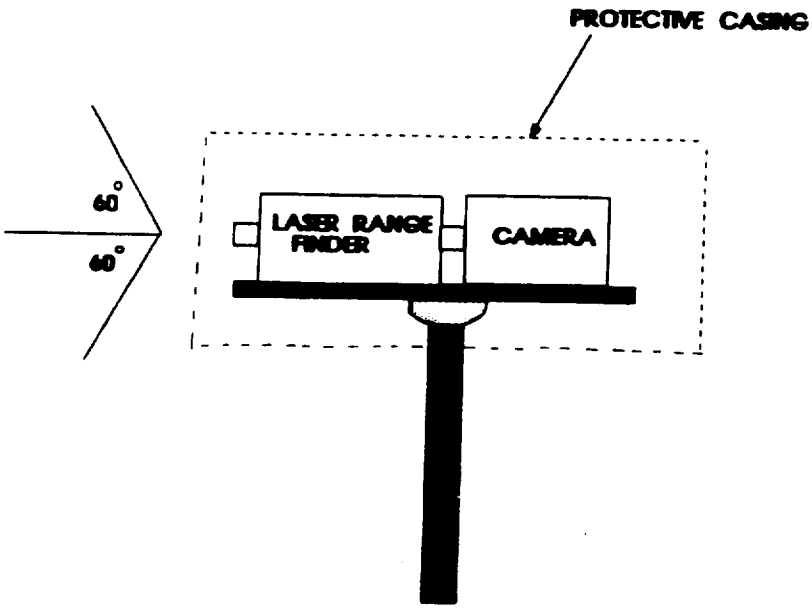

Figure 12.3

Corner optical aid arrangement. One arrangement per corner of the vehicle.

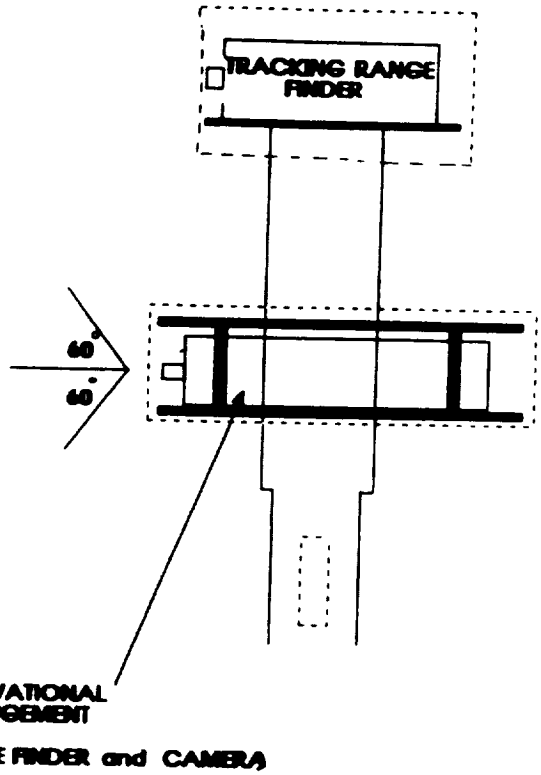

Figure 12.4

Preliminary optical array. Located in the center of the vehicle.

These rangefinders will aid the earth station in determining distances of objects that are being viewed by a certain light/camera/rangefinder arrangement. An example of one of the corner arrangements can be seen in figure 12.3 and the main arrangement in figure 12.4.

The laser rangefinder that will be used in aiding navigation during the unmanned mission will also be located on the main arrangement stand with the exception that it will be located a fixed distance of 20 feet from the surface. The beam that is emitted by this devise will be locked on to a stationary retroreflector to which navigation will be referenced.

Some of the performance abilities of the laser rangefinding devices are as follows (Reference 82):

- Operating range from a minimum of some cm to a maximum of some km.
- Range accuracies of approximately 1% of the distance for long ranges and some mm for short range.
- Range rate accuracy (radial velocity) of some mm/s to some cm/s
- A field of view (FOV) of 30 x 30.
- Small in size, light-weight and low power draw.
- Simplicity and Reliability

12.5 ENVIRONMENTAL PROTECTION OF EQUIPMENT

The harsh environment of the Moon provides several design obstacles such as heat dissipation, solar radiation, and solar flares. Each of these problems must be addressed and methods of copping with them designed.

The heat that is generated by the equipment will be dissipated to the radiator coils which contain a circulating ethylene-glycol fluid. This heat will then be carried away to the radiator array. The radiator is further discussed in section 7 of this report.

In order to protect the components from the effects of the sun (i.e., solar radiation and flares) a protective casing will enclose all of the components of the system. This casing will be constructed of an aluminum alloy which is wrapped with a reflective material cover comprised of a beta cloth and teflon mixture to lessen the heating ability of the sun (Reference 86).

12.6 CONCLUSIONS

After considering all of the design constraints that were set upon the development of the optical means of the LCUV the configuration shown in figure 12.1 was chosen for utilization. The lighting, viewing by camera and distance determination of the vehicle by a choice of five different light/camera/rangefinder configuration stands gives optical analysis capabilities of any point around the vehicle by at least three cameras.

The laser rangefinder that will be used in conjunction with a stationary retroreflector will aid the Earth based station in the navigation of the vehicle by position determination and tracking. The way that this system will be controlled has not as of yet been determined although it is known to be possible.

All of the components that were discussed will be protected from the harsh environment of the Moon by a protective casing and a reflective thermal cover. The heat that is generated by the devices will be first conducted to the radiator coils and then carried away by the working fluid to the radiator array.

Although the system has not been entirely designed the concepts that have been introduced are credible and do abide by the design constrains that have been outlined.

APPENDIX A

```
100 REM  THIS PROGRAM COMPUTES THE SAFE BEARING LOAD, TRACTIVE
110 REM  EFFORT, RESISTANCE TO MOTION, AND DRAWBAR PULL FOR A
120 REM  TRACKED LUNAR CONSTRUCTION VEHICLE.
130 REM
140 REM  CONSTANTS:
150 REM
160 REM  c  = 360 N/m²
170 REM  Nc = 65
180 REM  Nq = 37
190 REM  y  = 400 N/m³
200 REM  Ny = 35
210 REM  p  = 35°
220 REM  Kp = 41158.5 N/m²
230 REM
240 REM  VARIABLES
250 REM
260 REM  w  - SAFE BEARING LOAD (N)
270 REM  m  - MASS (kg)
280 REM  b  - TRACK WIDTH (m)
290 REM  l  - TRACK LENGTH (m)
300 REM  A  - TRACK AREA (m²)
310 REM  H  - TACTIVE EFFORT (N)
320 REM  R  - TRACK RESISTANCE (N)
330 REM  DP - DRAWBAR PULL (N)
340 REM
350 REM  BEGIN PROGRAM
360 REM
370 Z=0
380 DIM A(100) B(100) H(100) L(100) R(100) M(100) W(100) DP(100)
390 C=360: NC=65: NQ=37: NY=35: Y=400: P=36*2*PI/360: KP=41158.5:
400 L=2.4
410 CLS
420 Z=Z+1
430 INPUT " INPUT TRACK WIDTH IN m"; B(Z)
440 A(Z)=B(Z)*L
450 REM  COMPUTE BEARING LOAD
460 W(Z)=4*A(Z)*(C*NC+Y*B(Z)*NY)
470 M(Z)=W(Z)/9.81
480 WM(Z)=M(Z)*1.635
490 H(Z)=2*(A(Z)*C+(WM(Z))*(TAN(P)))
500 R(Z)=2*((1/B(Z)*KP))*((WM(Z)/(2*L))^2)
510 DP(Z)=H(Z)-R(Z)
520 INPUT " RUN WITH NEW WIDTH ?  1-YES 2-NO";O
530 IF O=1 THEN GOTO 420
540 CLS
550 PRINT TAB(3)"A";TAB(10)"W";TAB(20)"M";TAB(30)"H"
        TAB(40)"R";TAB(50) "DP"
560 PRINT TAB(0)"(m²)";TAB(10)"(N)";TAB(18)"(kg)"
        TAB(29)"(N)";TAB(39)"(N)";TAB(49)"(N)"
570 PRINT "-----------------------------------------------"
```

```
580 FOR N=1 TO Z
590 PRINT TAB(0)A(N);TAB(7)WM(N);TAB(17)M(N);TAB(27)H(N);
        TAB(37)R(N);TAB(47)DP(N);
600 NEXT N
610 PRINT;PRINT;PRINT;PRINT;PRINT
620 INPUT " INPUT SPECIFIC MASS FOR TRACK ? 1-YES 2-NO";O
630 IF O=2 THEN END
640 U=U+1
650 INPUT " INPUT TRACK WIDTH AND MASS ";B(U),M(U)
660 A(U)=B(U)*L
670 W(U)=M(U)*1.635
680 H(U)=2*(A(U)*C+W(U)*TAN(P))
690 R(U)=2*((1/B(U)*KP))*((W(U))/(2*L))^2)
700 DP(U)=(H(U)-R(U))
710 INPUT " INPUT ANOTHER WIDTH AND MASS ? 1-YES 2-NO";O
720 IF O=1 THEN GOTO 640
730 CLS
740 PRINT TAB(3)"A";TAB(10)"W";TAB(20)"M";TAB(30)"H"
        TAB(40)"R";TAB(50) "DP"
750 PRINT TAB(0)"(m²)";TAB(10)"(N)";TAB(18)"(kg)"
        TAB(29)"(N)";TAB(39)"(N)";TAB(49)"(N)"
760 PRINT "-----------------------------------------------"
770 FOR N=1 TO U
780 PRINT TAB(0)A(N);TAB(7)WM(N);TAB(17)M(N);TAB(27)H(N);
        TAB(37)R(N);TAB(47)DP(N);
790 NEXT
800 END
    END
```

APPENDIX B

SYMBOLS

AR	prime radiator area, sq meters
Cp	specific heat of fluid, KJ/(KG)(K)
F	shape factor or view factor
Gs	solar constant, 1.356 KW/sq meters
Hr	convective heat-transfer coefficient, KW/(sq meters)(K)
D	diameter of pipe, meters
Nu	Nusselt number
K	thermal conductivity of cooling fluid, KW/(meters)(K)
In	solar energy rate reflected per moon unit area, KW/sq meters
Q	total heat-rejection rate, KW
q	heat-rejection flow rate for a .305 by .305 meter section of radiator, KW/sq meter
S	entropy, KJ/(kg)(K)
T	temperature, K
Ts	effective sink temperature, K
w	fluid flow rate, kg/second
α_s	solar absorptance
ϵ	emittance of radiator
ϕ	angle between sun and normal to radiating surface
σ	Stefan-Boltzmann Constant, 5.6671 x 10 KW/(sq meters)(K)

SUBSCRIPTS

av	integrated average
f	fluid
i	inlet
M	moon
o	outlet
R	radiator
w	wall

APPENDIX C

```
10   '
20   '
30   '              COMPUTER PROGRAM TO SIZE RADIATOR
40   '              LUNAR CONSTRUCTION UTILITY VEHICLE
50   '              GROUP 2
60   '              PROGRAM NAME: RADIATE
70   '
80   '              DESCRIPTION OF VARIABLES
90   '
100  'COOL    : NAME OF THE COOLING FLUID BEING ANALYZED
110  'D       : DIAMETER OF PIPE USED TO CARRY COOLING FLUID (METERS)
120  'W       : MASS FLOW RATE OF COOLING FLUID (KG/SEC)
130  'CP      : SPECIFIC HEAT OF THE COOLING FLUID (KJ/(KG)(K))
140  'VIS     : DYNAMIC VISCOSITY OF COOLING FLUID ((N)(SEC)/SQ METERS)
150  'PR      : PRANTL NUMBER OF COOLING FLUID
160  'K       : THERMAL CONDUCTIVITY OF COOLING FLUID (KW/(METERS)(K))
170  'HR      : CONVECTIVE HEAT TRANSFER COEFFICIENT (KW/(SQ METERS)(K))
180  'RE      : REYNOLDS NUMBER
190  'NU      : NUSSELT  NUMBER
200  'TFI     : TEMPERATURE OF COOLING FLUID AT THE RADIATOR INLET (K)
210  'TFO     : TEMPERATURE OF COOLING FLUID AT THE RADIATOR OUTLET (K)
220  'DELTATF: TEMPERATURE DIFFERENCE OF COOLING FLUID AT THE RADIATOR INLET
230  '          AND OUTLET (K)
240  'TM      : LUNAR SURFACE TEMPERATURE (K)
250  'ANGLE   : ANGLE BETWEEN SUN AND NORMAL TO RADIATOR SURFACE (DEGREES)
260  'GS      : SOLAR CONSTANT (KW/SQ METERS)
270  'SBC     : STEPHAN-BOLTZMANN CONSTANT (KW/(SQ METERS)(K^4))
280  'PCELL   : POWER OUTPUT OF THE FUEL CELL (KW)
290  'NCELL   : EFFICIENCY OF THE FUEL CELL
300  'PMTR    : POWER OUTPUT OF EACH MOTOR (KW)
310  'NMTR    : EFFICIENCY OF THE MOTOR
320  'N       : NUMBER OF MOTORS USED
330  'Q       : TOTAL HEAT REJECTION FLOW RATE (KW)
340  'A       : SOLAR ABSORPTANCE
350  'E       : EMITTANCE OF RADIATOR
360  'TS      : EFFECTIVE SINK TEMPERATURE (K)
370  'TWI     : INLET RADIATOR WALL TEMPERATURE (K)
380  'TWO     : OUTLET RADIATOR WALL TEMPERATURE (K)
390  'TWAV    : RADIATOR AVERAGE WALL TEMPERATURE (K)
400  'AREA    : PRIME RADIATOR AREA (SQ METERS)
410  '
420  '              SUBROUTINES
430  '
440   GOSUB 550    'INPUT VALUES
450   GOSUB 760    'RATE OF HEAT REJECTION
460   GOSUB 810    'TEMPERATURE OF COOLING FLUID AT THE RADIATOR OUTLET
470   GOSUB 870    'EFFECTIVE SINK TEMPERATURE
480   GOSUB 940    'CONVECTIVE HEAT TRANSFER COEFFICIENT
490   GOSUB 1170   'RADIATOR WALL TEMPERATURES
500   GOSUB 1480   'RADIATOR AVERAGE WALL TEMPERATURE
510   GOSUB 1580   'PRIME RADIATOR AREA
520   GOSUB 1630   'PROGRAM OUTPUT
530   END
540  '
550  '              INPUT VALUES
560  '
570   CLS
580   INPUT "COOLING FLUID BEING TESTED ";COOL$
581   INPUT "OPERATING CONDITION OF LCUV ";OPER$
590   INPUT "DIAMETER OF PIPE USED TO CARRY COOLING FLUID (METERS) =";D
```

```
600   INPUT "MASS FLOW RATE OF THE COOLING FLUID (KG/SEC) =";W
610   INPUT "SPECIFIC HEAT OF THE COOLING FLUID (KJ/(KG)(K))";CP
620   INPUT "TEMPERATURE OF COOLING FLUID AT THE RADIATOR OUTLET (K) =";TFO
630   INPUT "SOLAR ABSORPTANCE =";A
640   INPUT "EMITTANCE OF RADIATOR =";E
650   INPUT "LUNAR SURFACE TEMPERATURE (K) =";TM
660   INPUT "ANGLE BETWEEN SUN AND NORMAL TO RADIATOR SURFACE (DEGREES) =";ANGLE
670   INPUT "SOLAR CONSTANT (KW/SQ METERS) =";GS
680   INPUT "STEPHAN-BOLTZMANN CONSTANT (KW/(SQ METERS)(K^4)) =";SBC
690   INPUT "POWER OUTPUT OF THE FUEL CELL (KW) =";PCELL
700   INPUT "EFFICIENCY OF THE FUEL CELL =";NCELL
710   INPUT "POWER OF EACH MOTOR (KW) =";PMTR
720   INPUT "EFFICIENCY OF THE MOTOR =";NMTR
730   INPUT "NUMBER OF MOTORS USED =";N
740   RETURN
750  '
760  '              RATE OF HEAT REJECTION
770  '
780   Q=PCELL*(1/NCELL-1)+N*PMTR*(1/NMTR-1)
790   RETURN
800  '
810  '              TEMPERATURE OF COOLING FLUID AT THE RADIATOR OUTLET
820  '
830   DELTATF=Q/(W*CP)
840   TFI=TFO+DELTATF
850   RETURN
860  '
870  '              EFFECTIVE SINK TEMPERATURE
880  '
890   PI=3.14159
900   ANGLE=ANGLE*(PI/180)
910   TS=(TM^4/2+(GS/(2*SBC))*(A/E)*COS(ANGLE))^.25
920   RETURN
930  '
940  '              CONVECTIVE HEAT TRANSFER COEFFICIENT
950  '
960   MEANTF=(TFO+TFI)/2
970   CLS
980   PRINT
990   PRINT "TEMPERATURE OF COOLING FLUID AT RADIATOR INLET =" TFI "K"
1000  PRINT
1010  PRINT "TEMPERATURE OF COOLING FLUID AT RADIATOR OUTLET =" TFO "K"
1020  PRINT
1030  PRINT "MEAN TEMPERATURE OF COOLING FLUID =" MEANTF "K"
1040  PRINT
1050  PRINT "THE PROPERTIES REQUIRED TO CALCULATE THE CONVECTIVE HEAT TRANSFER"
1060  PRINT "COEFFICIENT SHOULD BE EVALUATED AT THE MEAN TEMPERATURE OF THE"
1070  PRINT "COOLING FLUID."
1080  PRINT
1090  INPUT "VISCOSITY OF THE COOLING FLUID ((N)(SEC)/SQ METERS) =";VIS
1100  INPUT "PRANTL NUMBER OF COOLING FLUID =";PR
1110  INPUT "THERMAL CONDUCTIVITY OF COOLING FLUID (KW/(METERS)(K)) =";K
1120  RE=(4*W)/(PI*D*VIS)
1130  NU=.023*(RE^.8)*(PR^.4)
1140  HR=(NU*K)/D
1150  RETURN
1160 '
1170 '              RADIATOR WALL TEMPERATURES
1180 '
1190  TWI=TFI
```

```
1200  CHECK1=1
1210  WHILE (CHECK1).0001)
1220     F1=TFI-(SBC*E/HR)*(TWI^4-TS^4)-TWI
1230     DF1=4*(SBC*E/HR)*TWI^3-1
1240     TWI=TWI-F1/DF1
1250     CHECK1=ABS(F1/DF1)
1260  WEND
1270  TWO=TFO
1280  CHECK2=1
1290  WHILE (CHECK2).0001)
1300     F2=TFO-(SBC*E/HR)*(TWO^4-TS^4)-TWO
1310     DF2=4*(SBC*E/HR)*TWO^3-1
1320     TWO=TWO-F2/DF2
1330     CHECK2=ABS(F2/DF2)
1340  WEND
1350  IF TWI>TS AND TWO>TS GOTO 1460
1360  CLS
1370  PRINT
1380  PRINT "INVALID RESULTS: THE EFFECTIVE SINK TEMPERATURE CANNOT BE"
1390  PRINT "                 GREATER THAN THE INLET OR OUTLET RADIATOR"
1400  PRINT "                 WALL TEMPERATURE."
1410  PRINT
1420  INPUT "DO YOU WANT TO CONTINUE PROGRAM (0=NO:1=YES) ";ANSWER
1430  PRINT
1440  IF ANSWER=0 GOTO 1950
1450  IF ANSWER=1 GOTO 440
1460  RETURN
1470  '
1480  '            RADIATOR AVERAGE WALL TEMPERATURE
1490  '
1500  NUM=TWI-TWO+(E*SBC/HR)*(TWI^4-TWO^4)
1510  DEN1=(1/HR)*LOG((TWI^4-TS^4)/(TWO^4-TS^4))
1520  DEN2=LOG(((TWI-TS)*(TWO+TS))/((TWO-TS)*(TWI+TS)))
1530  DEN3=2*(ATN(TWI/TS)-ATN(TWO/TS))
1540  DEN=E*SBC*(DEN1+(1/(4*E*SBC*TS^3))*(DEN2-DEN3))
1550  TWAV=((NUM/DEN)+TS^4)^.25
1560  RETURN
1570  '
1580  '            PRIME RADIATOR AREA
1590  '
1600  AREA=Q/(E*SBC*(TWAV^4-TS^4))
1610  RETURN
1620  '
1630  '            PROGRAM OUTPUT
1640  '
1650  LPRINT TAB(25) "PROGRAM OUTPUT"
1660  LPRINT
1670  LPRINT
1680  LPRINT "COOLING FLUID USED IN THIS ANALYSIS : " COOL$
1690  LPRINT
1700  LPRINT
1701  LPRINT "OPERATING CONDITIONS OF LCUV : " OPER$
1703  LPRINT
1710  LPRINT "PROPERTIES OF THE FLUID USED FOR COOLING"
1720  LPRINT
1730  LPRINT "MASS FLOW RATE =" W "KG/SEC"
1740  LPRINT "SPECIFIC HEAT =" CP "KJ/(KG)(K)
1750  LPRINT "DYNAMIC VISCOSITY =" VIS "(N)(SEC)/SQ METERS
1760  LPRINT "REYNOLDS NUMBER =" RE
1770  LPRINT "PRANTL NUMBER =" PR
```

```
1780  LPRINT "THERMAL CONDUCTIVITY =" K "KW/(METERS)(K)
1790  LPRINT "CONVECTIVE HEAT TRANSFER COEFFICIENT =" HR "KW/(SQ METERS)(K)
1800  LPRINT "TEMPERATURE OF COOLING FLUID AT RADIATOR INLET =" TFI "K"
1810  LPRINT "TEMPERATURE OF COOLING FLUID AT RADIATOR OUTLET =" TFO "K"
1820  LPRINT
1830  LPRINT
1840  LPRINT "PROPERTIES OF THE RADIATOR"
1850  LPRINT
1860  LPRINT "TOTAL HEAT REJECTION RATE =" Q "KW"
1870  LPRINT "SOLAR ABSORPTANCE =" A
1880  LPRINT "EMITTANCE =" E
1881  LPRINT "LUNAR SURFACE TEMPERATURE =" TM "K"
1890  LPRINT "EFFECTIVE SINK TEMPERATURE =" TS "K"
1900  LPRINT "INLET RADIATOR WALL TEMPERATURE =" TWI "K"
1910  LPRINT "OUTLET RADIATOR WALL TEMPERATURE =" TWO "K"
1920  LPRINT "RADIATOR AVERAGE WALL TEMPERATURE =" TWAV "K"
1930  LPRINT "PRIME RADIATOR AREA =" AREA "SQ METERS
1940  RETURN
1950  END
```

PROGRAM OUTPUT

```
COOLING FLUID USED IN THIS ANALYSIS : ETHYLENE GLYCOL


OPERATING CONDITIONS OF LCUV : NORMAL (SOLAR NIGHT)

PROPERTIES OF THE FLUID USED FOR COOLING

MASS FLOW RATE = .54 KG/SEC
SPECIFIC HEAT = 2.682 KJ/(KG)(K)
DYNAMIC VISCOSITY = .002677 (N)(SEC)/SQ METERS
REYNOLDS NUMBER = 10111.65
PRANTL NUMBER = 27.586
THERMAL CONDUCTIVITY = .2612 KW/(METERS)(K)
CONVECTIVE HEAT TRANSFER COEFFICIENT = 1425.609 KW/(SQ METERS)(K)
TEMPERATURE OF COOLING FLUID AT RADIATOR INLET = 364.1429 K
TEMPERATURE OF COOLING FLUID AT RADIATOR OUTLET = 360 K


PROPERTIES OF THE RADIATOR

TOTAL HEAT REJECTION RATE = 6 KW
SOLAR ABSORPTANCE = .18
EMITTANCE = .85
LUNAR SURFACE TEMPERATURE = 120 K
EFFECTIVE SINK TEMPERATURE = 100.9082 K
INLET RADIATOR WALL TEMPERATURE = 364.1423 K
OUTLET RADIATOR WALL TEMPERATURE = 359.9995 K
RADIATOR AVERAGE WALL TEMPERATURE = 362.0633 K
PRIME RADIATOR AREA = 7.292251 SQ METERS
```

PROGRAM OUTPUT

COOLING FLUID USED IN THIS ANALYSIS : ETHYLENE GLYCOL

OPERATING CONDITIONS OF LCOV : MAXIMIUM (SOLAR NOON)

PROPERTIES OF THE FLUID USED FOR COOLING

MASS FLOW RATE = .54 KG/SEC
SPECIFIC HEAT = 2.682 KJ/(KG)(K)
DYNAMIC VISCOSITY = .002575 (N)(SEC)/SQ METERS
REYNOLDS NUMBER = 10512.19
PRANTL NUMBER = 26.591
THERMAL CONDUCTIVITY = .2614 KW/(METERS)(K)
CONVECTIVE HEAT TRANSFER COEFFICIENT = 1450.269 KW/(SQ METERS)(K)
TEMPERATURE OF COOLING FLUID AT RADIATOR INLET = 368.2857 K
TEMPERATURE OF COOLING FLUID AT RADIATOR OUTLET = 360 K

PROPERTIES OF THE RADIATOR

TOTAL HEAT REJECTION RATE = 12 KW
SOLAR ABSORPTANCE = .18
EMITTANCE = .85
LUNAR SURFACE TEMPERATURE = 336.1 K
EFFECTIVE SINK TEMPERATURE = 282.6253 K
INLET RADIATOR WALL TEMPERATURE = 368.2853 K
OUTLET RADIATOR WALL TEMPERATURE = 359.9996 K
RADIATOR AVERAGE WALL TEMPERATURE = 364.0676 K
PRIME RADIATOR AREA = 22.26659 SQ METERS

14.0 REFERENCES

1. Minnick, Elbert, C., Pyramidal Truss Core Panel Compared to Corrugated Core (Navtruss) Panel, For Dr. R.L. Ash, MEM 435 Senior Seminar, October 25, 1988.

2. Goetzel, Claus, G., Rittenhouse, John, B., Singletary, John, B., Space Materials Handbook, Addison-Weseley Publishing Company Inc., Reading, Massachusetts, pp.425-442, pp.519-532.

3. Draper, Charles, F., Radiation Shielding for a Lunar Base Module, For Dr. R.L. Ash, MEM 435 Senior Seminar, October 25, 1988.

4. Everhart, John, L., Titanium and Titanium Alloys, Reinhold Publishing Corp., New York, New York, p. 13.

5. The Aluminum Association, Aluminum Construction Manual: Specifications for Aluminum Structures, The Aluminum Association, New York, New York, Third Edition, 1970, p.53.

6. Shigley, Joseph, E., Mitchell, Larry, D., Mechanical Engineering Design, McGraw Hill Publishing Co., New York, New York, 4th Edition, 1983, p.800.

7. M.G. Bekker. Off the Road Locomotion, Research and Development in Terramechanics. Edited by Ann Arbur. University of Michigan Press, 1961.

8. H.T. McAdams, P.A. Reese, and G.M. Lewandowski, prepared by Cornell Aeronautical Laboratory, Inc. Traffacicability and Visibility Analysis of the Lunar Surface. NASA contract report CR-1881, July 1971.

9. M.G. Becker Theory of Land Locomotion (The Mechanics of Vehicle Mobility). Edited by Ann Arbur, University of Michigan Press, 1960

10. G. Davis, M. Hooker, T. Nordtredt, C. Bryant, N. Lebigot. NASA/USRA Advanced Summer Design Report. August 1988.

11. Executive Summary Report Lockheed Missile and Space Company. Design, Fabrication and Delivery of an Improved Single Elastic Loop Mobility System (ELMS). 1972.

12. Smith and William. Principles of Materials Science and Engineering. McGraw Hill Book Company, 1984.

13. Goetael,Claus,G. Rittenhouse, John,B.,Singletary,John, B. Space Materials Handbook, Addison-Weseley Publishing Co. Inc.,Reading Massachusetts.

14. Greenwood,Donald G.,Principles ofDynamics,PrenticeHall,1988.

15. " Macpherson Strut Suspension",Motor Age ,Semptember 1982

16. Fogiel,M.,Handbook of mathematical,Scientific, and Engineering Formulas, Tables, Functions,Graphs,Transforms

22. Parrish, M. A., "Fuel Cells-A Survey," Materials in Engineering, Scientific and Technology Press, Surrey, England, Vol. 2, No. 2, Dec. 1980, pp. 68-72.

23. Angrist, Stanley W., Direct Energy Conversion, Allyn and Bacon, Inc., Boston, Massachusetts, Fourth edition, 1982.

24. Schubert, F. H., Hoberecht, M. A., Le, M., "Alkaline Water Electrolysis Technology for Space Station Regenerative Fuel Cell Energy Storage," Proceedings of the 21st Intersociety Energy Conversion Engineering Conference, American Chemical Society, Washington, D. C., August 1986, pp. 1617-1626.

25. McAdams, H.T., Reese, P. A., Lewandowski, G. M., Trafficability and Visibility Analysis of the Lunar Surface, NASA Contract Report NASA Cr-1881, Correll Aeronautical Laboratory, Inc., Buffalo, New York, July 1971, pp. 63-75.

26. Le, Mike, Engineer, Johnson Space Center, Phone conversation,
Febuary 17, 1989.

27. McDougall, Angus, Fuel Cells, Halstead Press, New York, New York, First edition, 1976.

28. Kenyo, T., "Chromium-Doped Raney Nickel Catalyst for Hydrogen Electrodes in Alkaline Fuel Cells," Journal of the Electrochemical Society, Electrochemical Society, Inc., Manchester, New Hampshire, Vol. 132, No. 2, Febuary 1985, pp. 383-386.

29. Bayazitoglu, Y.,Smith, G., Curl, R., Hydrogen Energy Part B, Edited by T. Nejat Veziroglu, Plenum Press, New York, New York, 1974.

30. Bufkin, A.L., T.O. Tri, and T.C. Trevino. 1988. EVA Concerns for a Future Lunar Base. Lunar Bases & Space Activities in the 21st Century. Paper no. lbs-88-214

31. Electro-Craft Corporation. 1980. DC Motors, Speed Controls, Servo Systems. Fifth edition. Hopkins, Minnesota: Electro-Craft Corporation

32. Schuring,D.J., H.T.McAdams, P.A. Reese, and G.M. Lewandowski. 1971. Trafficability and Visibility Analysis of the Lunar Surface. NASA CR-1881. Washington D.C.

33. Pacific Scientific Motor Co. DC motor catalog. 1987.

34. Phone conversation with Dr. Richard K. Barton, Senior Electro-Mechanical Engineer, General Electric Co., East Lake Road, Eire, PA. 16531

35. Dallas, Thomas, Diaguila, Anthony J., Saltsman, James F., Design Studies on the Effects of Orientation, Lunation, and Location on the Performance of Lunar Radiators, Lewis ResearchCenter, Cleveland, Ohio, March 1971.

36. Design Criteria for Controlling Stress Corrosion Cracking, Prepared by Materials and Process Laboratory, George C. Marshall Space Flight Center, Alabama, 1977.

37. ASHRAE Handbook 1985 Fundamentals, American Society of Heating, Refrigerating and Air-Conditioning Engineers, Inc., Atlanta, Georgia, 1985.

38. Incropera, Frank P., Dewitt, David P., Fundamentals of Heat and Mass Transfer, John Wiley & Sons Inc., New York, New York, Second edition, 1985.

39. Skylab Extravehicular Mobility Unit, NASA Report s-531.

40. G.R. Evans and W.E. Price, The Effects of High Energy Radiation in Infared Optical Materials, SB-61-25, Lockneed Missiles and Space Company, Sunnyvale, California, May 1961.

41. F.V. Tooley, Handbook of Glass Manufacture, Vol 2, Ogden Publishing Company, New York, 1960.

42. G. Artutunian and F.C. Seppi, The Effects of Ionizing Radation Upon Transparent Materials, Report RR-1, Ordnance Tank-Automotive Command, Detroit. Arsenal, Centerline Michigan, October 1959.

43. T.E. Lusk, "Infrared-Transmission Materials Would Be Unaffected by Radiation in Space, "Electronic Design, p74, 62 October 1960.

44. C.G. Gortzel, J.B. Rittenhouse, and J.B. Singletory, ed., Space Materials Handbook, Lockneed Missles and Space Company, Addison-Wesley Publishing Company, Inc. Reading, Massachusetts, 1965.

45. J.P. Heppner, et.al, Project Vanguard MagneticField Instrumentation and Measurements, NASA TND-486, September 1961.

46. E.K. Welhart & CH. Johnston, Sealing of Manned Spacecraft, McDonnell Aircraft Corporation, 24 September 1963.

47. Press Information", Space Shuttle Transportation Systems, Rockwell Intertional Corporations, 1984.

48. H. Misko, personal conversation, 3/22/89, Corning Glass Company.

49. D. Higgons, personal conversations, 3/24/89, PPG Industries.

50. R. Zobrowski, personal conversation, 4/4/89, OCLA Laboratories.

51. A. Abbott, personal conversation, 4/3/89, American Flat Glass,Inc.

52. F.H. Samonski, Jr., E.M. Tucker, "Apollo Experience Report", Command And Service Module Environmental Control System, Manned Spacecraft Center, NASA, Huston, Texas, May 24 1971.

53. J. Buckley, personal conversation, 3/21/89, NASA-Langley.

54. D. Powell, personal conversations, 3/1/89, EI.Du Pont De Nemours and Company.

55. G. Graf, "Upon The Farm", Space World, April 1987.

56. P. Romans secretary, personal conversation, March 25, 1989 Owens Lorning Corporation.

57. "Properties, Processing, and applications of teflon TFE -Fluorocarbon Fiber", Du pont Technical Information; Fibers, Bulletin TF-2, May 1978.

58. H. Mallory, personal conversation, March 31, 1989, EI. Du Pont De Nemours and Company.

59. "Properties of DuPont Industrial Filament Yarns", Dupont Fibers Technical Information, Multifiber Bulletin X-272, July 1988.

67. Muehldorf, Eugene, I., and Richard F. Filipowsky, Space Communication Systems. Englewood Cliffs New Jersey: Prentice-Hall, 1965.

68. Krassner, George, N. and Jackson Michaels, Introduction to Space Communication Systems. New york: McGraw, 1964.

69. Tomasi, Wayne, Advanced Electronic Communication Systems. Englewood Cliffs New Jersey: Prentice-Hall, 1987.

70. Balakrishnan, A.V., ed., Space Communications. New York: McGraw, 1963.

71. Wolff, Edward, A., Antenna Analysis. New York: John Wiley and Sons, 1975.

72. Morris, D.J., Communications for Command and Control Systems.Elmsford New york: Pergamon Press, 1983.

73. Brazell, J.W., Williams, W.M., et.al., Lunar Base Construction Equipment, April 1988.

74. Mendell, W.W. ed., Lunar Bases and Space Activities of the 21st Centrury, Lunar and Planetary Institute, Houston, 1985.

75. Aardayfio, D.D., Pottinger, H.J., Computer Control of Robotic Manipulators, Mechanical Engineering, August 1982, pp.40-

76. Nobbe, Thomas A., Shuttle Arm to Gain Eye, Brain, and Muscle, Machine Design, vol.58, April 10, 1986, pp.23-28.

77. Dooling, Dave, "Canadian Arm Aids Shuttle Program"

78. Wilson, J., Hydraulic and Electrical Actuation Systems for Robotic Use on the Moon, Old Dominion University.

79. Lunar Base Surface Missions Operations, Lunar Base Sysyems Study (LBSS) task 4.1, Johnson Space Center NASA ontract No. NAs9-1878 p.74.

80. Kuell, D.E., Butler G.V., Advances in the Astronautical Sciences; Shuttle/Spacelab The New Transportation System and its Utilization;Proceedings of the Third Dglriaas Sympossium, Hanover, Germany, April 28-30, 1980.

81. Lindberg, G.M., Canadian stretches Shuttle Reach, Aerospace America, May, 1985, pp.70-74.

82. Schwarte, R.. 1984. Performance capabilities of Laser Ranging Sensors. Proc. ESA Workshop on Space Laser Applications and Technology, 26-30 March (ESA SP-202,May 1984)

83. Forrester, P., and K.F. Hulme. 1981. Review of Laser Rangefinders. Optical and Quantum Electronics 3, no. 13:259-293

84. Wilson, P.. 1982. Use of Powerful Lasers and Lidars for Ranging and Positioning. Optical and Quantum Electronics 2, no. 3:37-39

85. Halliday, D., and R. Resnick. 1978. Physics Parts 1&2. New York: John Wiley & Sons

86. Skylab EVA Mobility Unit. NASA Document S531, 1982

NASA
FORMAL
REPORT

FFNo 665 Aug 65